

Studies on the effect of randomness on the
synchronization of coupled systems and on
the dynamics of intermittently driven
systems

Manu Punnen John.

International School of Photonics
Cochin University of Science and Technology
Kochi 682 022, India

Thesis submitted to Cochin University of Science and Technology in
partial fulfillment of the requirements for the award of the Degree of
Doctor of Philosophy

January 2009

Studies on the effect of randomness on the synchronization of coupled systems and on the dynamics of intermittently driven systems

Author:

Manu Punnen John.

Research Fellow

International School of Photonics,

Cochin University of Science and Technology,

Kochi, 682022, India

E-mail: mpjohn@gmail.com

Research Advisor:

Dr. V. M. Nandakumaran

Professor

International School of Photonics,

Cochin University of Science and Technology,

Kochi, 682022, India

E-mail: nandak@cusat.ac.in

International School of Photonics,

Cochin University of Science and Technology,

Kochi, 682022, India

www.photonics.cusat.edu

January 2009

Dedicated to
My Family and Friends

CERTIFICATE

Certified that the research work presented in the thesis entitled “*Studies on the effect of randomness on the synchronization of coupled systems and on the dynamics of intermittently driven systems*” is based on the original work done by Mr. Manu Punnen John under my guidance in the International School of Photonics, Cochin University of Science and Technology, Kochi 682 022 and has not been included in any other thesis submitted previously for the award of any degree.

Kochi
26 January, 2009

Dr. V. M. Nandakumaran
(Supervising Guide)
International School of Photonics
CUSAT

DECLARATION

Certified that the work presented in the thesis entitled “*Studies on the effect of randomness on the synchronization of coupled systems and on the dynamics of intermittently driven systems*” is based on the original work done by me under the guidance and supervision of Dr. V. M. Nandakumaran, Professor, International School of Photonics, Cochin University of Science and Technology, Kochi 682 022, India and has not been included in any other thesis submitted previously for the award of any degree.

Kochi

26 January, 2009

Manu Punnen John

Acknowledgements

With a feeling of profound thankfulness and deep sense of gratitude, I acknowledge the invaluable help and consistent guidance rendered to me by Prof. V. M. Nandakumaran. His insight and objective thinking about research problems were an inspiration for me during the course of the work.

At this juncture, I cannot forget all the encouragement and support provided by Prof. C. P. Girijavallabhan, Prof. V. P. N. Nampoori, Prof. Radhakrishnan and Mr Kailasnath throughout my life in ISP, hence I thank them wholeheartedly.

I acknowledge Prof M. Lakshmanan, Prof M. Daniel, Prof. Jürgen Kurths, Dr. M. P. Joy, Dr. P. Indic, Prof. Rajarishi Roy and Prof. Thomas Kuruvilla for fruitful discussions.

I owe much to Dr. S. Rajesh and Dr. Bindu M. Krishna for all the help and sound advices, without which I would have been lost at times. Also I acknowledge fertile discussions and waves of encouragement from Mrs. Parvathi Abin and Mr. Jijo P. Ulahannan. Appreciations and criticisms from Mrs. Chitra Radhakrishnan was also helpful in several occasions.

As lion's share of my work was computational, a lot of software and hardware related help given by Mr. V. C. Kishore, Mr. Emmanuel Thompson and Mr. Vinu V. Nampoothiri is gratefully acknowledged, without which I could not have completed my work successfully. Above all, I acknowledge my earnest gratitude to Mr. P. P. Vinod Kumar in this regard who always has been the doctor on call for my computational systems and related problems.

I also acknowledge my colleagues in ISP and my friends who gave me support, encouragement and a treasure of pleasant memories.

Financial support from the Council for Scientific and Industrial Research (CSIR) is gratefully acknowledged, without which my life as a research student would have been impossible. I thank the 'Cochin University of Science and Technology' for all the support and for being a second home during my postgraduate and research years.

Manu Punnen John.

Preface

Nonlinear dynamics has emerged into a prominent area of research in the past few decades, particularly after the wide availability of low cost and fast computation. Today nonlinear systems are being investigated in almost every discipline. It has also contributed to the development of a unique stream of interdisciplinary research. Turbulence, Pattern formation, Multistability etc are some of the important areas of research in nonlinear dynamics apart from the study of chaos.

Chaos theory is perhaps the one which has provided most counter intuitive results in comparison with other branches of nonlinear dynamics. The study of chaos theory started in the modern sense with the investigations of Edward Lorentz in mid 60's. Later developments in this subject provided systematic development of chaos theory as a science of deterministic but complex and unpredictable dynamical systems.

Synchronization of chaotic systems is one of the most important developments in chaos theory. It is found that two (or even more) chaotic systems, though each by itself is complex and unpredictable, can be made to behave identically if they are suitably coupled. Soon it was also found that such synchronized systems can be used to encrypt messages which led to the development of chaotic encryption based cryptographic schemes. In addition to this, the synchronization of coupled complex systems has also contributed tremendously to our understanding of collective phenomenon of interacting systems in nature.

It has been shown recently that systems driven with random pulses show the signatures of chaos, even without nonlinear dynamics. This shows that the relation between randomness and chaos is much closer than as it was understood earlier. The

effect of random perturbations on synchronization can be also different. In some cases identical random perturbations acting on two different chaotic systems induce synchronization. However most commonly, the effect of random fluctuations on the synchronization of chaotic systems is to destroy synchronization .

This thesis deals with the effect of random fluctuations with its associated characteristic timescales on chaos and synchronization. We try to unearth yet another manifestation of randomness on chaos and synchronization . This thesis is organized into six chapters as follows.

In chapter 1 we introduce the basic concepts of nonlinear dynamics and chaos. It includes the basic definitions of the terms used in chaos theory and also some well known chaotic systems are discussed. Basic computational tools are dealt with and we have discussed how they are used in quantifying and characterizing chaotic dynamics. In this chapter we also introduce the notion of synchronization of chaotic systems. Also we briefly discuss its main technological application: Chaotic encryption based cryptographic schemes.

In chapter 2, brief discussions on the theoretical concepts and the dynamical systems specific to this work are given. We introduce the concept of noise, and two familiar types of noise are discussed. The classifications and representation of white and colored noise are introduced. Based on this we introduce the concept of randomness that we deal with as a variant of the familiar concept of noise. The dynamical systems introduced are the Rossler system, directly modulated semiconductor lasers and the Harmonic oscillator. The directly modulated semiconductor laser being not a much familiar dynamical system, we have included a detailed introduction to its relevance in Chaotic encryption based cryptography in communication.

In chapter 3 the studies on the effect of a fluctuating parameter mismatch associated with characteristic timescales on the synchronization is presented. The studies are performed on the Rossler system and directly modulated semiconductor laser systems. We show that the effect of a fluctuating parameter mismatch on synchronization is to destroy the synchronization. Further we show that the relation between

synchronization error and timescales can be found empirically but there are also cases where this is not possible.

In chapter 4 we present the results of the investigations on a modified harmonic oscillator. We assume that the freely running drive and the oscillator are coupled only when the trajectory is within a strip of small width located around the origin of the position momentum space. There is no coupling between the drive and the oscillator when the trajectory is outside the strip. The system exhibits chaos. We have also replaced the deterministic driving with a random forcing and we found that the stochastic system mimics its deterministic analogue. The dynamics in deterministic and stochastic cases are characterized by standard tools in chaos theory. We also found that the nature of the effective fluctuations which affect the stochastic system is similar to the fluctuations introduced in chapter 3.

In chapter 5 we consider another modified version of the system that we have presented in chapter 4. The oscillator was subjected to a drive which is spatially modulated with a rapidly decaying exponential function of the position variable. Such a modification induces nonlinearities necessary for chaotic behavior. Studies show that under the variation of the parameters, the system becomes chaotic, which appears to be the period doubling route to chaos. We also discuss the synchronization properties of this system.

In chapter 6 we summarize and conclude the present work. A few directions for future works has also been suggested.

List of Publications

Journal Papers

- **Manu P. John** and V. M. Nandakumaran, *Interplay of determinism and randomness in a piecewise linear chaotic system*, communicated.
- M. R. Parvathi, Bindu M. Krishna, S. Rajesh, **M. P. John** and V. M. Nandakumaran, *Hopf bifurcation in parallel polarized Nd:YAG laser*, to appear in Chaos, Solitons and Fractals.
- **Manu P. John**, P. U. Jijo and V M Nandakumaran *Effect of a fluctuating parameter mismatch and the associated timescales on coupled Rossler oscillators*, to appear in Pramana.
- M.R. Parvathi, Bindu M. Krishna, S. Rajesh, **M. P. John** and V.M. Nandakumaran, *Synchronization and control of chaos in coupled chaotic multimode Nd:YAG lasers*, Phys. Lett. A 373, 96, 2008.
- Bindu M. Krishna, **Manu P. John** and V M Nandakumaran *Performance characteristics of positive and negative delayed feedback on chaotic dynamics of directly modulated InGaAsP semiconductor lasers*, Pramana 71, No. 6, 1259, 2008.
- Ritty J. Nedumpara, **P. J. Manu**, C.P.G. Vallabhan, V.P.N. Nampoore, P. Radhakrishnan *Energy transfer studies in dye mixtures in different solvent environments*, Optics and Laser Technology 40, iss. 7, 953, 2008.
- Jayasree V. K, Shaija P. J, **Manu P. John**, P. Radhakrishnan, *An Optoelectronic Sensor Configuration for the Determination of Age Related Indices Using Blood Volume Pulse*, Sensors & Transducers Journal 87, Issue 1, 39, 2008.

Mathematica demonstrations

- *Chaotic Dynamics of a Modulated Semiconductor Laser* from The Wolfram Demonstrations Project, Contributed by: Manu P. John and V. M. Nandakumaran

Talks

- **M. P. John**, P. U . Jijo and V. M. Nandakumaran, Effect of a fluctuating parameter mismatch in the synchronization of a chaotic system, National Conference on Current Trends in Material Science (CTMS-07), organized by the Department of Physics Christian College, Chengannur, March 25-27 2007
- **M.P. John**, P. U. Jijo, and V. M. Nandakumaran, *Fast Fluctuations do not Destroy Synchronization*, National Conference on Nonlinear Systems and Dynamics, Ramanujam Institute for Advanced Study in Mathematics, University of Madras, Chennai, 6-8, February 2006, Proceedings, Allied Publishers Chennai(peer reviewed).
- Jijo P. Ulahannan, **Manu P. John**, and V. M. Nandakumaran, *Bistability and Hysteresis in the Dynamics of Directly Modulated Multiple Quantum Well Lasers*, Proceedings of the OSA conference Frontiers in Optics 2007 Laser Science XXIII, San Jose, California, USA, September 16-20, 2007 (peer reviewed).
- Parvathi. M. R, Bindu M Krishna, **M. P .John** and V. M. Nandakumaran, *Hopf bifurcation and phase transition in Nd:YAG lasers*, Recent Developments in Nonlinear Dynamics, RDND 2008 Bharatidasan University Tiruchirappally Feb 13-16, 2008.
- M.R.Parvathi, Bindu.M.Krishna, M. P. John and V.M.Nandakumaran, Nonlinear dynamics of coupled chaotic multimode Nd:YAG laser, NCNSD 2008, PRL, Ahmedabad.

Poster presentations

- M. P. John, P. U. Jijo, and V. M. Nandakumaran, *Effect of parameter fluctuations in directly modulated semiconductor laser systems*, *Proceedings*, Photonics 2004, Cochin, December 8-11 (2004).
- P. U. Jijo, M. P. John, S. Rajesh and V. M. Nandakumaran, *Control of chaos and noise induced instabilities in a Duffing oscillator with amplitude modulated feedback*, Perspectives in Nonlinear Dynamical Systems 2004 (PNLD - 2004), Chennai, July 12-15, 2004 (a Satellite meeting of the STAPHYS 22, IISc, Bangalore, India).
- M. R. Parvathi, M. P. John and V. M. Nandakumaran, *Nonlinear dynamics of a two mode intracavity doubled Nd:YAG laser*, National Conference on recent trends in Optoelectronics and Laser technology, NCOL 2007 University of Kerala, Thiruvananthapuram.
- M. R. Parvathi, M. P. John and V. M. Nandakumaran, *Transition from phase to complete synchronization in coupled chaotic multimode Nd:YAG lasers with a parameter mismatch*, National Laser Symposium NLS 2007 Indore.
- M. R. Parvathi, Bindu.M.Krishna, S.Rajesh, **Manu P. John** and V. M. Nandakumaran, Dynamics of Nd:YAG laser under delayed optoelectronic feedback, National Laser Symposium, 2008, Delhi.

Table of Contents

	Preface	xi
	Table of Contents	xvii
1	Introduction	1
1.1	Chaos	1
1.2	Chaotic dynamical systems	2
1.3	Mathematical representation of discrete dynamical systems.	3
1.4	Logistic map	4
1.4.1	Chaos in continuous dynamical systems	4
1.5	The Lorenz system	7
1.6	Poincare sections	11
1.7	Power spectrum	12
1.8	Lyapunov exponents	15
1.9	Attractors and dimensions	17
1.10	Routes to chaos	17
1.11	Unstable periodic orbits	19
1.12	Synchronization of Chaos	21
1.12.1	Coupling schemes	21
1.13	Types of synchronization	24
1.13.1	Perfect or Exact synchronization	24
1.13.2	Phase and Lag synchronization	24
1.13.3	Generalized Synchronization	24
1.14	Secure communication using Chaos	25
1.15	Conclusion	26
	Bibliography	27

2	Randomness in synchronization and chaos	31
2.1	Introduction	31
2.2	White and coloured noise	31
2.2.1	White noise	32
2.2.2	Coloured noise	33
2.2.3	Correlations in time	34
2.2.4	When is a noise considered delta correlated ?	34
2.2.5	Fluctuations with large timescales and randomness	34
2.3	Systems under consideration	35
2.3.1	Rossler Attractor	35
2.3.2	Harmonic Oscillator	37
2.4	Directly modulated semiconductor lasers	45
2.4.1	Laser model	47
2.5	Conclusion	49
	Bibliography	50
3	Effect of parameter fluctuations on coupled chaotic systems	55
3.1	Introduction	55
3.2	Parameter fluctuations	56
3.3	Effect on synchronization	57
3.4	Discussion	64
3.5	Effect of fluctuations in Laser dynamics	68
3.6	Laser model	68
3.7	Parameter fluctuations	70
3.7.1	Numerical results	70
3.8	Conclusion	73
	Bibliography	74
4	Chaos in an intermittently driven damped oscillator	79
4.1	Introduction	79
4.2	Basic model	80
4.3	Deterministic driving	81
4.3.1	Dynamical equations	81
4.3.2	Numerical results	81
4.4	Random driving	88
4.4.1	Dynamical equations	88
4.4.2	Numerical results	90

4.5	Nature of the forcing	95
4.6	Conclusion	95
	Bibliography	96
5	Harmonic oscillator with exponential damping	99
5.1	Introduction	99
5.2	Parameter variations	102
5.3	Synchronization	108
5.4	Conclusions	114
	Bibliography	115
6	Summary, conclusions and future prospects	117
6.1	Summary and conclusion	117
6.2	Future prospects	118

Chapter 1

Introduction

Nonlinear dynamics deals with systems in which the equation of motion involve nonlinear differential equations or difference equations. Many of the nonlinear equations are difficult to solve analytically. Also in some cases, no stable analytic solutions exist. Thus the only option in dealing with most of these equations is numerical solutions. This need a huge amount of arithmetic calculations, which were impossible for humans before the advent of computers. However, with the advent of low cost computation many of these equations are solved numerically. It was found that nonlinear systems often exhibit surprising behaviors, drastically different from those of their approximately linear counterparts.

As of now, nonlinear dynamics is an interdisciplinary area of research that deals with phenomenon like multistability [1, 2, 3], pattern formation [4] and chaos [6, 7, 8, 9, 10]. Much of the findings in this area have contributed to our understanding of nature, and also in the advancement of technology.

1.1 Chaos

In English language, the word Chaos is used to describe a situation which is unpredictable or irregular. In nonlinear dynamics, chaos refers to the complex evolution

of a deterministic system, which is highly sensitive to initial conditions. A proper understanding of this phenomenon started with Lorentz's observations of a dynamical system derived from a weather model [5]. He found that the system is bounded, aperiodic and highly sensitive to initial conditions. His paper remained unnoticed for a while, but around late 70's chaos theory became an active area of research. The mathematical frame work that describe the theory is so versatile that it could be applied to a variety of natural phenomenon. This has lead to the development of a strong interdisciplinary component, which includes secure communication [11], biological systems [12, 13, 14, 15], and social interactions [16].

1.2 Chaotic dynamical systems

A dynamical system is a system that evolves in time. A dynamical system can be deterministic or stochastic. The evolution of a deterministic system is determined by it past according to some mathematical rule or formula. A stochastic dynamical system evolves according to some random process, such as the rolling of a dice or the tossing of a coin.

The dynamical system could either be continuous dynamical system or discrete dynamical system, depending on whether time is continuous or discrete. The dynamics in the phase space is represented by differential equations in case of continuous systems and difference equations in case of discrete systems. Such dynamics can again be classified into two groups. Flows or mappings which conserves phase space volume or conservative systems and dissipative systems where the phase space volume is not conserved. Physical systems in reality is usually continuous dissipative systems. Mappings or discrete systems usually appear as derived from the dynamics of continuous systems. Conservative systems have been studied in great detail particularly because of their applications in celestial mechanics.

We first discuss discrete maps, and introduce some of the basic tools and concepts

required in understanding chaotic dynamics. Later we introduce continuous dynamical systems and the additional tools like Poincare section that is required for studying such continuous systems.

1.3 Mathematical representation of discrete dynamical systems.

Mathematically, dynamical systems are described by the rule that determines the evolution of the system in time. That is, given the state of the system at time $t = n$, the dynamical equations gives the state of the system at time $t = n + 1$. Consider a system defined by the variables x_1, x_2, \dots, x_k and the parameters p_1, p_2, \dots, p_m . The dynamical system can be represented as

$$\begin{aligned}
 x_{1 \ n+1} &= f_1(p_1, p_2, \dots, p_m, x_{1n}x_{2n}\dots x_{kn}) \\
 x_{2 \ n+1} &= f_2(p_1, p_2, \dots, p_m, x_{1n}x_{2n}\dots x_{kn}) \\
 &\cdot \quad \cdot \\
 &\cdot \quad \cdot \\
 &\cdot \quad \cdot \\
 x_{k \ n+1} &= f_k(p_1, p_2, \dots, p_m, x_{1n}x_{2n}\dots x_{kn})
 \end{aligned} \tag{1.3.1}$$

According to the values of the parameters, the system can be chaotic or periodic. A chaotic system usually undergoes a series of period doublings and ends up in chaos, with the variation of these parameters. This transition of the state of the system can be represented by a bifurcation diagram. In a bifurcation diagram, specially chosen points from the phase space of the attractor is plotted against the instantaneous values of a varying parameter. Bifurcation points are those values of the parameter at which there occurs a qualitative change in the dynamical system (eg: one cycle-two cycle

or periodic to aperiodic and chaotic). Thus the periodic and chaotic behavior can be distinguished from the way the points are distributed in the bifurcation diagram. Another tool that is used in the visual characterization of discrete dynamical systems is the return map. In a return map, the $(n + 1)^{th}$ value of a variable is plotted against the n^{th} value of the parameter. If the slope of such a map is greater than 1, the map is chaotic. These ideas will be demonstrated in the case of the logistic map.

1.4 Logistic map

The logistic map [17] is one of the widely studied discrete system in chaos theory. It is a simple system that display almost all features that is unique to a chaotic system. The equation for the logistic map is given by the equation,

$$x_{n+1} = f(x_n) \tag{1.4.1}$$

where,

$$f(x_n) = \mu x_n(1 - x_n) \tag{1.4.2}$$

The dynamics is one dimensional, with a single bifurcation parameter μ . The function $f(x)$ represents a one-hump map in the interval zero and one. The bifurcation diagram in figure 1.1 shows the transition from a fixed point to periodic cycles and finally to chaos in a logistic map. The return map is shown in figure 1.2. It can be seen that it is similar to the function $f(x)$ which determines its dynamics. The bifurcation diagrams and return maps are also useful in the study of continuous systems.

1.4.1 Chaos in continuous dynamical systems

The dynamical systems in which time is continuous is called a continuous system. Such systems are usually represented by a set of coupled differential equations. As in the case of discrete systems, the variables denote the state of the system in the phase

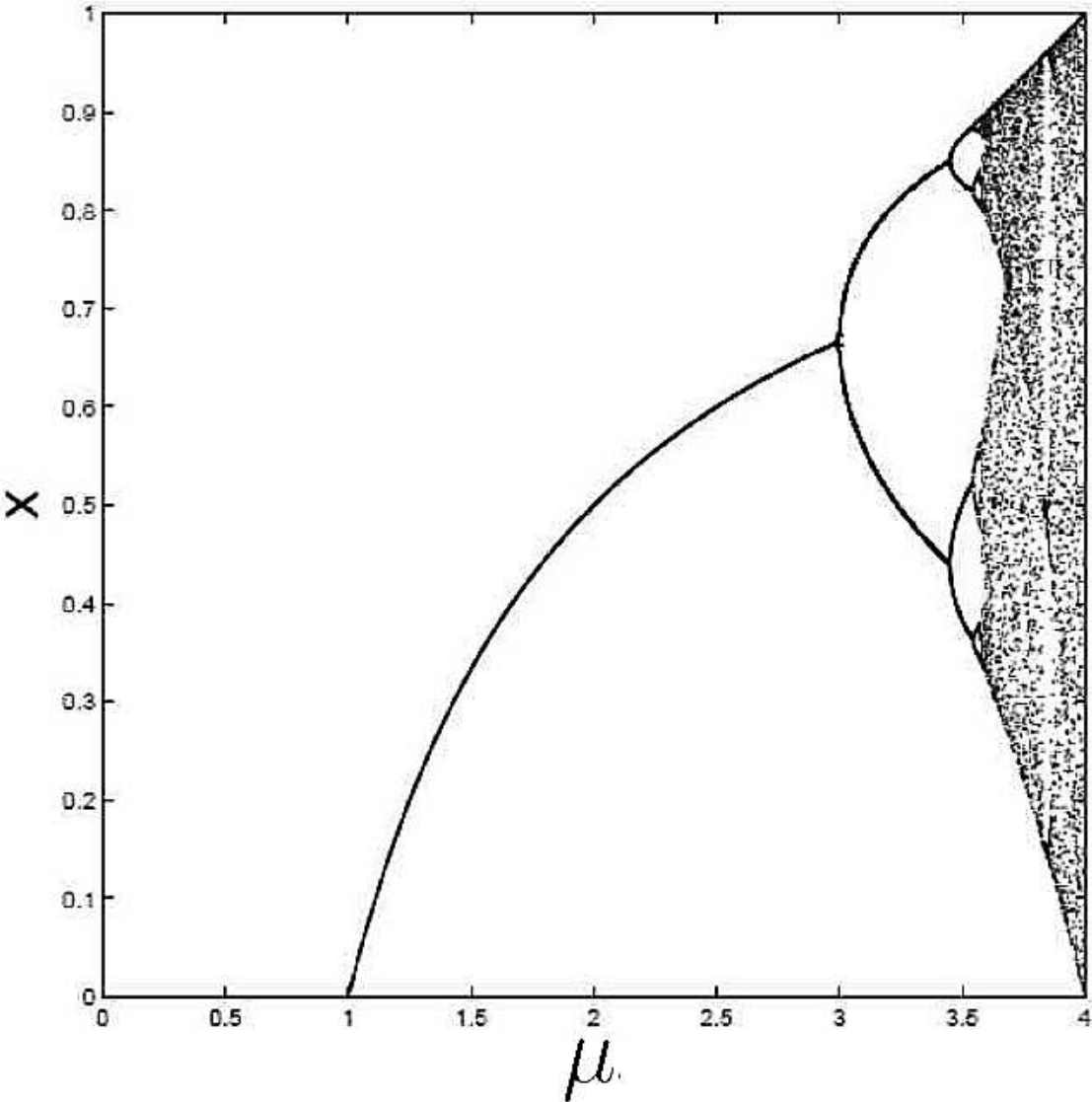


Figure 1.1: The bifurcation diagram of a logistic map.

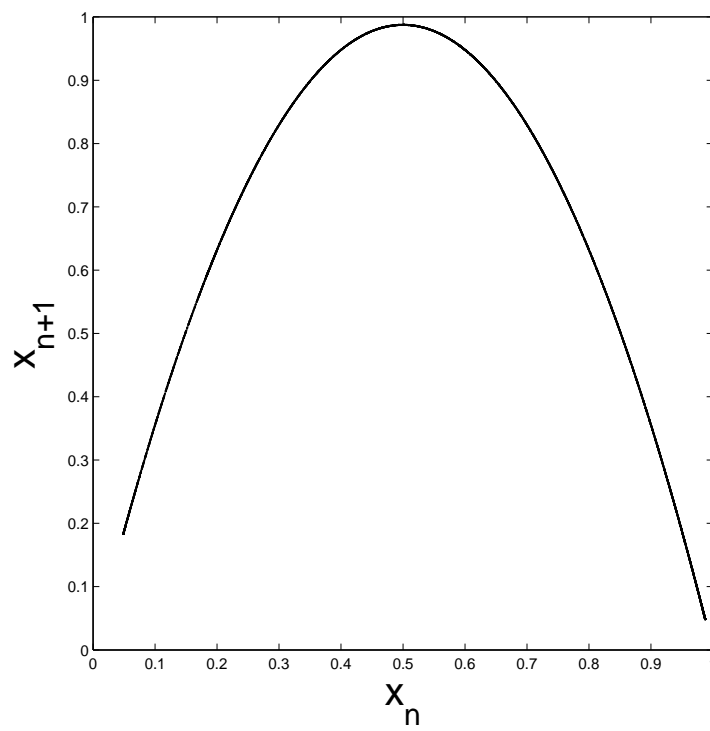


Figure 1.2: The return map of a logistic map.

space and the nature of the dynamics is determined by the parameters. In general, a continuous dynamical system can be represented by the following set of equations,

$$\begin{aligned}
 \dot{x}_1 &= f_1(p_1, p_2, \dots, p_m, x_1, x_2, \dots, x_k) \\
 \dot{x}_2 &= f_2(p_1, p_2, \dots, p_m, x_1, x_2, \dots, x_k) \\
 &\cdot \quad \cdot \\
 &\cdot \quad \cdot \\
 &\cdot \quad \cdot \\
 \dot{x}_k &= f_k(p_1, p_2, \dots, p_m, x_1, x_2, \dots, x_k),
 \end{aligned} \tag{1.4.3}$$

where the dots represents time derivatives.

Nonlinear coupled differential equations can be chaotic in certain regions of the parameter space. The parameters in this equations, if varied, the system exhibits both chaotic and periodic behavior. A return map can be obtained from the maxima of the time series. This is by plotting the $(n + 1)^{th}$ maxima against the n^{th} maxima. Such a return map can be used to study the dynamical features of the system: like the absence of a stable periodic behavior. Also a well defined return map means that the system can actually be reduced to a one dimensional dynamical system. The reduction of a dynamical system represented by coupled dynamical equations to an equivalent one dimensional system is discussed in [18].

1.5 The Lorenz system

A well known example of a continuous chaotic system is the Lorenz system [5]. It is a truncated version of the Rayleigh-Benard model of convection of heat through fluids. This system was studied by Lorenz, and is the first example of a continuous dynamical system showing chaotic behavior. The dynamical equations for the Lorenz

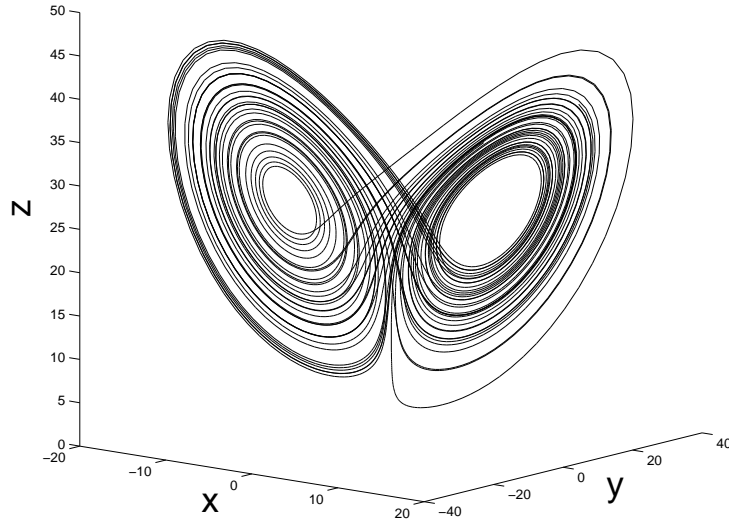


Figure 1.3: Phase space of a Lorenz attractor.

system is given by,

$$\dot{x} = \sigma(y - x) \quad (1.5.1)$$

$$\dot{y} = x(\rho - z) - y$$

$$\dot{z} = xy - \beta z$$

The typical values of the parameters for chaos are: $\sigma = 10$, $\rho = 28$ and $\beta = 8/3$. The phase space trajectory of the system is given in figure 1.3. The system shows chaotic as well as periodic behavior as the parameters are varied. The bifurcation diagram obtained by varying ρ is given in figure 1.4. The return map of the Lorenz attractor is well defined and with a slope greater than 1, and was in fact used by Lorenz as a proof that the time series of this system is chaotic. Figure 1.5 shows the return map of the Lorenz system.

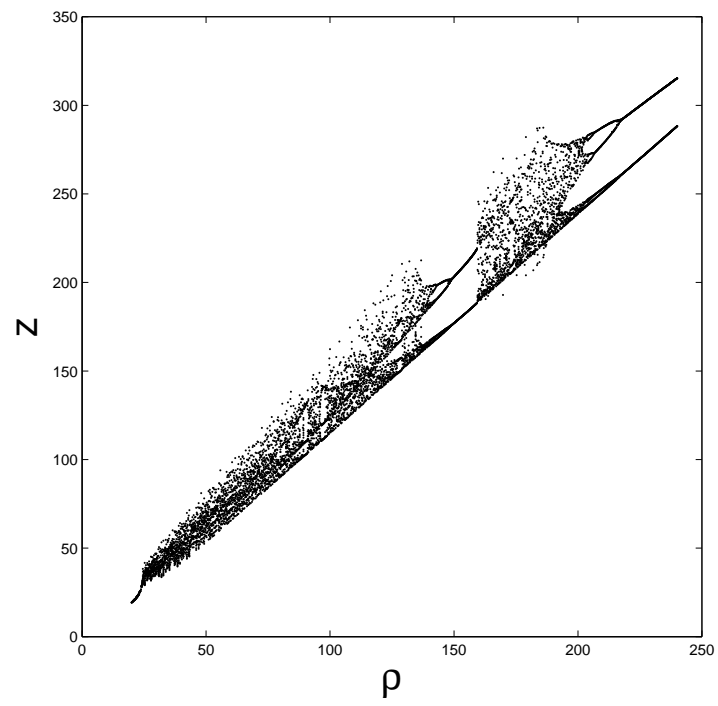


Figure 1.4: The bifurcation diagram of a Lorenz system.

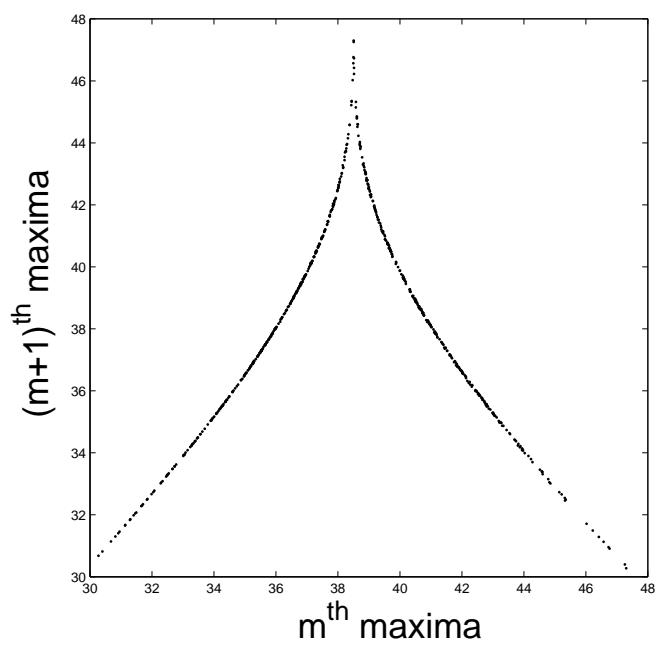


Figure 1.5: The return map of a Lorenz system. The maxima s were obtained from the time series of the variable z of the system.

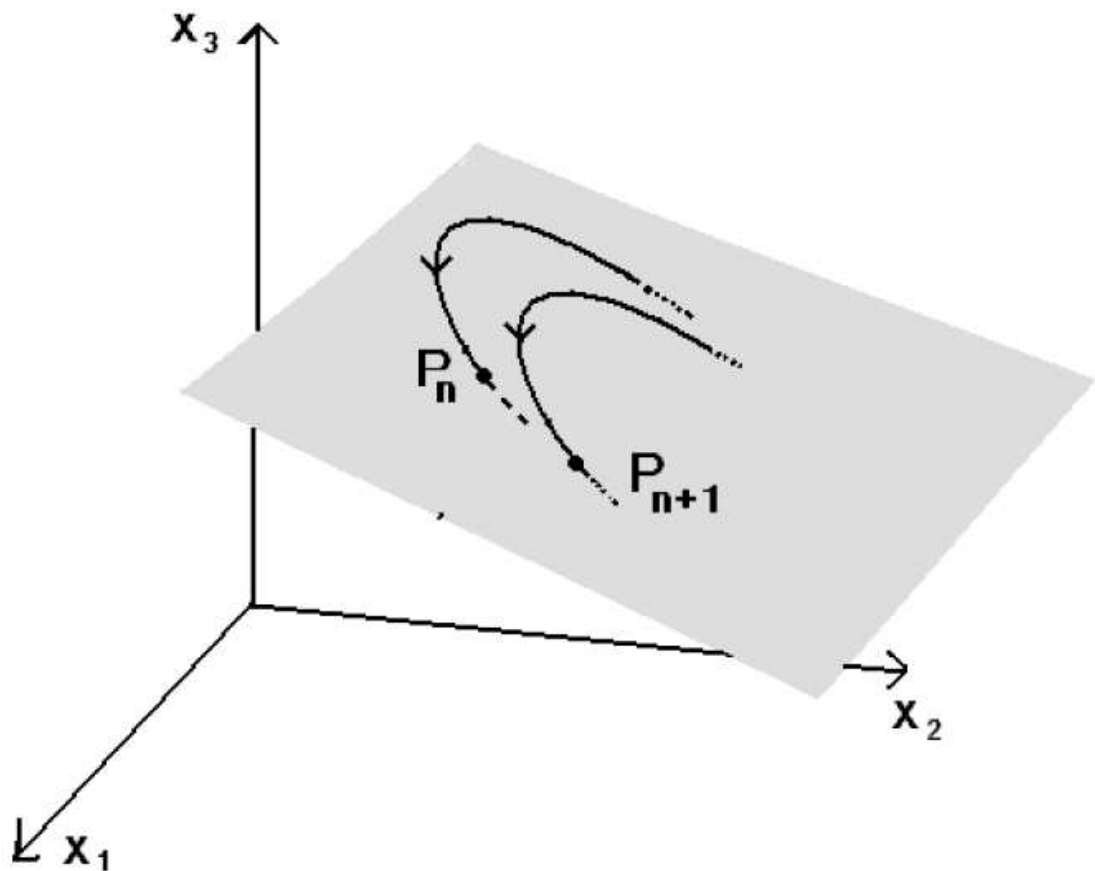


Figure 1.6: The schematic diagram of a Poincare section.

1.6 Poincare sections

We have seen in equation 1.12.2 that a dynamical system can be multi dimensional, and chaotic behavior is possible only in spaces with at least three dimensions. But many of the quantities that characterize chaotic behavior in a system can be obtained by studying the dynamics in a lower dimensional space. A systematic way of doing this is by constructing a Poincare section. In constructing a Poincare section we consider a subspace of dimension $n - 1$ in an n dimensional space. For example, a two dimensional plane defined in the phase space of a three dimensional attractor is a Poincare section. The method of constructing Poincare sections is illustrated in

figure 1.6. The phase space trajectories that passes through the section is recorded. But a constraint imposed: *the encounters of the trajectory only in one direction is considered*. Let P_1, P_2, \dots, P_n be N such points recorded in such an evolution. For a point P_k there will be coordinates p_1 and p_2 associated with it. Typically, a mapping of the form,

$$\begin{aligned} p_{m+1}^1 &= f_1(p_m^1, p_m^2) \\ p_{m+1}^2 &= f_2(p_m^1, p_m^2) \end{aligned} \quad (1.6.1)$$

can also be defined. This can be used for several purposes including the calculation of invariant parameters of the dynamics.

1.7 Power spectrum

Fourier methods in which a signal in time domain t , $f(t)$ is represented in the frequency domain ω , $f(\omega)$, is widely used in all branches of science. The power spectrum of a times series gives the distribution of the power as a function of the component frequencies. For a periodic sequence, or a regular time series, it consists of finite number of frequency components in a given frequency range. But the power spectrum of an irregular time series will contain an infinite number of frequencies. The power spectrum is widely used as a first test for chaotic behavior. Due to the irregular nature of the dynamics, the power spectrum of a chaotic time series will be broad. Usually there can be significantly high power distributions corresponding to some frequencies. This corresponds to the characteristic frequencies of the system. Figure 1.7 shows the time series and power spectrum of a Lorenz system with $\rho = 150.35$, where it is periodic. It can be seen that the majority of power is distributed within a few frequencies. In figure 1.8, the time series of a chaotic Lorenz system and its power spectrum is given. The broad power spectrum is a signature of chaotic behavior. However, chaotic behavior can only be confirmed after calculating the Lyapunov

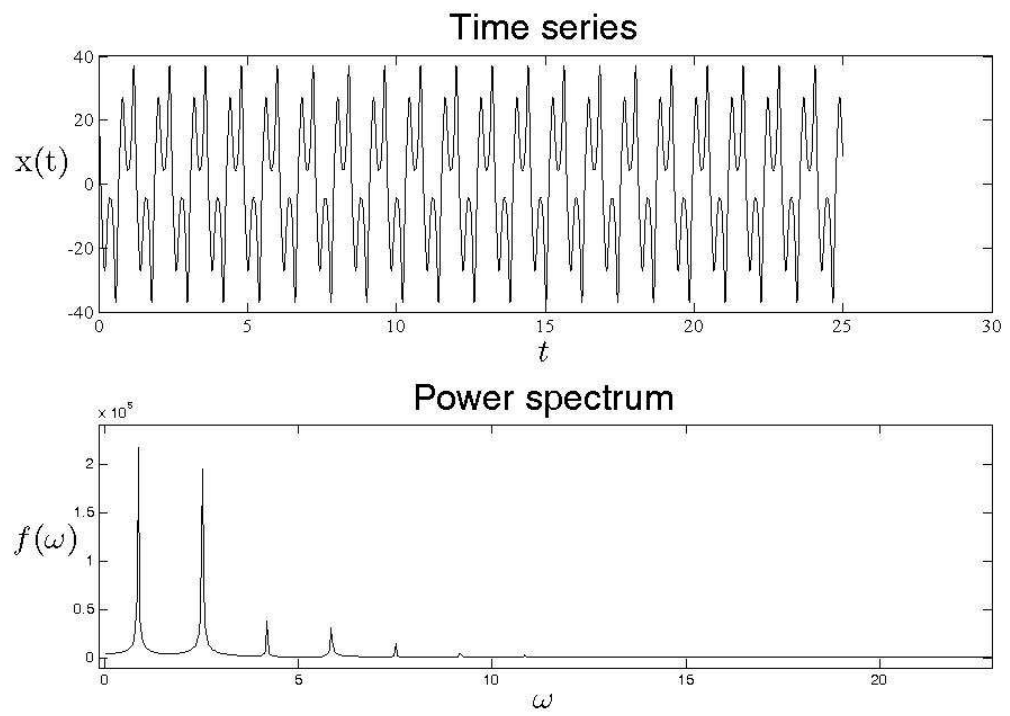


Figure 1.7: The time series and power spectrum of a periodic Lorenz system.

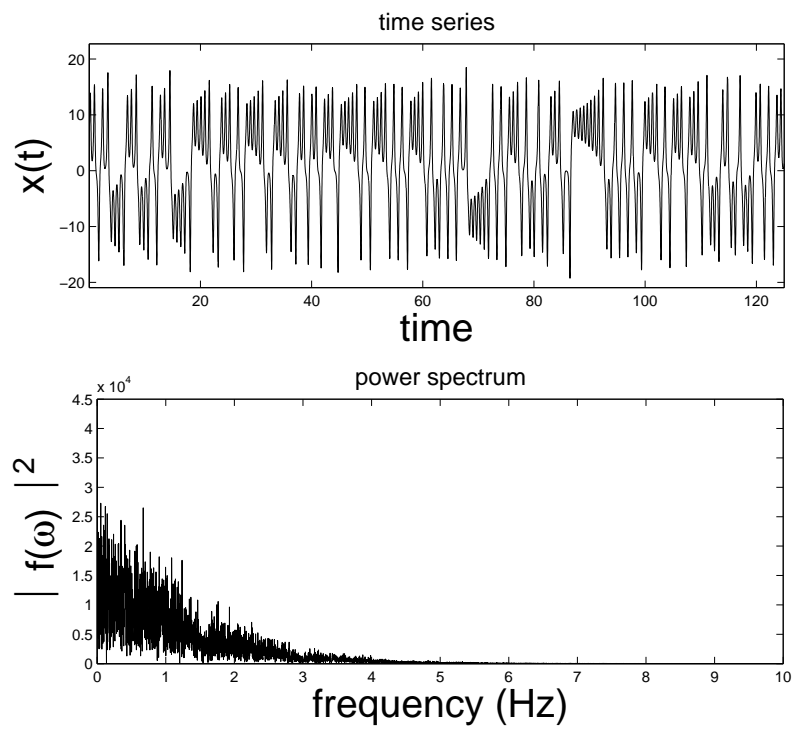


Figure 1.8: The time series and power spectrum of a chaotic Lorenz system.

exponents.

1.8 Lyapunov exponents

The most important feature of chaotic dynamics is its *sensitivity to initial conditions*. Trajectories that start with small differences in the initial conditions diverge exponentially. Mathematically, the divergence of trajectories (see figure 1.9) of two flows which differ in the initial conditions by an amount ΔX , which can be written as,

$$\Delta X(t) = \Delta X(0) \exp(\lambda t) \quad (1.8.1)$$

where λ is the Lyapunov exponent which determines how fast the separation between two such trajectories converge or diverge. One can calculate the rate of exponential divergence or the Lyapunov exponents from this equation, but not used in practice because of two reasons. One is that here λ depends on the initial conditions and another reason is that the arbitrarily chosen trajectories may not belong to the attractor.

Lyapunov exponents as an invariant measure of the divergence of an attractor are obtained by the Wolf's algorithm [19]. There the divergence is calculated by the evolution of a linearized system corresponding to an actual system. The error vectors that evolves according to the linearized dynamical equations undergo stretching and folding in chaotic flow. The rate of divergence is calculated as the ratio of initial and final norms. The error vectors are normalized after the calculation of the norm. The process repeats and the Lyapunov exponents are obtained by dividing the average rate of divergence by the time of evolution. This method can be extended to delay differential equations by approximating them to finite dimensional maps [20]. Delay differential equations arise if the dynamics involves a delay feedback.

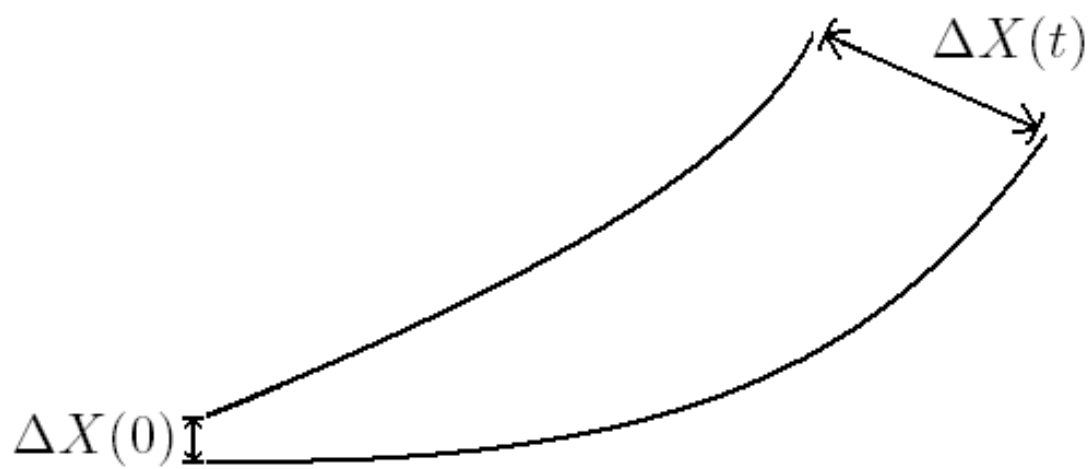


Figure 1.9: The trajectories that start with small errors diverge in course of the evolution.

1.9 Attractors and dimensions

A dynamical system starts its evolution in the phase space with some initial conditions. In most of the cases the initial conditions may not be on the phase space trajectory on to which a system would eventually settle down. Asymptotically, the trajectories are "attracted" to a bounded region in phase space, called attractors, which are of lower dimension which is a subset of the phase space.

Attractors in the phase space are associated with a characteristic dimension. This is defined according to the density distribution of the points in the phase space that a chaotic trajectory visits. Two important dimensions that are used in chaos theory are the *capacity dimension* and *correlation dimension* [6, 7, 8, 9, 10]. The capacity dimension is related to the scaling properties of the attractor, or the way the attractor fill the phase space. The correlation dimension is related to the local inhomogeneity of the attractor, that is the frequency of the visits of the trajectory to a region in phase space.

A fixed point in phase space is a zero dimensional attractor. A periodic limit cycle have dimension one and for a quasiperiodic torus having two frequencies have the dimension two. Attractors resulting from chaotic time evolution possess non integer dimension and are called strange attractors. This comes from the fact that the system does not visit every region of the phase space. The regions that come under the span of the phase space varies in frequency of the trajectory visits in an irregular but a systematic way. However, certain non chaotic attractors can also be strange [21].

1.10 Routes to chaos

The routes to chaos are usually referred to the sequence of intermediate states when a system transforms from one of the stable states to a chaotic state under parameter variation. Most common route is the period doubling route. The period of the

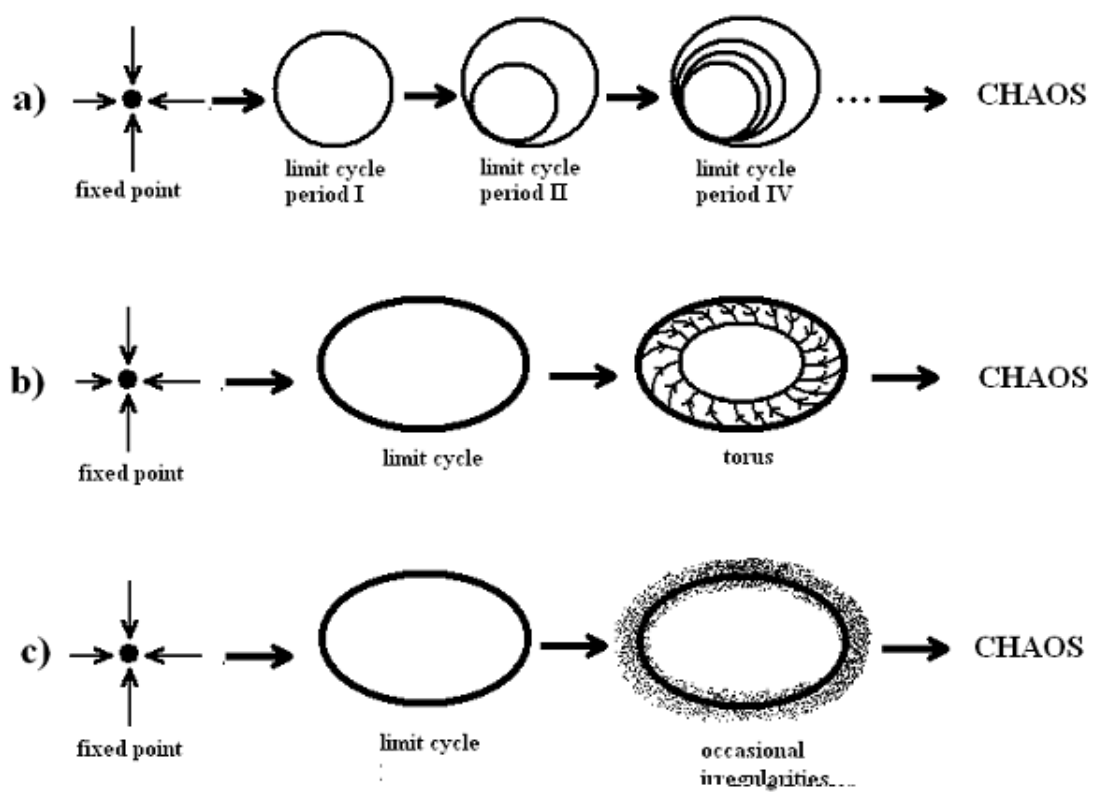


Figure 1.10: Routes to chaos: (a) period doubling route (b) quasiperiodicity route (c) intermittency route.

oscillations doubles as the parameter is varied and it undergoes a succession of such period doublings and it reaches a state where the period is infinite, that is a chaotic state. Another route is the breaking of a quasiperiodic torus in phase space. In some systems, the transition to chaos is preceded by short irregular interruptions in the periodic behavior. Such a transition to chaos from a stable state is called the intermittency route. In addition to this, there are other routes, but is uncommon. In figure 1.10 a schematic representation of the main routes to chaos are shown.

1.11 Unstable periodic orbits

In the previous section we have seen that the transition to the chaotic state involve a sequence of periodic states. A system in the chaotic state can still have periodic orbits that are hidden in irregularities. Let,

$$x_{n+1} = f(x_n) \tag{1.11.1}$$

be a discrete map. Consider x^* such that $f(x^*) = x^*$, that is a point that get mapped to itself. Such a point represents a periodic oscillation of the system. One can actually calculate periodic orbits by solving the equation.

$$f(x^*) - x^* = 0. \tag{1.11.2}$$

The orbit corresponding to x^* may be stable or unstable according to the derivative of $f(x)$ evaluated at x^* ,

$$\left. \begin{array}{l} \left| \frac{df(x)}{dx} \right| < 1 \text{ stable} \\ \left| \frac{df(x)}{dx} \right| > 1 \text{ unstable.} \end{array} \right\} \tag{1.11.3}$$

In the chaotic regime, all the periodic orbits are unstable. The system continues in a periodic orbit if the initial conditions are on a periodic orbit and if no external perturbations occur. But this is not possible always due to the limited precision of the computing device. In an actual physical system, small perturbations or noise

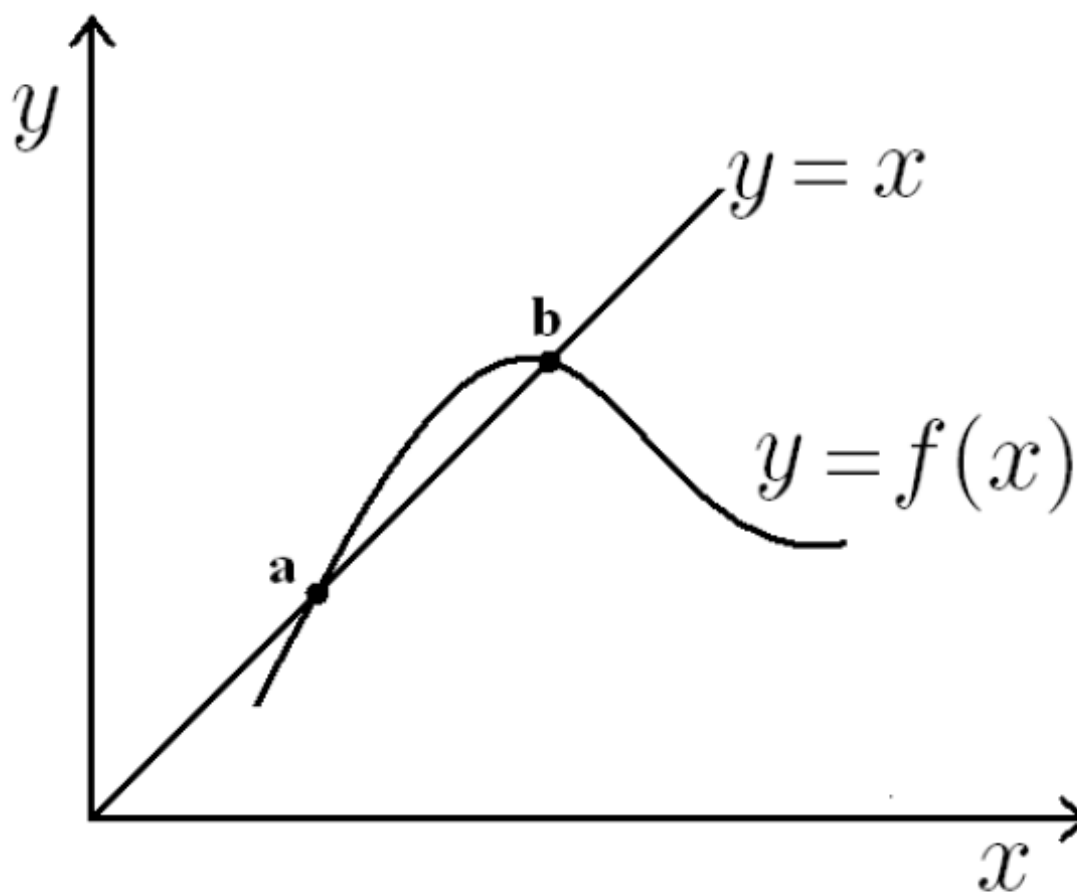


Figure 1.11: Periodic orbits as the intersection of $y = x$ line to the mapping functions. The point a represents an unstable periodic orbit with $\left| \left(\frac{df(x)}{dx} \right)_{x=a} \right| > 1$ and the point b represents a periodic orbit as $\left| \left(\frac{df(x)}{dx} \right)_{x=b} \right| < 1$.

always affect the dynamics and it is difficult if not impossible to maintain a totally error free dynamics in reality.

Unstable periodic orbits(**UPOs**) are highly significant in determining the nature of the chaotic dynamics occurring in a system. Many invariant parameters of a chaotic system can be extracted from **UPOs** [22]. In addition to this, stabilization of a **UPO** can also suppress chaotic behavior [23] with a delayed feed back. Also this is one of the most widely used methods to control chaos in a variety of systems.

1.12 Synchronization of Chaos

Synchronization[24] in physical systems has been known for three centuries. Christian Huygens in 1665 noted that two clocks hanging from the same support leads to the synchronization of their pendulums. Synchronization, in one form or another is present in many of engineering and physical problems [11, 26, 27, 25, 24].

It sounds incredible that chaotic systems, which evolve unpredictably and irregularly can be synchronized. However, Yamada and Fujisaka[25] and Pecora and Carol [26, 27] have shown that this is possible. Synchronization of chaotic systems is now one of the hottest areas of research in physics and in other fields. It finds direct application in chaotic encryption-based cryptographic schemes, which is widely used in secure communication[11]. Apart from technological applications, synchronization is one of the highly successful attempt to understand organized behavior in nature [24].

1.12.1 Coupling schemes

The most common method used for synchronization is to couple two such chaotic systems. The coupling can be unidirectional or bidirectional. In a unidirectional coupling, one of the systems is left to evolve on its own and the dynamics of the other is modified so as to achieve synchronization. In bidirectionally coupled systems, the

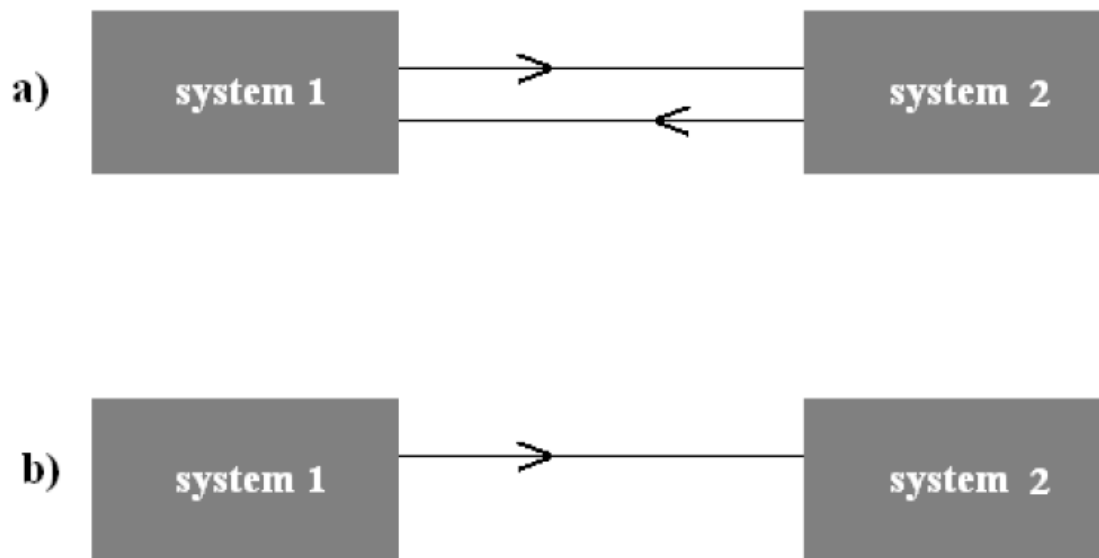


Figure 1.12: (a)bidirectional coupling, (b) unidirectional coupling.

mutual coupling modifies the dynamics of both of the systems so as to maintain synchrony. In fig. 1.12 unidirectional and bidirectional coupling schemes are illustrated. Mathematically such coupling can be expressed as,

$$\begin{aligned}\dot{X} &= f(X) + C\Phi_{x,y}(X, Y) \\ \dot{Y} &= f(Y) + C\Phi_{y,x}(X, Y)\end{aligned}\tag{1.12.1}$$

where $X = (x_1 \ x_2 \dots x_n)^T$, $Y = (y_1 \ y_2 \dots y_n)^T$, and $\Phi(X, Y) = (\phi_1(x, y) \ \phi_2(x, y) \dots \phi_n(x, y))^T$ are the vectors and the coupling functions that define the evolution. The coupling functions can be any function of the phase space variables. The method that is most

commonly used for synchronization is a diffusive coupling, where the coupling function is simply the difference between any of the two similar variables of the coupled system. The final mathematical form of such a coupled evolution can be,

$$\begin{aligned}
 \dot{x}_1 &= f_1(p_1, p_2, \dots, p_m, x_1, x_2 \dots x_k) \\
 \dot{x}_2 &= f_2(p_1, p_2, \dots, p_m, x_1, x_2 \dots x_k) \\
 &\cdot \quad \cdot \\
 \dot{x}_m &= f_m(p_1, p_2, \dots, p_m, x_1, x_2 \dots x_k) + c_{x,y}(y_m - x_m) \\
 &\cdot \\
 &\cdot \quad \cdot \\
 \dot{x}_k &= f_k(p_1, p_2, \dots, p_m, x_1, x_2 \dots x_k) \\
 \dot{y}_1 &= f_1(p_1, p_2, \dots, p_m, y_1, y_2 \dots y_k) \\
 \dot{y}_2 &= f_2(p_1, p_2, \dots, p_m, y_1, y_2 \dots y_k) \\
 &\cdot \quad \cdot \\
 \dot{y}_m &= f_m(p_1, p_2, \dots, p_m, y_1, y_2 \dots y_k) + c_{y,x}(x_m - y_m) \\
 &\cdot \quad \cdot \\
 &\cdot \quad \cdot \\
 \dot{y}_k &= f_k(p_1, p_2, \dots, p_m, y_1, y_2 \dots y_k)
 \end{aligned} \tag{1.12.2}$$

here, $c_{x,y}$ and $c_{y,x}$ are appropriately chosen coupling strengths. In a unidirectional coupling scheme, either $c_{x,y}$ or $c_{y,x}$ is zero. One of the main advantages of this type of diffusive coupling is that the dynamics of the coupled systems are affected only according to its deviation from synchrony. In a perfectly synchronized state, the perturbations vanish. We mainly focus on this coupling scheme in the present thesis.

1.13 Types of synchronization

The nature of the synchronization between two coupled systems depends on various dynamical aspects. The most important are: the extent to which the systems are identical and the coupling strength.

1.13.1 Perfect or Exact synchronization

Consider two chaotic systems represented by $X(t)$ and $Y(t)$, which are coupled in any of the coupling scheme. If $|X(t) - Y(t)| \rightarrow 0$ as $t \rightarrow \infty$, the synchronization is said to be Exact Synchronization or Perfect Synchronization. The stability of such a synchronized state is determined by Transverse Lyapunov Exponents (**TLE**) introduced by Pecora and Carol [28]. Transverse Lyapunov exponents are Lyapunov exponents in the direction normal to the synchronization manifold $X(t) = Y(t)$ [28].

1.13.2 Phase and Lag synchronization

Defining a phase for chaotic oscillations is not as straightforward as in regular oscillations. However, using Hilbert transform, the phase of Chaotic oscillations can be derived from a given time series. A weak entrainment between two coupled chaotic system may lead to their phase difference to be within a small, well defined constant. Such a phenomenon is called Phase Synchronization [29]. It usually happens if the coupling strength is low or the systems are not identical, even if coupling strength is appreciable. Coupled nonidentical chaotic oscillators with high coupling strength leads to Lag Synchronization. Lag Synchronization refers to the case where the synchronization occur with a time lag between the two systems [30].

1.13.3 Generalized Synchronization

In some situations, even though the behavior of the coupled systems are not identical, a functional relationship can be established between them. Such a phenomenon is

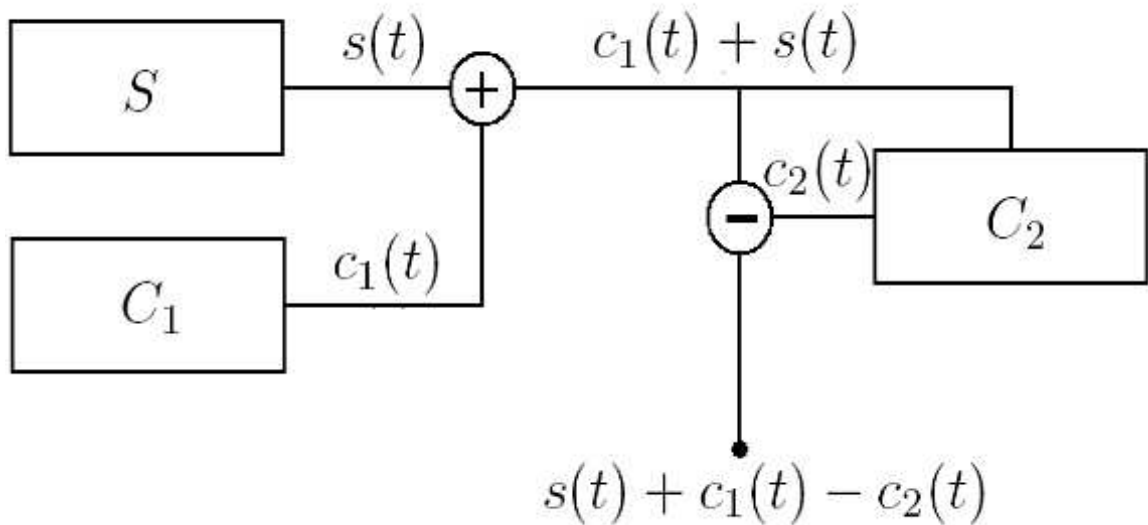


Figure 1.13: Schematic diagram of a secure communication scheme.

called Generalized Synchronization [31].

1.14 Secure communication using Chaos

Consider two chaotic systems C_1 and C_2 whose outputs are $c_1(t)$ and $c_2(t)$ respectively and are synchronized to due a coupling. Let S be the source which produce the signal $s(t)$ that has to be communicated. The signal is mixed with the chaotic oscillations in low amplitudes and is transmitted through the communication channel. At the receiving end, $c_2(t)$ is subtracted from the incoming signal which gives $s(t) + c_1(t) - c_2(t)$. In an ideally synchronized case $c_1(t) = c_2(t)$, and the signal is retrieved with high fidelity. Due to the fact that the parameter values of the chaotic systems used for encryption is kept secret, an eavesdropper is unable to synchronize his system with the transmitter and will never get the transmitted data with any reasonable fidelity. Thus chaotic encryption can provide reasonable security needed for data transmissions in reality. Now, is this method cent percent secure ? The answer is no. But that is equally true with all cryptographic schemes.

Though chaotic encryption schemes are demonstrated successfully, both numerically and experimentally, it is still far away from being implemented commercially. One of the main reasons is the sensitivity of a chaotic state to external perturbations. Signal which is transmitted through a communication channel is affected by noise before it reaches the receiving end. Also the parameters of the system can change considerably according to the changes in the environment. This induce mutual parameter mismatches that damage synchronization. Thus the practical implementation of chaotic encryption based cryptographic schemes require many of these issues to be addressed.

1.15 Conclusion

We have introduced the basic concepts regarding chaos theory and synchronization of chaotic systems. Also we have discussed the basic computational tools that are used in chaos theory.

Bibliography

- [1] U. Feudel, C. Grebogi, B. R. Hunt and J. A. Yorke, Phys. Rev. E **20**, 71, (1996)
- [2] U. Feudel, C. Grebogi, CHAOS 20, 597, 1997.
- [3] A. P. Kanjamala and A. F. J. Levi, Appl. Phys. Lett 72, 2214, 1998.
- [4] R. Kapral, Phys. Rev. A 31, 3868, 1985.
- [5] E. N. Lorenz, Journal of the Atmospheric Sciences 20, 130 1963.
- [6] E. Atlee Jackson, Perspectives of Nonlinear Dynamics, Cambridge University Press, New York 1991.
- [7] J. Guckenheimer and P. Holmes, Nonlinear Oscillations, Dynamical System, and Bi- furcations of Vector Fields, Springer - Verlag, New York 1983.
- [8] E. Ott, Chaos in dynamical system, Cambridge University Press 2002
- [9] S. Neil Rasband, Chaotic Dynamics of Nonlinear Systems, Wiley Interscience, New York 1997.
- [10] J. C. Sprott, *Chaos and Time-series analysis*, Oxford University Press, Oxford, 2003.
- [11] K. Cuomo and A. V. Oppenheim, Phys. Rev. Lett. 71, 65 1993.
- [12] S. Sinha and R. Ramaswamy, BioSystems 20, 341 1987.

- [13] Heinz G. Schuster (ed) *Chaos Control in Biological Systems*, Wiley-VCH Verlag GmbH 1999.
- [14] *Chaos in Biological Systems*, Proceedings of a NATO ARW held at Duffryn House, Cardiff, Wales, December 8-12, 1986, Degn, Hans; Holden, Arunn V.; Olsen, Lars Folke (Eds.)
- [15] Becks L, Hilker FM, Malchow H, Jurgens K and Arndt H, : *Nature*, 435(7046):1226, 2005.
- [16] P. Akritas et al, *Chaos, Solitons & Fractals* 14, 595, 2002.
- [17] R. M. May, *Nature* 261, (5560):459, 1976
- [18] S. H. Strogatz, *Nonlinear Dynamics and Chaos: With Applications to Physics, Biology, Chemistry and Engineering*, Perseus Books Group, New York, 2001.
- [19] A. Wolf, J. B. Swift, H. L. Swinney and J. A. Vatsano *Physica D* 16, 285, 1985.
- [20] J. D. Farmer, *Physica D*, 366 1982.
- [21] F. Romieras and E. Ott , *Phys. Rev. A* 35, 4404, 1987.
- [22] D. Auerbach, et. al., *Phys. Rev. Lett.* 8, 2387 1990.
- [23] K. Pyragas, *Phys. Lett. A* 170, 421, 1992.
- [24] A. Pikovsky, M. Rosenblum, J. Kurths, *Synchronization: A Universal Concept in Nonlinear Sciences* Cambridge, UK: Cambridge University Press, 2001
- [25] T. Yamada and H. Fujisaka, *Prog. Theor. Phys.* 70, 1240, 1983.
- [26] L. M. Pecora and T. L. Carroll, *Phys. Rev. Lett* 64, 821, 1990.
- [27] T. L. Carroll and L. M. Pecora, *IEEE Trans. Circuits Syst.* 38 II, 453, 1991.

- [28] Louis M. Pecora, Thomas L. Carroll, Gregg A. Johnson, and Douglas J. Mar, Chaos 7, 520, 1997.
- [29] M. G. Rosenblum and A. S. Pikovsky and J. Kurths, Phys. Rev. Lett. 76, 1804, 1995.
- [30] M. G. Rosenblum, A. S. Pikovsky and J. Kurths, Phys. Rev. Lett. 78, 4193, 1997.
- [31] Kocarev and U Parlitz, Phys. Rev. Lett. 76, 1816, 1996.

Chapter 2

Randomness in synchronization and chaos

2.1 Introduction

Chaos and synchronization are two well understood notions in nonlinear dynamics, but the term randomness is a much more general notion and its interpretation can be ambiguous. In this chapter, we introduce the concept of randomness that we have used in the present work. We first introduce noise, i.e. we discuss two of the most familiar kind of noises and discuss how they are classified and represented. Then we introduce the concept of randomness as a variant of the concept of noise. In addition to this, we also give a brief introduction of the dynamical systems that we have employed in our studies.

2.2 White and coloured noise

Noise in actual dynamical systems originates as the result of some physical processes. For example, the thermal noise which originates as the result of the agitation of the

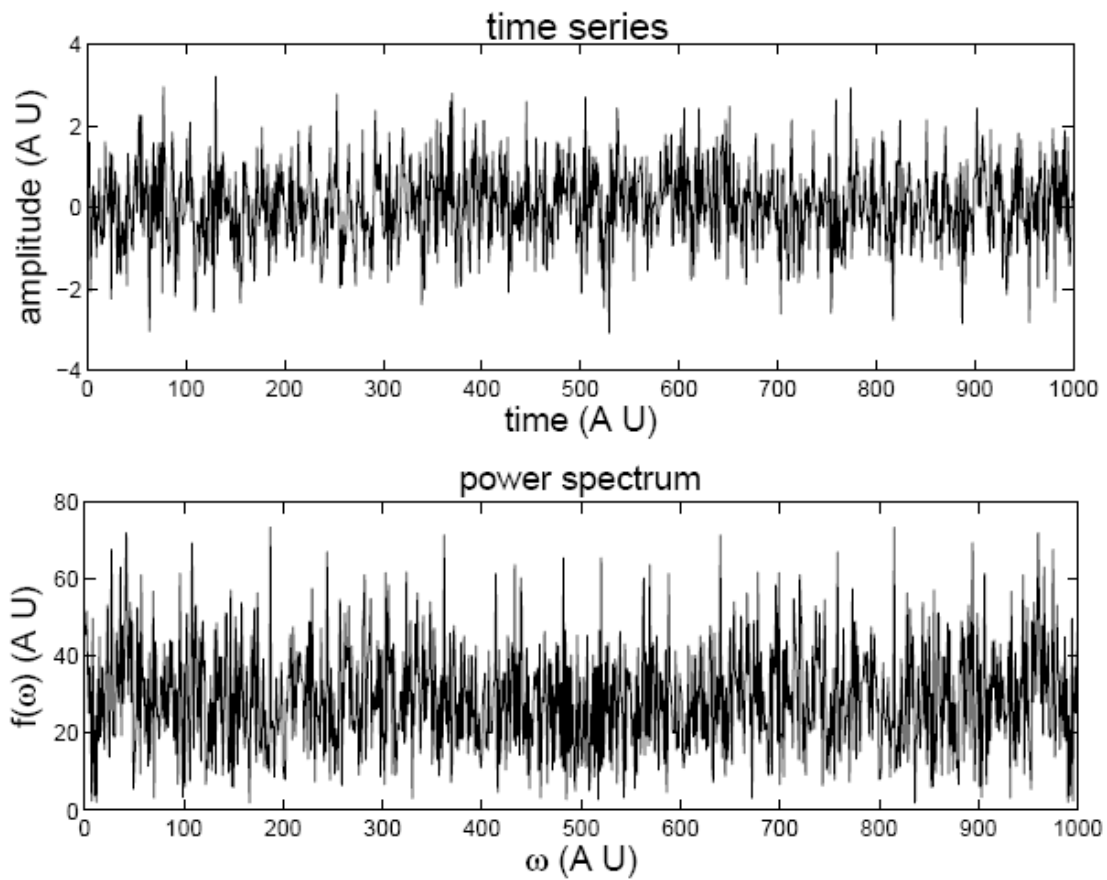


Figure 2.1: The time series and frequency spectrum of white noise.

charge carriers in a conductor. On the basis of the fourier spectrum, noise is classified mainly into two categories: the white noise and the coloured noise.

2.2.1 White noise

If the amplitudes of all the frequency components of a noise are uniform, it is called white noise. In fig 2.1 the time series and the power spectrum of a white noise source are shown. It can be seen that all the components have identical amplitudes and the fluctuations about zero are frequent. Also no typical trend can be found in these

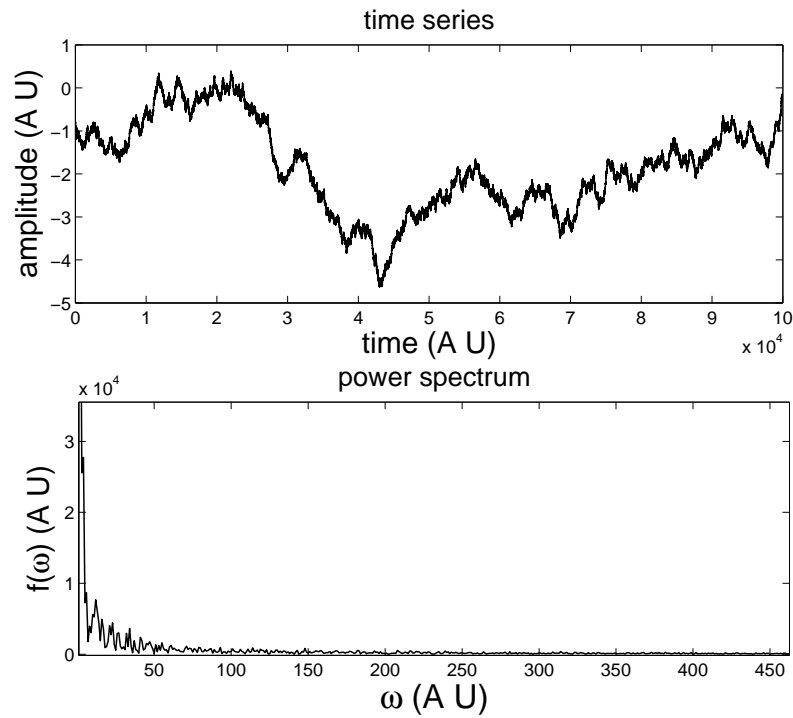


Figure 2.2: The time series and frequency spectrum of coloured noise.

fluctuations.

2.2.2 Coloured noise

The most familiar form of coloured noise resembles the time series of a random walk. Figure 2.2 shows the timeseries and the power spectrum of a colored noise source. It can be seen that the time series is irregular and the power spectrum is inhomogeneous with relatively high amplitudes for the lower frequencies. Time series of the colored noise shows local trends, which can be interpreted as the system retaining some memory about its past. This leads to short range temporal correlations.

2.2.3 Correlations in time

The correlations in time is an important factor when considering the features of a noise source. Such correlations decide the effect of the fluctuations on the dynamics [1]. The correlations in time for white noise dies out very quickly. The correlation function for white noise can be expressed as

$$\langle \xi(t)\xi(t_1) \rangle = 2D\delta(t - t_1) \quad (2.2.1)$$

Here D is the strength of the noise.

Colored noise possess correlations that decay slowly and is exponential in most of the cases. The relation,

$$\langle \xi(t)\xi(t_1) \rangle = 2D\lambda \exp(-\lambda |t - t_1|) \quad (2.2.2)$$

gives the correlation in time for coloured noise.

2.2.4 When is a noise considered delta correlated ?

At this point, one should ask the question, can a fluctuating quantity be really delta correlated. In reality there exist no fluctuation that is totally uncorrelated to any of the previous instances, because all such perturbations arise as a result of some physical process. But, If the correlation time is much less compared to any characteristic timescale of the system under consideration, it is considered to be delta correlated. For example in equation 2.2.2 $\lambda \rightarrow \infty$ represents a delta correlated noise.

2.2.5 Fluctuations with large timescales and randomness

When the timescales or the correlation time associated with the fluctuations is very large, the features of the fluctuation become more pronounced in the dynamics as casual random modifications. In this situation, many estimates regarding the effect of perturbations can be made without strict statistical considerations. For example,

the effect of fluctuations in phase on the coherence properties of a monochromatic wave [2] assumes the fluctuations to be associated with large timescales. In the present work we study random fluctuations with time scales much higher than that of the systems under consideration.

2.3 Systems under consideration

In this section we discuss the basic systems that we have used in our investigations. We introduce the Rossler attractor, Directly modulated semiconductor laser and the Driven damped harmonic oscillator.

2.3.1 Rossler Attractor

Coupled Rossler systems are one of the most widely used dynamical systems in the study of synchronization. Rossler systems gained popularity mostly due to its simplicity, its ability to synchronize, simplicity and the interesting nature of the results obtained. The Rossler system is represented by the dynamical equations,

$$\begin{aligned} \dot{x} &= -y - z \\ \dot{y} &= x + 0.18y \\ \dot{z} &= 0.2 + z(x - 10) \end{aligned} \tag{2.3.1}$$

The phase space trajectory of the system is given in figure 2.3. This system exhibits both chaotic and periodic behavior according to the values of the parameters.

The exact synchronization of coupled Rossler systems is widely discussed in [4].

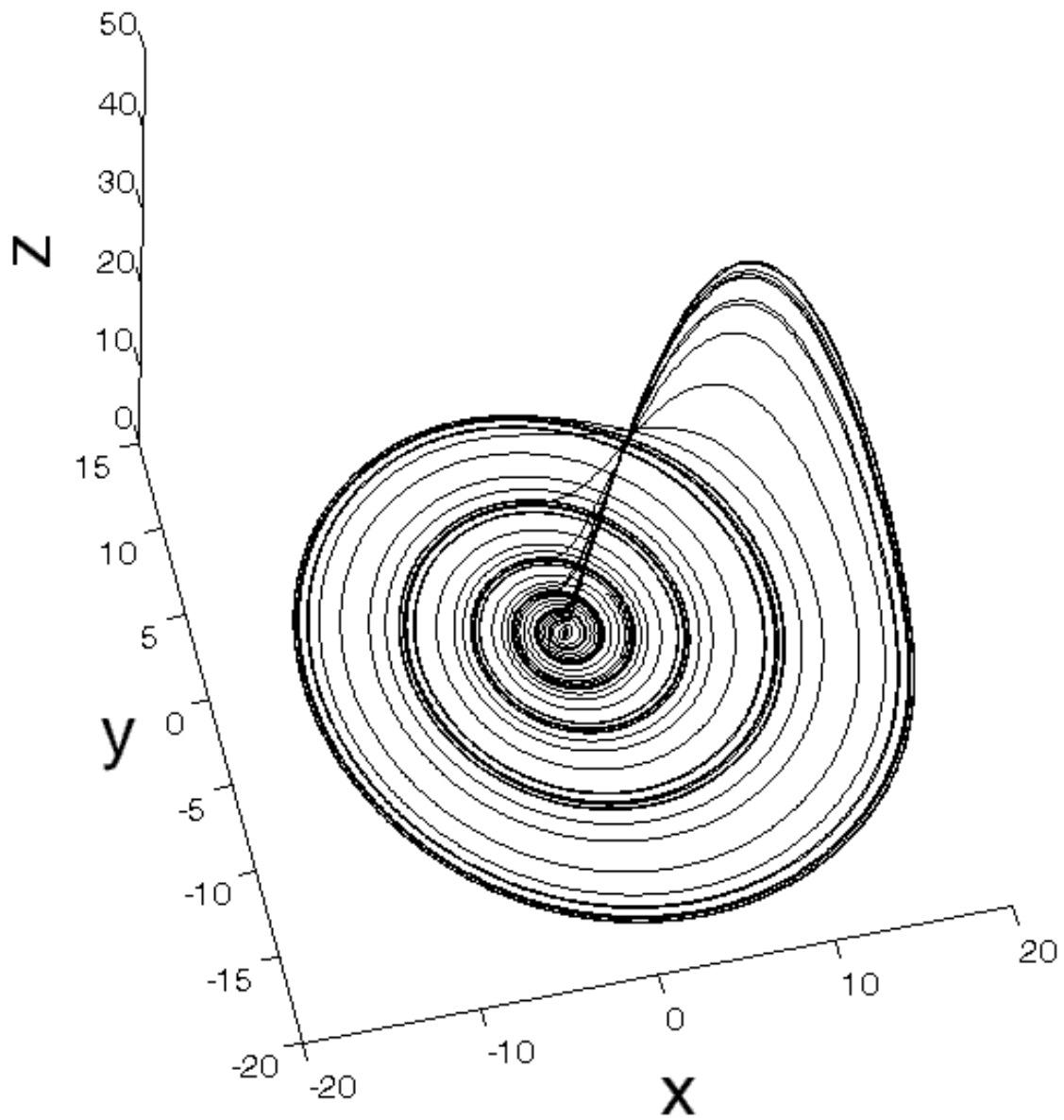


Figure 2.3: The phase space of the Rossler oscillator.

Rossler oscillators coupled diffusively can be represented as follows,

$$\begin{aligned}\dot{x}_{1,2} &= -y_{1,2} - z_{1,2} \pm \alpha(x_{2,1} - x_{1,2}) \\ \dot{y}_{1,2} &= x_{1,2} + p_{1,2}y_{1,2} \\ \dot{z}_{1,2} &= 0.3 + z_{1,2}(x_{1,2} - 10).\end{aligned}\tag{2.3.2}$$

The synchronization of two coupled chaotic systems is usually illustrated by synchronization plots wherein two of the corresponding variables of the coupled systems are plotted against each other. Exact synchronization will give the typical $y = x$ line, and deviations from exact synchrony can easily be identified as the deviation from this pattern. The synchronization plot corresponding to $c = 0.3$ for the diffusively coupled Rossler oscillators is shown in figure 2.4. It can be seen that the behavior the variables x_1 and x_2 are identical in time. But synchronization is destroyed with a lower coupling strength $c = 0.1$, as shown in figure 2.5. Stability of synchronization can be determined by Conditional Lyapunov Exponents (**CLE**). The stability of the synchronized states of Rossler systems in terms **CLE** is given in [4]. It is shown that the coupled Rossler systems with identical parameter values give stable synchronization for a wide range of coupling strengths. The coupling strength c ranges from 0.25 to 1.4 and the most stable synchronization is achieved around 0.9. In coupled Rossler systems, exact synchronization is impossible if the parameter values are not identical. On increasing the coupling strength, phase synchronization occurs and with further increase in coupling strength the systems attain a state of lag synchronization[3].

2.3.2 Harmonic Oscillator

The harmonic oscillator is an oscillator whose frequency is independent of the amplitude and initial conditions. Not all oscillators are harmonic oscillators. For example, consider a simple pendulum, which is almost harmonic when the amplitude is low. But for higher amplitudes, the frequency depends on the amplitude. Interestingly the

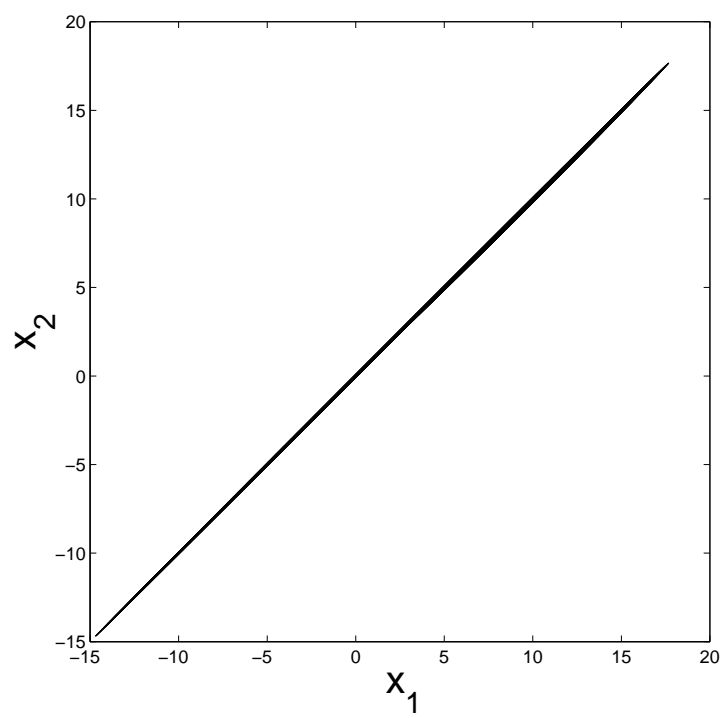


Figure 2.4: Synchronization plot for a coupled system with a high coupling strength.

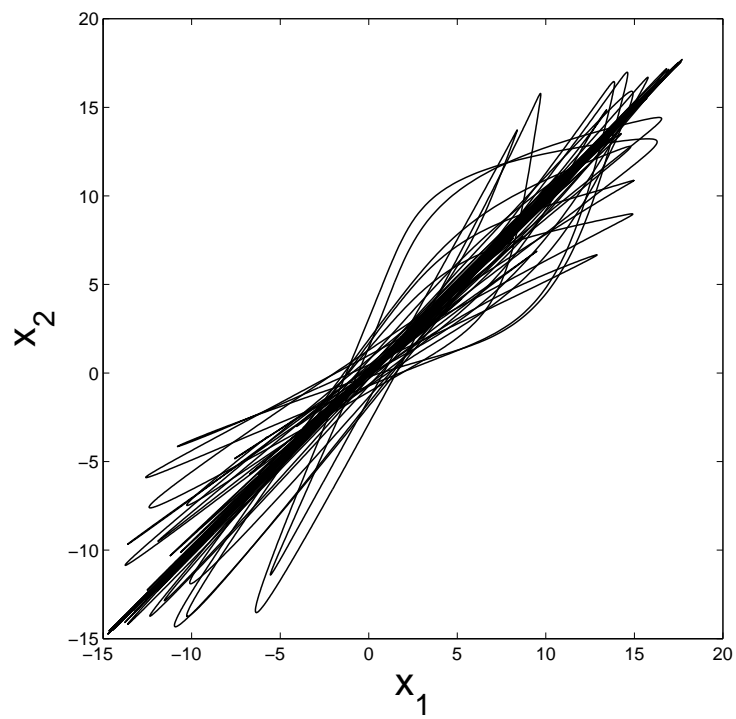


Figure 2.5: Synchronization plot for a coupled system with a low coupling strength.

frequency can be infinite for the highest amplitude as shown in figure 2.6.

The most common examples of harmonic oscillators are the spring-mass system and an **LCR** circuit shown in figure 2.7. In the spring-mass system, a mass which is allowed to slide on a plane is attached to a spring whose one end is fixed. The harmonic oscillations arise in the **LCR** circuit as a result of the oscillations of the charge that is stored in the capacitor. We focus on the spring mass system because it is more suitable from a mechanical point of view. The dynamical equation of a spring-mass system can be written as,

$$\frac{d^2x}{dt^2} + \Omega^2x = 0 \quad (2.3.3)$$

Here, Ω represents the angular frequency of the drive. A general solution to this equation can be written as,

$$x(t) = A \sin \Omega t + \Phi \quad (2.3.4)$$

where Φ is the initial phase of the oscillator. The position and momentum oscillate sinusoidally with a mutual phase difference of $\frac{\pi}{2}$. This results in a circular phase space trajectory as shown in figure 2.8.

In reality all oscillators are associated with damping. The equations of motion of such oscillators also include a damping and driving terms in addition to the quantities present in equation 2.3.3.

The dynamical equation of the damped driven harmonic oscillator is given by,

$$\frac{d^2x}{dt^2} + \gamma \frac{dx}{dt} + \Omega^2x = a \sin(\omega t) \quad (2.3.5)$$

Here, γ , Ω and ω represents the damping coefficient, the angular frequency of the oscillator and the angular frequency of the drive respectively. The term a represents the amplitude of the forcing. The behavior in time, after the transients have vanished can be represented by the equation,

$$x(t) = \frac{a}{\sqrt{(\omega^2 - \Omega^2)^2 + \gamma\omega^2}} \sin(\omega t - \delta) \quad (2.3.6)$$

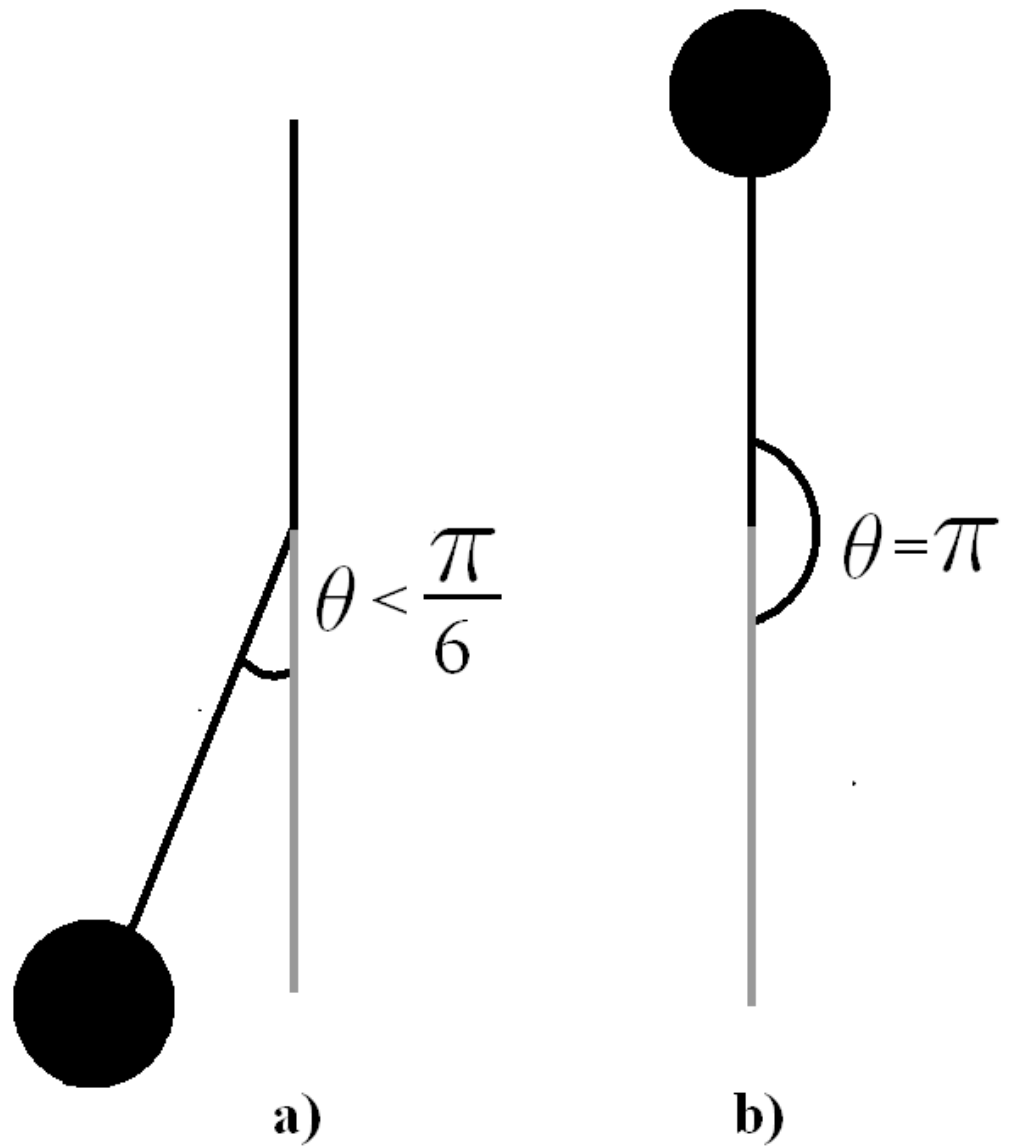


Figure 2.6: Dependence of the frequency on the amplitude in the case of a simple pendulum. a) the frequency is almost independent of the amplitude. b) the frequency can be zero for some initial conditions.

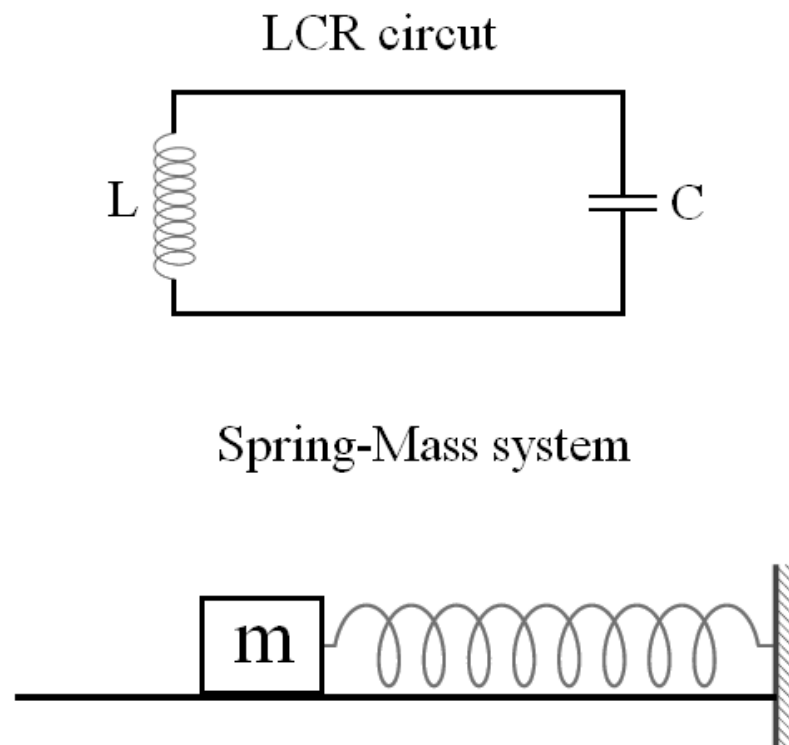


Figure 2.7: Examples of harmonic oscillators: the LCR circuit and spring mass system.

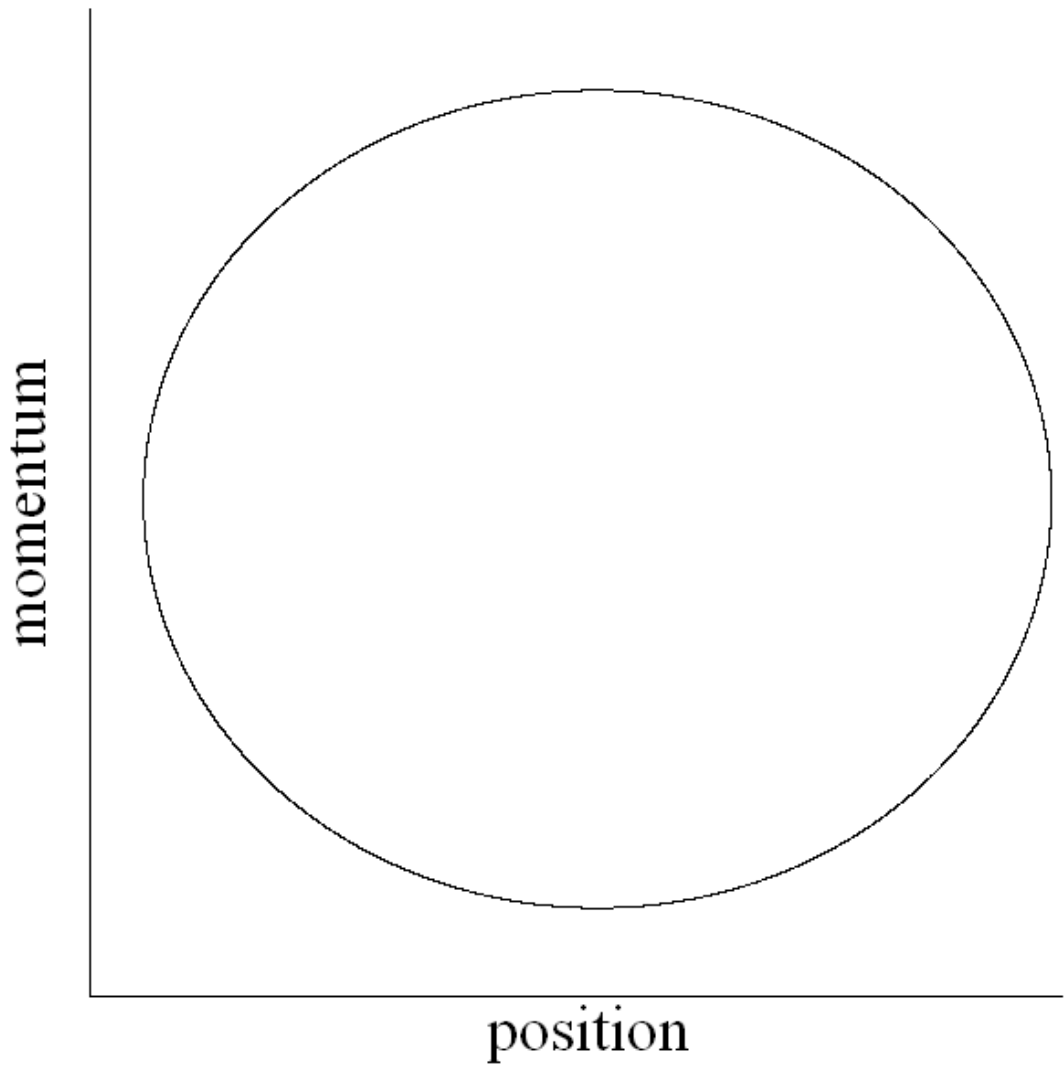


Figure 2.8: The phase space trajectory of a harmonic oscillator.

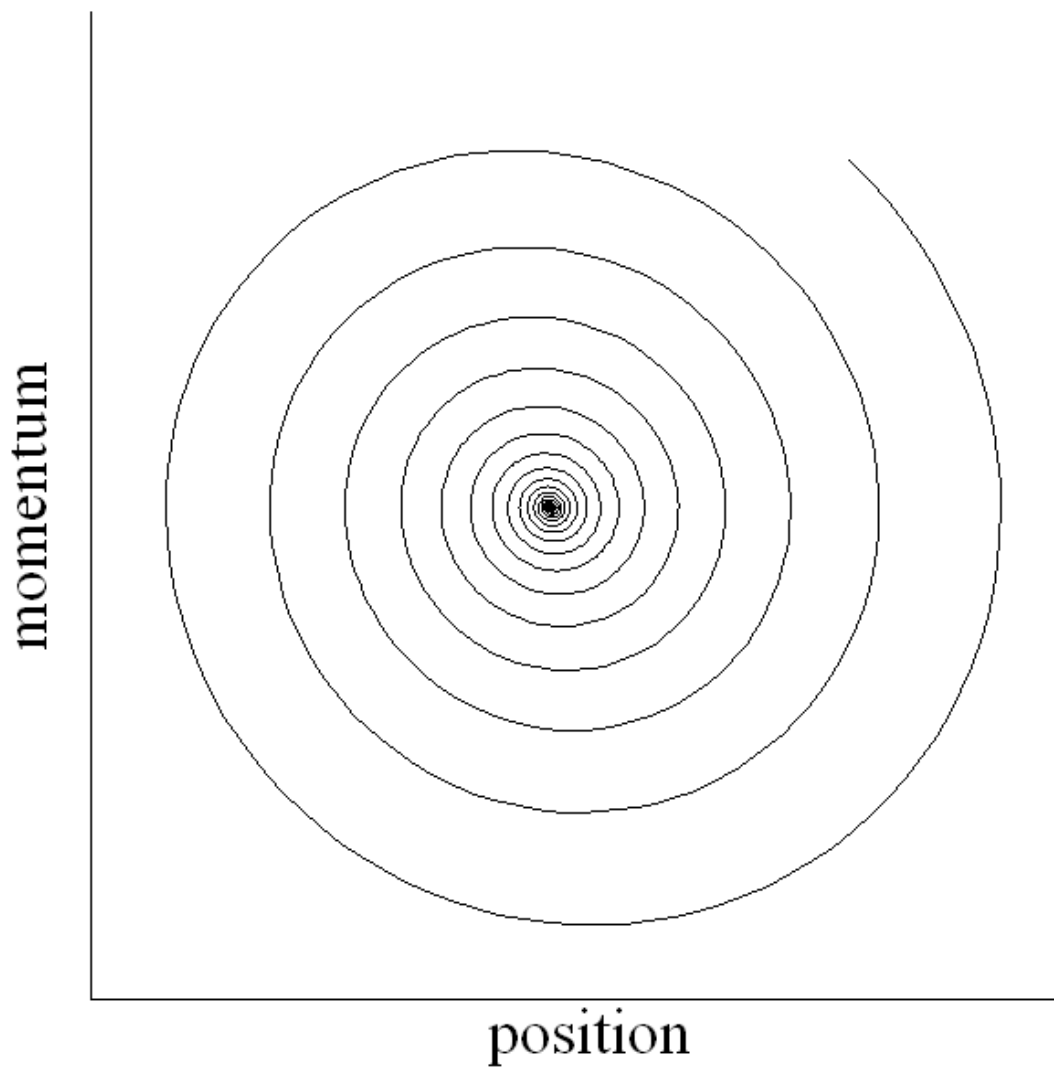


Figure 2.9: When not driven, the trajectories of a harmonic oscillator spirals down to a fixed point in the position-momentum space.

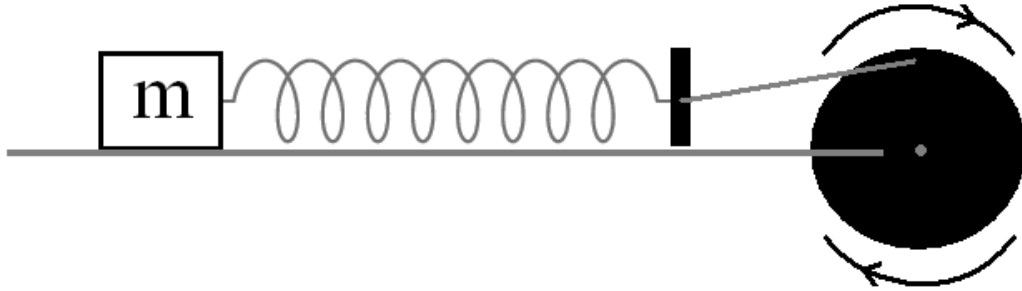


Figure 2.10: Schematic diagram of a mechanical driven harmonic oscillator.

The term δ represents the phase difference between the drive and the oscillator, which is equal to $\tan^{-1} \frac{\gamma\omega}{\Omega^2 - \omega^2}$. When not driven, or with $|a| = 0$, the system spirals down to a fixed point in the position momentum space. This is illustrated in figure 2.9.

A physical realization of this is shown in figure 2.10. Here the end of the spring is connected to a moving rotating disc in order to realize the driving modulations. An interesting mathematica demonstration of this is also available [5].

2.4 Directly modulated semiconductor lasers

Study of chaotic dynamics of semiconductor lasers have received much attention in the past few decades due to the applicability of chaotic synchronization of such systems in the field of optical secure communication [6, 7, 8, 9, 10, 11, 12, 13]. Semiconductor lasers are generally very stable systems when operated with only a dc bias current. However, instabilities are induced in their dynamics by the inclusion of additional degrees of freedom. The different methods proposed for producing chaotic outputs are giving external optical injection [14, 15, 16, 17], giving optical feedback [18, 19, 20],

direct GHz current modulation [21, 22, 23, 24, 25, 26, 27, 28] and giving delayed optoelectronic feedback [29, 30, 31, 32, 33]. Positive delayed optoelectronic feedback is the conventional method of generating ultra-short pulses [34] from semiconductor lasers. The dynamics of semiconductor lasers with direct current modulation has been widely studied [35, 36, 37, 38, 39]. It has already been proved that the effect of mode gain reduction occurring due to nonlinear processes is suppression of chaotic dynamics [40]. A bi-directional coupling between two such lasers is also found to suppress chaotic dynamics [41]. A positive delayed optoelectronic feedback combined with strong current modulation is found to suppress chaotic dynamics and bistability in semiconductor lasers [42, 43]. The effect of such a combination in inducing chaotic dynamics through a quasiperiodic route in quantum-well lasers also has been studied [30].

The most preferred light source in the optical communication systems is the directly modulated semiconductor lasers with GHz modulation. Chaotic synchronization of two such lasers is a widely investigated topic because of its applicability in optical secure communication [44, 45, 46, 47]. For InGaAsP lasers used in optical communication systems, the nonlinear gain reduction is very strong and its direct consequence on the dynamics of such lasers is the suppression of chaotic outputs. Earlier studies on the dynamics of directly modulated semiconductor lasers based on the rate equations for carrier and photon population inside the laser cavity, predicted period doubling and chaos in some range of modulation frequency and modulation depth [23, 24]. These rate equations have to be modified to include a small power dependent reduction in mode gain occurring due to phenomenon such as spectral hole burning [48, 49]. The dynamic response of semiconductor laser strongly depends on the nonlinear gain and therefore it has a significant role in modeling semiconductor laser dynamics [50, 51]. The optimum value of nonlinear gain reduction factor for InGaAsP lasers is between 0.03 and 0.06 and it has been proved that this system exhibits chaotic dynamics only for nonlinear gain reduction below 0.01 [40]. This makes the investigations on the methods of producing chaotic outputs from such lasers under

optimum parameter values very important for their applicability in secure communication systems.

2.4.1 Laser model

Semiconductor lasers with direct current modulation can be represented by the following rate equations for the photon density (P), carrier density (N), and the driving current (I) [26, 40]

$$\frac{dN}{dt} = \left(\frac{1}{\tau_e}\right)\left[\left(\frac{I}{I_{th}}\right) - N - \left\{\frac{(N - \delta)}{(1 - \delta)}\right\}P\right] \quad (2.4.1)$$

$$\frac{dP}{dt} = \left(\frac{1}{\tau_p}\right)\left[\frac{N - \delta}{1 - \delta}(1 - \epsilon P)P - P + \beta N\right] \quad (2.4.2)$$

$$I(t) = I_b + I_m \sin(2\pi ft) \quad (2.4.3)$$

where τ_e and τ_p are the electron and photon lifetimes, N and P are the carrier and photon densities, I is the driving current, $\delta = \frac{n_0}{n_{th}}$, $\epsilon = \epsilon_{NL}S_0$ are dimensionless parameters where n_0 is the carrier density required for transparency, $n_{th} = \frac{\tau_e I_{th}}{eV}$ is the threshold carrier density, ϵ_{NL} is the factor governing the nonlinear gain reduction occurring with an increase in S , $S_0 = \Gamma \frac{\tau_p}{\tau_e} n_{th}$, I_{th} is the threshold current, e is the electron charge, V is the active volume, Γ is the confinement factor and β is the spontaneous emission factor. $I_b = b \times I_{th}$ is the bias current where b is the bias strength, $I_m = m \times I_{th}$ is the modulation current where m is the modulation depth and fm is the modulation frequency [35]. Parameter values for which the system output will be chaotic are: $\tau_e = 3 \text{ ns}$ and $\tau_p = 6 \text{ ps}$ are the electron and photon life times. $\delta = 692 \times 10^{-3}$ and $\beta = 5 \times 10^{-5}$ and $I_{th} = 26 \text{ mA}$. In figure 2.11 the phase space [52] of the laser in the chaotic regime is shown with the given parameters. However, the delay feedback can also induce chaos in this laser system, notably for lower values of epsilon [53].

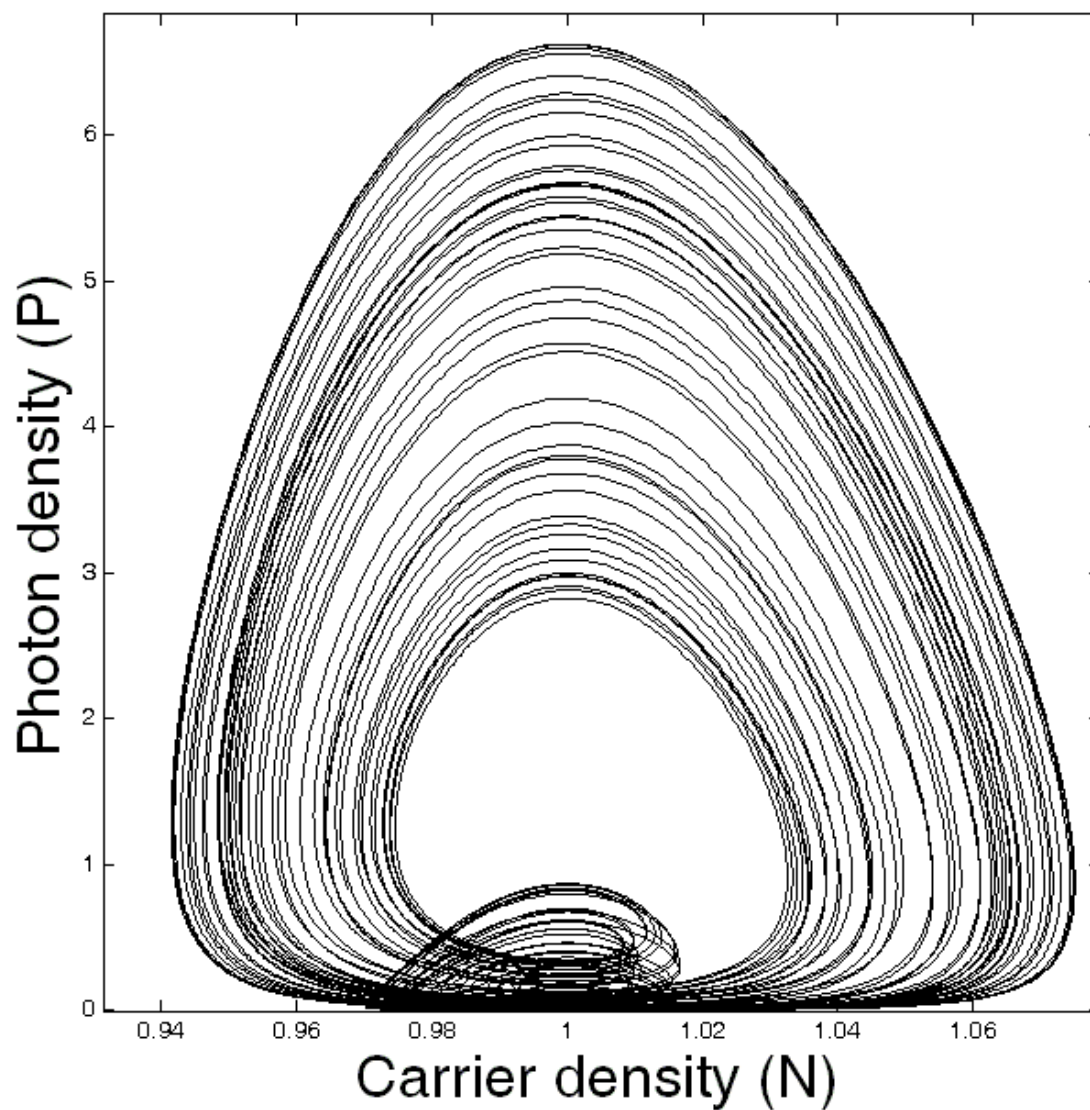


Figure 2.11: The phase space of a directly modulated semiconductor laser in the chaotic regime.

2.5 Conclusion

In this chapter we have clarified the concept of randomness that we study in this work. The systems that we consider are also introduced.

Bibliography

- [1] M. Gitterman, Nosi oscillator *The first hundred years from Einstein untill now* World Scientific, Singapore 2005.
- [2] G. R. Fowles, *Introduction to Modern Optics* New York, Holt, Rinehart and Winston, 1968.
- [3] Pikovsky, M. Rosenblum, J. Kurths, *Synchronization: A Universal Concept in Nonlinear Sciences* Cambridge, UK: Cambridge University Press, 2001
- [4] Louis M. Pecora, Thomas L. Carroll, Gregg A. Johnson, and Douglas J. Mar, Chaos 7, 520, 1997.
- [5] "Driven Damped Oscillator" from The Wolfram Demonstrations Project <http://demonstrations.wolfram.com/DrivenDampedOscillator/> Contributed by: Mark Robertson-Tessi.
- [6] I. Fisher, Y. Liu, P. Davis, Phys. Rev. A 62, 011801R, 2000.
- [7] S. Tang, H.F. Chen, S.K. Hwang, J.M. Liu, IEEE Trans. Circ. Sys.I 49, 163, 2002.
- [8] H.D.I. Abarbanel, M.B. Kennel, L. Illing, S. Tang, H.F. Chen, J.M. Liu, IEEE J.Quantum Electron. 37,1310 (2001)
- [9] S. Sivaprakasam,K.A. Shore, IEEE J. Quantum Electron. 36, 35, 2000.
- [10] J.P.Goedgebuer, L. Larger, H. Porte, Phys. Rev. Lett. 80,2249 (1998)

- [11] P. Colet, R. Roy, *Opt.Lett.* 19,2056, 1994.
- [12] G.D. Van Wiggeren,R. Roy, *Science* 279, 1198, 1998.
- [13] J. Ohtsubo,IEEE *J.Quantum Electron.* 38, 1141, 2002.
- [14] V. Kovanis, A.Gavrielides, T.B. Simpson, J.M. Liu, *Appl. Phys. Lett.* 67, 2780, 1995.
- [15] T.B. Simpson, J.M. Liu, A. Gavrielides, V. Kovanis, P.M. Alsing, *Phys. Rev. A* 51, 4181, 1995.
- [16] T.B. Simpson, J.M. Liu, K.F. Huang, K. Tai, *Quantum Semiclass. Opt.* 9, 765, 1997.
- [17] V.A. Lodi, S. Donati, A. Scirius, *IEEE J. Quantum Electron.* 33, 1537, 1997.
- [18] J. Mork, B.Thornberg, J.Mark, *IEEE J. Quantum Electron.* 28, 93, 1992.
- [19] Y.Cho., T. Umeda, *Opt. Commun.* 59, 131, 1986.
- [20] L.Goldberger, H.F. Taylor, A. Dandridge, H.F. Weller, R.O. Miles, *IEEE J.Quantum Electron.* 18, 555, 1982.
- [21] S.Bennet, C.M.Snowden, S. Iezekiel, *IEEE J. Quantum Electron.* 33, 2076, 1997.
- [22] E.Hemery, L.Chusseau, J.M. Lourtioz, *IEEE J. Quantum Electron.* 26, 633, 1990.
- [23] C.H. Lee, T.H. Yoon, S.Y. Shin, *Appl. Phys. Lett.* 46, 95, 1986.
- [24] M. Tang, S. Wang, *Appl. Phys. Lett.* 47, 208, 1985.
- [25] H.G. Winful, Y.C. Chen, J.M. Liu, *Appl. Phys. Lett.* 48, 161, 1986.
- [26] H.F. Liu, W.F. Ngai, *IEEE J. Quantum Electron.* 29, 1668, 1993.
- [27] Y.Hori, H.Serisava, H.Sato, *J. Opt. Soc. Amer.B* 5, 1128, 1988.

- [28] M.Tang, S.Wang, *Appl. Phys. Lett.* 50, 1861, 1987.
- [29] F.Y.Lin, J.M. Liu, *IEEE J. Quantum Electron.* 39, 562, 2003.
- [30] C. Juang, S.M. Chang, N.K. Hu, C. Lee, W.W.Lin, *Jap. J. Appl. Phys.* 44, 7827, 2005.
- [31] E.V. Grigorieva, H.Haken, S.A. Kashchenko, *Opt. Commun.* 165, 279, 1999.
- [32] S. Tang, J.M. Liu, *IEEE J. Quantum Electron.* 37, 329, 2001.
- [33] C.H. Lee, S.Y. Shin, *Appl. Phys. Lett.* 62, 922, 1993.
- [34] T.C. Damen, M.A. Duguay, *Elec.Lett.* 16, 166, 1980.
- [35] H.F. Liu, W.F. Ngai, *IEEE J. Quantum Electron.* 29, 1668, 1993.
- [36] T.H. Yoon, C.H. Lee, S.Y. Shin, *IEEE J. Quantum Electron.* 25, 1993, 1989.
- [37] Y.G. Zhao, *IEEE J. Quantum Electron.* 28, *IEEE J. Quantum Electron.* 28, 992, 2009.
- [38] C.G. Lim, S. Iezekiel, C.M. Snowden, *Appl. Phys. Lett.* 78, 2384, 2001.
- [39] E.F. Manfra, I.L. Caldas, R.L. Viana, H.J. Kalinowski, *Nonl. Dyn.* 27, 185, 002.
- [40] G.P.Agrawal, *Appl. Phys. Lett.* 49, 1013, 1986.
- [41] T. Kuruvilla, V.M.Nandakumaran, *Phys. Lett. A* 254, 39, 1999.
- [42] S. Rajesh, V.M.Nandakumaran, *Phys. Lett. A* 319, 340, 2003.
- [43] S. Rajesh, V.M.Nandakumaran, *Physica D* 213, 113, 2006.
- [44] S.Tang, J.M. Liu, *IEEE J. Quantum Electron.* 39, 708, 2003.
- [45] H.F. Chen, J.M. Liu, *IEEE J. Quantum Electron.* 36, 27, 2000.

- [46] V.Bindu, V.M. Nandakumaran, Phys.Lett. A 277, 345, 2000.
- [47] V.Bindu, V.M. Nandakumaran, J.Opt.A:Pure Appl. Opt 4, 115, 2002.
- [48] B.Zee, IEEE J. Quantum Electron. 14,727, 1978.
- [49] Y.Seumatsu, K.Furuyyu, Trans. Inst.Electron. Commun. Eng. Jpn. E-60, 467, 1977.
- [50] R.S. Tucker,J.Lightwave Technol. LT-3, 1180, 1985.
- [51] T.L. Koch, R.A.Linke,Appl. Phys. Lett, 48, 613, 1986.
- [52] "Chaotic Dynamics of a Modulated Semiconductor Laser" from The Wolfram Demonstrations Project
<http://demonstrations.wolfram.com/ChaoticDynamicsOfAModulatedSemiconductorLaser/>
Contributed by: Manu P. John and V. M. Nandakumaran
- [53] Performance characteristics of positive and negative delayed feedback on chaotic dynamics of directly modulated InGaAsP semiconductor lasers, Bindu M. Krishna, Manu. P. John and V. M. Nandakumaran, Pramana 71, No. 6, 1259, 2008.

Chapter 3

Effect of parameter fluctuations on coupled chaotic systems

3.1 Introduction

In chapter 2 we discussed Rossler attractors and the directly modulated semiconductor laser systems. In this chapter we study the effect of parameter fluctuations on the synchronization properties of these systems. We consider a system of bidirectionally coupled Rossler attractors and unidirectionally coupled directly modulated semiconductor laser systems. Synchronization of coupled chaotic systems has generated a lot of research activities over the last several years.

Synchronization of chaos has been studied extensively in physical, chemical and biological systems. Different types of synchronization such as complete, generalized, lag and phase synchronization are described in literature. One of the methods by which the synchronization of chaotic systems can be achieved is by coupling two identical systems, which can be either unidirectional or bidirectional[1, 2, 3, 4, 5, 6, 10, 12, 11, 24, 7]. Synchronization in arrays of coupled laser systems has also been investigated under various coupling schemes[10, 12, 11, 24]. Complete synchronization

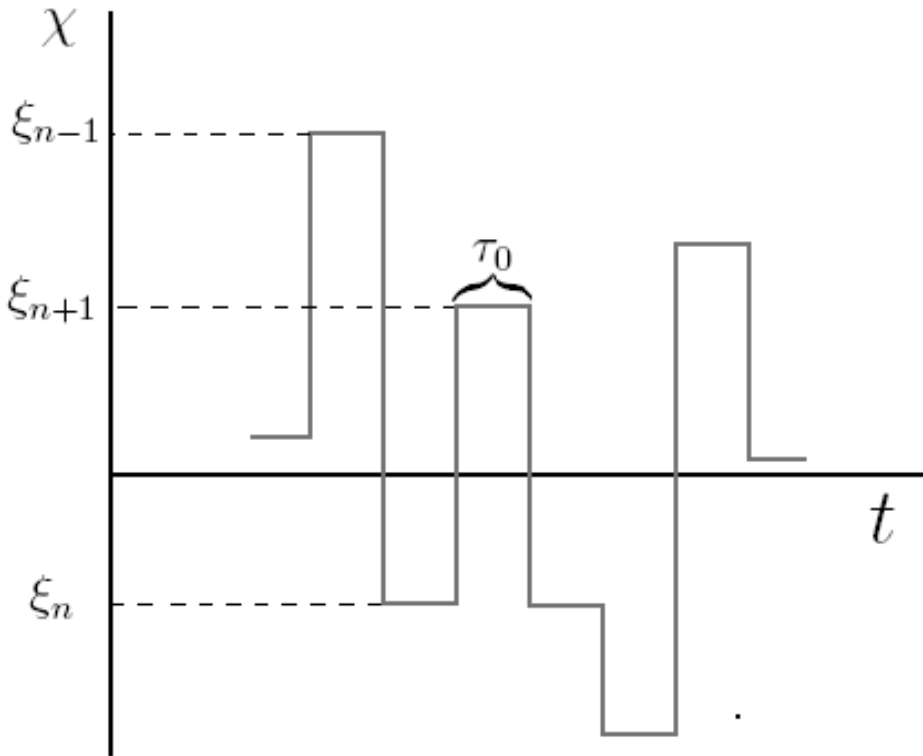


Figure 3.1: A schematic illustration of the fluctuation that affect the dynamics according to equation 3.7.1.

of identical chaotic systems is of considerable interest because of its applicability in secure communication[12, 24]. By identical systems we mean a set of systems whose parameters are exactly equal. It is found that complete synchronization is not possible when there is a small but finite mismatch of the parameters of the systems[9, 8, 7]. In coupled non autonomous systems, the effect of phase mismatch or a finite constant frequency detuning is to destroy the synchronization altogether[18].

3.2 Parameter fluctuations

To study the effect of fluctuations it is essential to identify a parameter whose mismatch is most effective in destroying synchronization. We denote this parameter as

p and the fluctuations to the parameter is assumed to occur in time as follows,

$$\begin{aligned} p_{1t} &= p_0 + \xi_{1t} \\ p_{2t} &= p_0 + \xi_{2t}, \end{aligned} \tag{3.2.1}$$

where ξ_{1t} and ξ_{2t} are two delta correlated zero mean random variables. In figure 3.1 such a fluctuation is illustrated.

We define $\widetilde{\Delta p}$, as a measure of the amplitude of fluctuations as follows,

$$\widetilde{\Delta p} = \langle |\delta p(t)| \rangle_t, \tag{3.2.2}$$

where $\delta p_t = p_{1t} - p_{2t}$ and $\langle \dots \rangle_t$ denotes time average.

In nature, parameter fluctuations are associated with characteristic time scales. In a laser this can be of the order of nano or micro seconds and in the case of biological systems the timescales can be of the order of hours or days.

To study the effect of time scales of parameter fluctuation on synchronization, we define the fluctuation rate ϕ , as *number of perturbations/unit time*. Different fluctuation rates can be achieved numerically by modifying the parameter as in eq. 3.7.1 in certain chosen time steps. Rest of the time the value of the parameter remains constant at the modified value. The error in synchronization is studied with respect to ϕ .

3.3 Effect on synchronization

Coupled Rossler oscillators are well known for numerical studies in synchronization. This is due to its simplicity and the ability to synchronize. Also, the results obtained [14, 16] can usually be generalized to other chaotic systems. We consider a system of

bidirectionally coupled Rossler oscillators given by the following equations,

$$\begin{aligned}
 \dot{x}_1 &= -y_1 - z_1 + c(x_2 - x_1) \\
 \dot{y}_1 &= x_1 + p_1 y_1 \\
 \dot{z}_1 &= 0.2 + z_1(x_1 - 10) \\
 \dot{x}_2 &= -y_2 - z_2 + c(x_1 - x_2) \\
 \dot{y}_2 &= x_2 + p_2 y_2 \\
 \dot{z}_2 &= 0.2 + z_2(x_2 - 10).
 \end{aligned} \tag{3.3.1}$$

The parameter values are chosen as $p_0 = 0.18$, $\widetilde{\Delta p} = 0.05$ and the coupling strength $c = 0.25$, for all the fluctuation rates. Keeping these parameters constant, we study the effect of the fluctuation rates on the quality of synchronization.

Fig.3.2 shows the synchronization plot in the presence of parameter fluctuations. It can be seen that the synchronization is robust. With the same value of $\widetilde{\Delta p}$ the synchronization is destroyed with a lower fluctuation rate as shown in fig.3.3. To quantify the synchronization error we used the similarity function defined by,

$$S^2(\tau) = \frac{\langle [x_1(t + \tau) - x_2(t)]^2 \rangle}{[\langle x_1^2(t) \rangle \langle x_2^2(t) \rangle]^{\frac{1}{2}}}. \tag{3.3.2}$$

Here τ is set to zero, which gives $S(0)$, the error in synchronization. Fig. 3.4 shows the plot of $S(0)$ vs. fluctuation rate. It can be seen that the error diminishes rapidly with the increase in the fluctuation rate. Keeping ϕ as a constant, and increasing the amplitude of fluctuations, it is found that $S(0)$ increases with $\widetilde{\Delta p}$. Also the rate of increase of $S(0)$ is higher for a lower value of ϕ , for a range of coupling strengths [15], as shown in figure 3.5.

In addition to random fluctuations to the parameter, we also investigated the effect of deterministic modulations to the parameter [16]. The parameters of the coupled systems are assumed to evolve in time as follows,

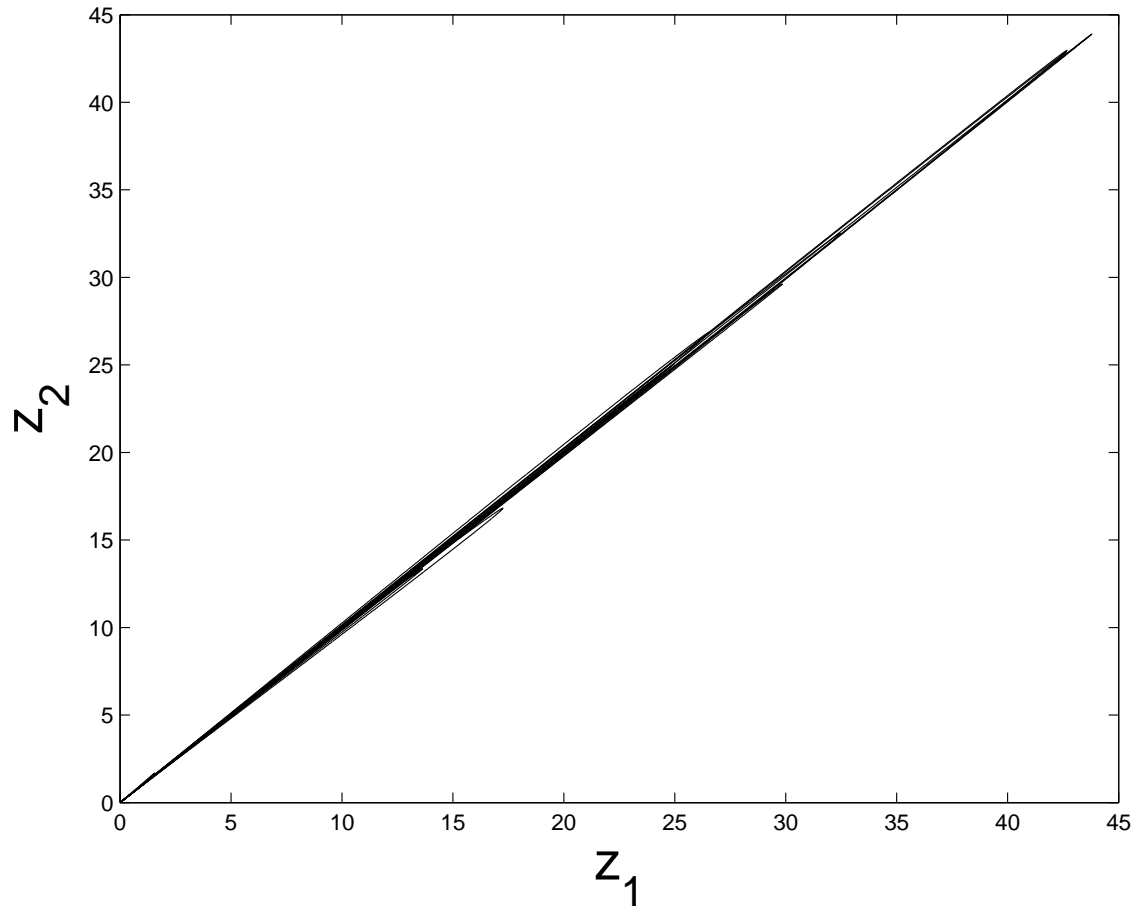


Figure 3.2: Synchronization is maintained in the presence of parameter fluctuations. $\phi = 1000$ and $\widetilde{\Delta p} = 0.05$

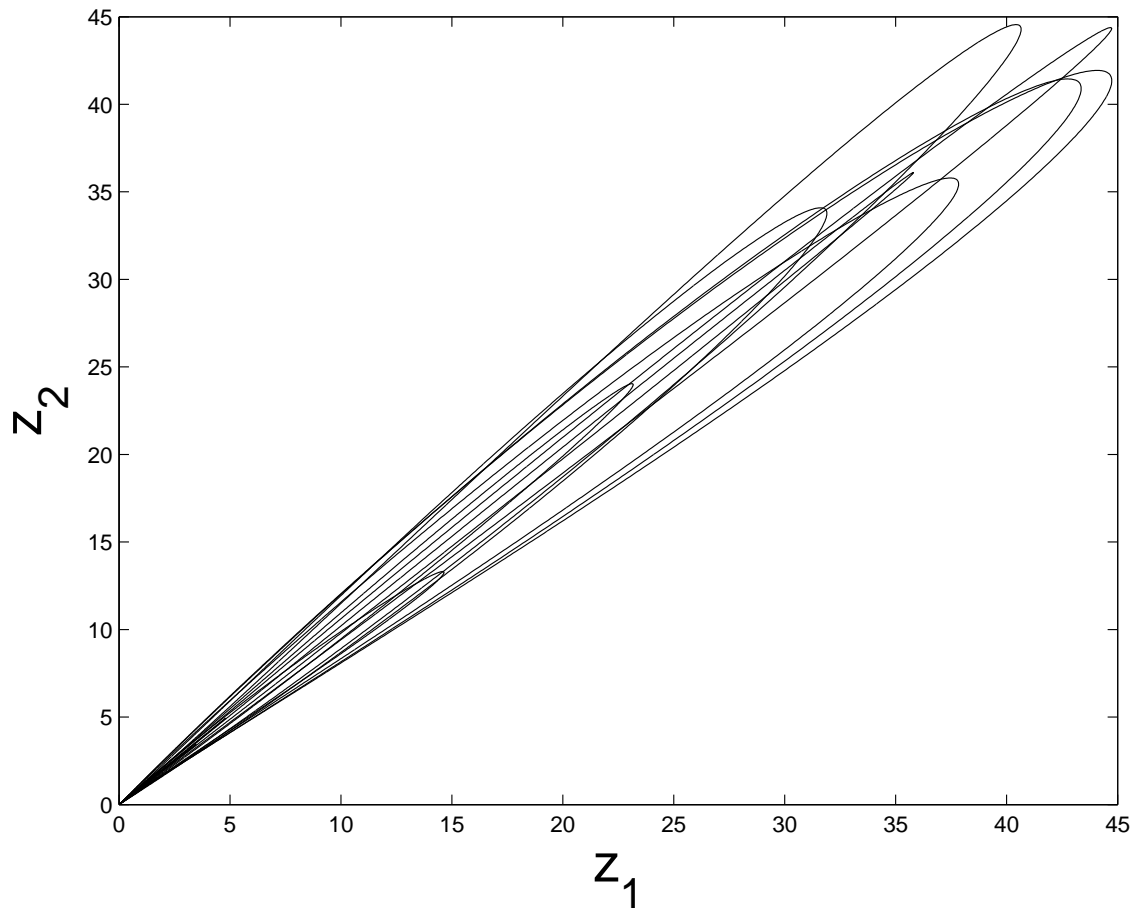


Figure 3.3: Synchronization is destroyed in the presence of parameter fluctuations with low fluctuation rates. Fluctuation rate $\phi = 25$ and $\widetilde{\Delta p} = 0.05$

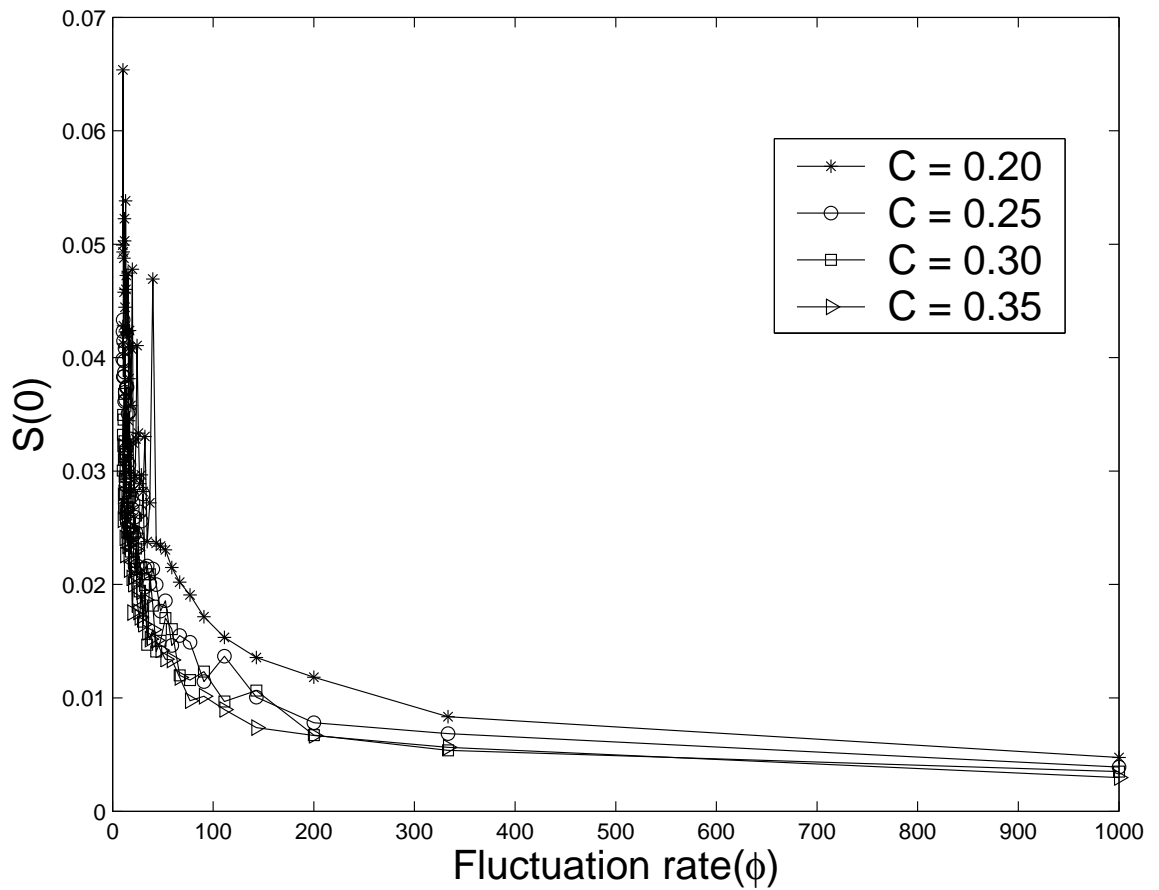


Figure 3.4: The synchronization error decreases with the increase in the fluctuation rate. It can be seen that high coupling could not stabilize synchronization with lower fluctuation rates. Here $\widehat{\Delta p} = 0.05$ and coupling strength $c = 0.5$.

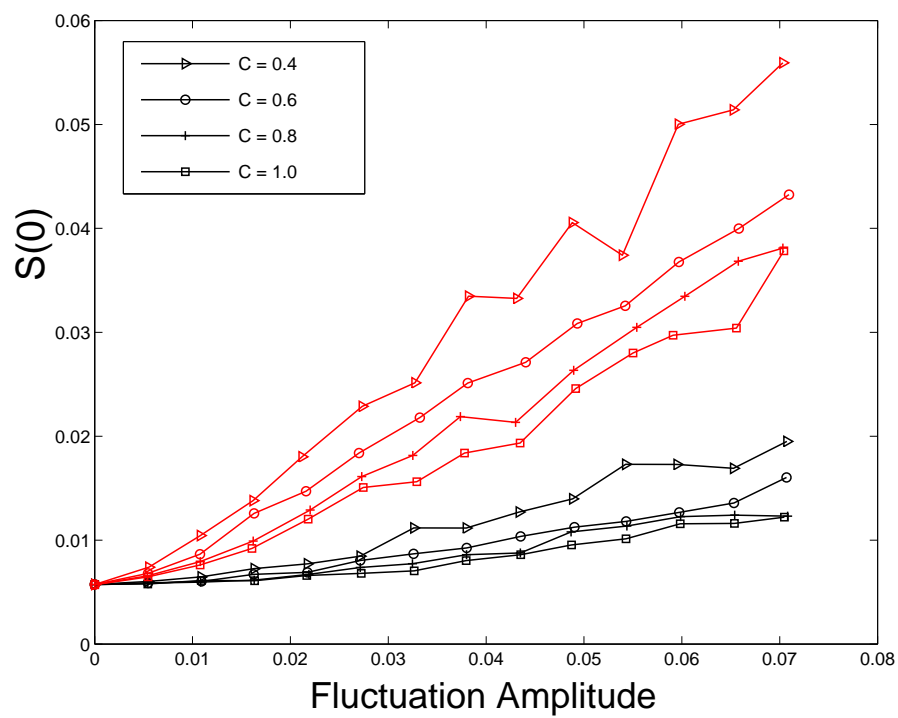


Figure 3.5: For two fluctuation rates, $\phi = 50$ (red) and $\phi = 500$ (black): the synchronization error grows as the amplitude of fluctuation is increased.

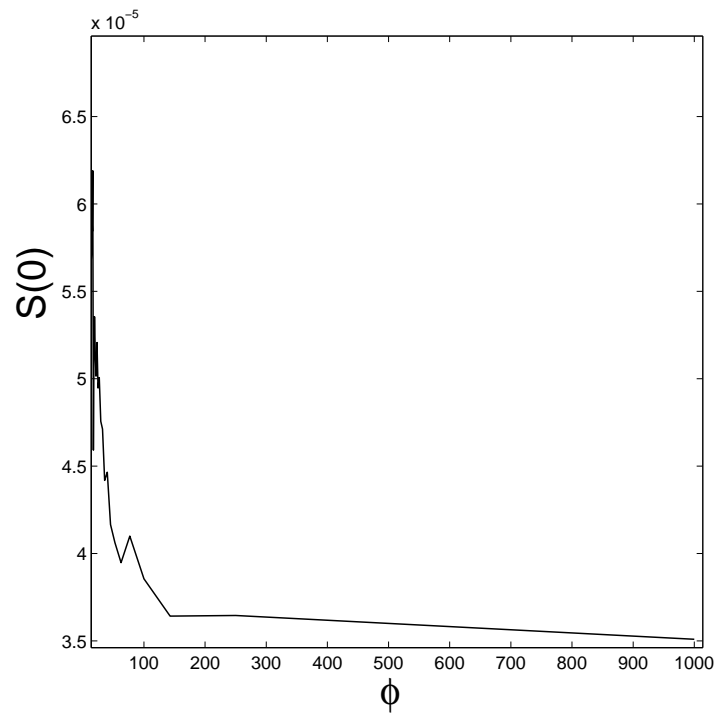


Figure 3.6: $S(0)$ vs. ϕ plot of coupled Rossler systems under fluctuations following uniform distribution. Here $\widetilde{\Delta p} = 0.05$.

$$\begin{aligned} p_1 &= p_0 + a \sin 2\pi ft, \\ p_2 &= p_0 - a \sin 2\pi ft, \end{aligned} \quad (3.3.3)$$

where the f the frequency of modulation and $a = 0.1$ is the amplitude of modulation. It can be seen in figure 3.7 that the synchronization error levels off as the frequency of modulation is increased. Note that high coupling strengths only reduce the synchronization error, but the stability of synchrony is achieved only at high modulation frequencies. Thus modulation frequency is important in determining the stability of synchronization.

3.4 Discussion

In general the robustness of synchronization with high fluctuation rates and destruction of synchronization with low fluctuation rates can be understood as follows. Let the evolution of the coupled systems in phase space be represented by the dynamical equations

$$\begin{aligned} \dot{X}_1 &= f_1(p_1, X_1) + Cf(X_2 - X_1) \\ \dot{X}_2 &= f_1(p_2, X_2) + Cf(X_1 - X_2). \end{aligned} \quad (3.4.1)$$

Where X represents the phase space variables, p the parameter whose fluctuation is considered, and C , the coupling constant.

With eq.3.4.1 we can write an equation for the rate of separation $X_1 - X_2$ of the trajectories as,

$$\frac{d(X_1 - X_2)}{dt} = \dot{X}_1 - \dot{X}_2 = M(p_1, p_2, X_1, X_2), \quad (3.4.2)$$

Where $M(p_1, p_2, X_1, X_2)$ is a function of the dynamical variables, the parameters of the coupled systems and Δp the parameter mismatch. This can be expanded in terms of Δp and the effect of fluctuations can be separated out.

$$M(p_1, p_2, X_1, X_2) = M_s(p_0, X_1, X_2) + E(p_0, X_1, X_2, \Delta p_1, \Delta p_2). \quad (3.4.3)$$

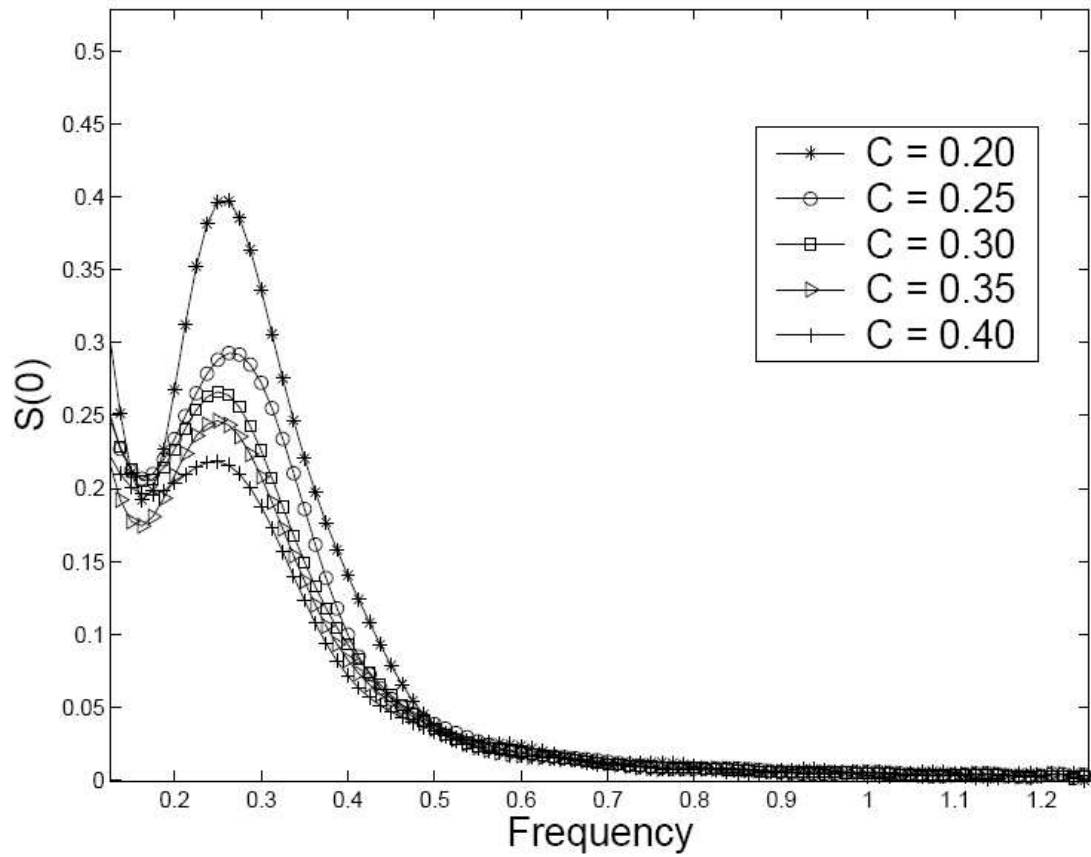


Figure 3.7: The synchronization error decreases with the increase in the in frequency of modulation. It can be seen that the modulation frequency is more important than coupling strength in determining the stability of synchronization. Here the amplitude of modulation $a = 0.1$.

where $E(p_0, X_1, X_2, \Delta p_1, \Delta p_2)$ can be written as,

$$E(p_0, X_1, X_2, \Delta p_1, \Delta p_2) = \Delta p_1 \frac{\partial M(p_1, p_2, X_1, X_2)}{\partial p_1} \Big|_{p_1=p_0} + \Delta p_2 \frac{\partial M(p_1, p_2, X_1, X_2)}{\partial p_2} \Big|_{p_2=p_0} .$$

This is valid for small Δp , neglecting its higher powers or if the higher derivatives of $M(p_1, p_2, X_1, X_2, \Delta p_1, \Delta p_2)$ with respect to p is zero. Also it should be noted that the parameter values are not near a bifurcation point.

Here $M_s(p_0, X_1, X_2)$ represents the quantity which offers a stable synchronization manifold, that is, when $M_s(p_0, X_1, X_2)$ alone is present on the right hand side of the separation equation, the coupled systems synchronize as $t \rightarrow \infty$. The conditions for such a synchronization is widely discussed in literature [6]. The term $E(p_0, X_1, X_2, \Delta p_1, \Delta p_2)$ represents the effect of the parameter mismatch. Coupled systems synchronizes if the overall effect of this term vanishes as $t \rightarrow \infty$.

In the present example of coupled systems (eq.3.3.1) the rate of separation of trajectories can be written as follows,

$$\begin{aligned} \frac{d(x_1 - x_2)}{dt} &= (y_1 - y_2) + (z_2 - z_1) + 2C(x_2 - x_1) & (3.4.4) \\ \frac{d(y_1 - y_2)}{dt} &= (x_1 - x_2) + p_1 y_1 - p_2 y_2 \\ \frac{d(z_1 - z_2)}{dt} &= (x_1 z_1 - x_2 z_2) + 10(z_2 - z_1) \end{aligned}$$

Assuming that we start from an approximately synchronized state, $x_1 \simeq x_2$, $y_1 \simeq y_2$ and $z_1 \simeq z_2$, we can write eq.3.4.4 as,

$$\begin{aligned} \frac{d(x_1 - x_2)}{dt} &\simeq 0 & (3.4.5) \\ \frac{d(y_1 - y_2)}{dt} &\simeq p_1 y_1 - p_2 y_2 \\ \frac{d(z_1 - z_2)}{dt} &\simeq 0. \end{aligned}$$

Here it can be seen that $M(p_1, p_2, X_1, X_2) = p_1 y_1 - p_2 y_2$ and $E(p_0, X_1, X_2, \Delta p_1, \Delta p_2)$ can be calculated as,

$$\begin{aligned}
 E(p_0, X_1, X_2, \Delta p_1, \Delta p_2) &= \Delta p_1 \frac{\partial(p_1 y_1 - p_2 y_2)}{\partial p_1} \Big|_{p_1=p_0} & (3.4.6) \\
 &+ \Delta p_2 \frac{\partial(p_1 y_1 - p_2 y_2)}{\partial p_2} \Big|_{p_2=p_0} \cdot \\
 &= \Delta p_1 y_1 - \Delta p_2 y_2 \\
 &= \xi_{1t} y_1 - \xi_{2t} y_2.
 \end{aligned}$$

as the instantaneous parameter mismatches $\Delta p_1 = \xi_{1t}$ and $\Delta p_2 = \xi_{2t}$. Also the form of $E(p_0, X_1, X_2, \Delta p_1, \Delta p_2)$ can be generalized to

$$E(p_0, X_1, X_2, \Delta p_1, \Delta p_2) = \sum_i \alpha_i \xi_{ti} x_i(t) \quad (3.4.7)$$

with many coupling schemes. Here ξ_t s are the the fluctuation terms, α s are constants and $x(t)$ s are the phase space variables of the coupled system. Perturbations of these nature are clearly multiplicative noise who's effect on synchronization has not been studied.

Here the effect of fluctuations vanishes because the ξ_{ti} 's are zero mean rapidly fluctuating quantities and $x(t)$'s are the phase space variables that evolve slowly when compared to the the rapid fluctuations or modulations of the parameter. Thus $x(t)$'s can be assumed to be constant, in the time required for the fluctuations to get summed to zero.

However with a low fluctuation rate the quantity $E(p_0, X_1, X_2, \Delta p_1, \Delta p_2)$ can affect the synchrony because the phase space evolution time is comparable to the interval where a fixed parameter mismatch persists. Thus with a lower fluctuation rate the system always get time to respond to the parameter mismatch before it being canceled out. In other words the sum on the R.H.S of eq.3.4.7 does not vanish without considerably modifying the phase space variables $x(t)$ when the fluctuation rates are low. Apart from gaussian random fluctuations, we also studied perturbations

with a uniform distribution. The results were qualitatively similar to that of gaussian perturbations as shown in figure 3.6. This suggests that the fluctuation rate ϕ is more significant than the statistical nature of the fluctuations.

In a case where the parameters are modulated the fluctuating terms ξ s are replaced by the oscillating terms. The mechanism of retaining stability of synchrony at high frequency modulations is similar to that of random parametric perturbations. The contributions of the parameter mismatch vanishes with fast zero mean oscillations. The analytical treatment of this is straight forward and not much different from that of random fluctuations.

3.5 Effect of fluctuations in Laser dynamics

In chapter II we have introduced the directly modulated semiconductor laser and its applications in secure communication. Investigations in this direction is still a hot topic of research [26, 27, 28]. Here we show that such laser systems are also considerably influenced by the fluctuations of the parameters. Another aim of our studies in lasers is to show that there are examples in which a well defined relation between the fluctuation rates (ϕ) and the synchronization error $S(0)$ cannot always be established.

3.6 Laser model

The dynamical equation of a directly modulated semiconductor laser can be expressed as [13],

$$\begin{aligned} \frac{dN}{dt} &= \left(\frac{1}{\tau_e}\right)\left[\left(\frac{I}{I_{th}}\right) - N - \left\{\frac{(N - \delta)}{(1 - \delta)}\right\}P\right] \\ \frac{dP}{dt} &= \left(\frac{1}{\tau_p}\right)\left[\frac{N - \delta}{1 - \delta}(1 - \epsilon P)P - P + \beta N\right] \end{aligned} \quad (3.6.1)$$

where, N and P are the normalized carrier and photon densities respectively. $\tau_e = 3 \text{ ns}$ and $\tau_p = 6 \text{ ps}$ are the electron and photon life times. $\delta = 692 \times 10^{-3}$ and $\beta = 5 \times 10^{-5}$ are two dimensionless parameters and $I_{th} = 26 \text{ mA}$ is the threshold current. The modulating current in the system is given by

$$I(t) = I_b + I_m \sin(2\pi ft). \quad (3.6.2)$$

Here, $I_b = 40.3 \text{ mA}$ is the biasing current, $I_m = 14.3 \text{ mA}$ is the modulating current and $f = 0.8 \times 10^9 \text{ Hz}$ the frequency of modulation. Two such laser systems can be synchronized by an optoelectronic feedback [23, 24]. In this scheme, the difference in photon densities of the drive and response systems is fed into the drive current of the response system.

The dynamics of the coupled system can be represented by the following equations,

$$\begin{aligned} \frac{dN_1}{dt} &= \left(\frac{1}{\tau_e}\right)\left[\left(\frac{I_1}{I_{th}}\right) - N_1 - \left\{\frac{(N_1 - \delta)}{(1 - \delta)}\right\}P_1\right] \\ \frac{dP_1}{dt} &= \left(\frac{1}{\tau_p}\right)\left[\frac{N_1 - \delta}{1 - \delta}(1 - \epsilon P_1)P_1 - P_1 + \beta N_1\right] \\ I_1(t) &= I_{b1} + I_{m1} \sin(\omega_1 t) \\ \frac{dN_2}{dt} &= \left(\frac{1}{\tau_e}\right)\left[\left(\frac{I_2}{I_{th}}\right) - N_2 - \left\{\frac{(N_2 - \delta)}{(1 - \delta)}\right\}P_2\right] \\ \frac{dP_2}{dt} &= \left(\frac{1}{\tau_p}\right)\left[\frac{N_2 - \delta}{1 - \delta}(1 - \epsilon P_2)P_2 - P_2 + \beta N_2\right] \\ I_2(t) &= I_{b2} + I_{m2} \sin(\omega_2 t) + 0.003105(P_1 - P_2). \end{aligned} \quad (3.6.3)$$

Such a system synchronizes when the parameters of both oscillators match [23]. Synchronization of coupled non-autonomous systems is highly sensitive to parameter mismatch [18], especially of the driving frequency. Being a non-autonomous system, this laser system is also highly sensitive to parameter mismatch, especially to those occurring in the driving frequency [25]. When we introduce parameter fluctuation, it is assumed that the average parameter values of both the systems are identical and are equal to the values for which they are designed for secure communication purpose [29].

3.7 Parameter fluctuations

Let ω_1 and ω_2 be the driving frequencies of the systems. Fluctuations in the system are incorporated as

$$\omega_1 = \omega_0 + \xi_1(t) \quad (3.7.1)$$

$$\omega_2 = \omega_0 + \xi_2(t), \quad (3.7.2)$$

where, ξ_1 and ξ_2 are zero mean delta correlated random variables. Once the frequency is modified, it remain constant for a characteristic timescale associated with the fluctuation, which is equal to $\frac{1}{\phi}$. With this modification, the angular frequencies of coupled systems fluctuates about $\omega_0 = 5.03 \times 10^9$, which is the mean angular frequency. The amplitudes of the fluctuations are quantified by $\widetilde{\Delta\omega}$ which is defined as,

$$\widetilde{\Delta\omega} = \langle |\delta\omega(t)| \rangle, \quad (3.7.3)$$

where, $\delta\omega(t) = \omega_1(t) - \omega_2(t)$. The Similarity function is used to quantify the synchronization error. In this case, the similarity function in terms of photon density can be written as,

$$S^2(\tau) = \frac{\langle [P_1(t + \tau) - P_2(t)]^2 \rangle}{[\langle P_1^2(t) \rangle \langle P_2^2(t) \rangle]^{\frac{1}{2}}}. \quad (3.7.4)$$

3.7.1 Numerical results

The variation of the synchronization error ($S(0)$) with respect to the fluctuation rate ϕ is studied. The error decreases as the fluctuation rate increases. The effect of Gaussian as well as uniform fluctuations on synchronization are studied. Figures 3.8 and 3.9 shows the variation of synchronization error for increasing values of fluctuation rates in the case of Gaussian and uniform perturbations respectively. It can be seen that in both the cases, the convergence of the $S(0)$ is not uniform as in the case of Rossler attractors. However for larger fluctuation rates, $S(0)$ falls to very low values.

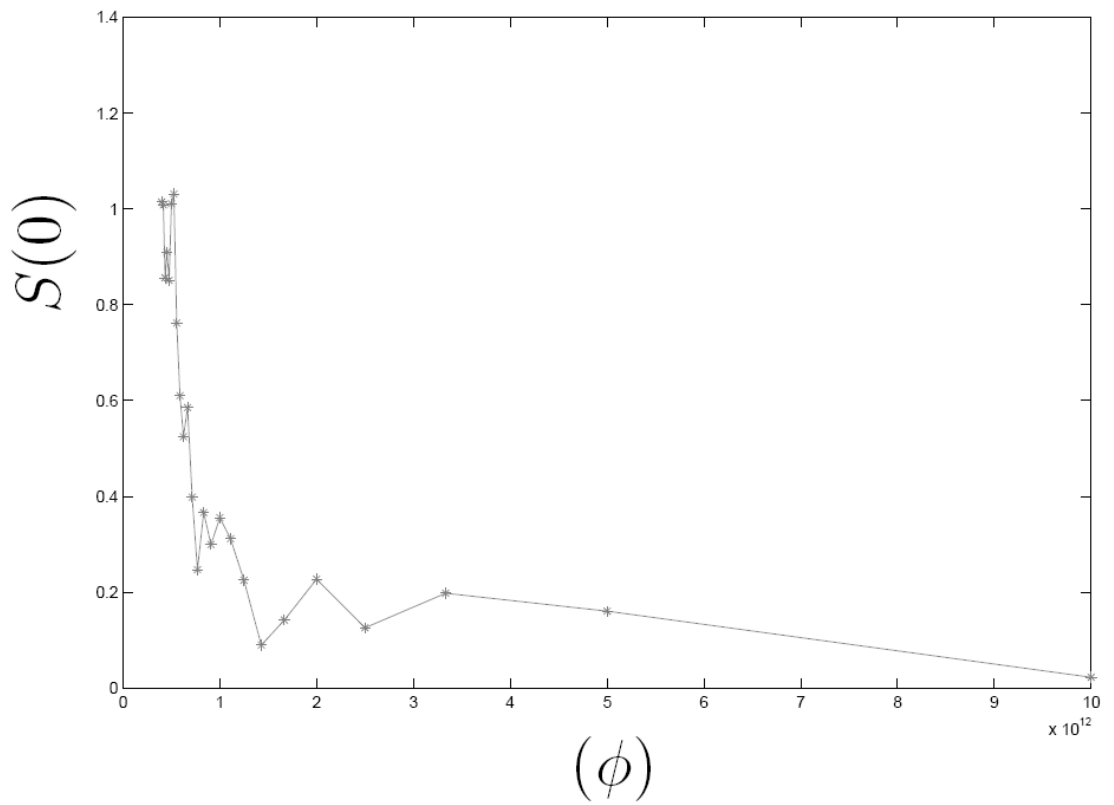


Figure 3.8: In coupled laser systems, the synchronization error $S(0)$ decays with the increase in the fluctuation rate. ξ 's follow gaussian distribution and $\widetilde{\Delta\omega} = 8.5761 \times 10^7$

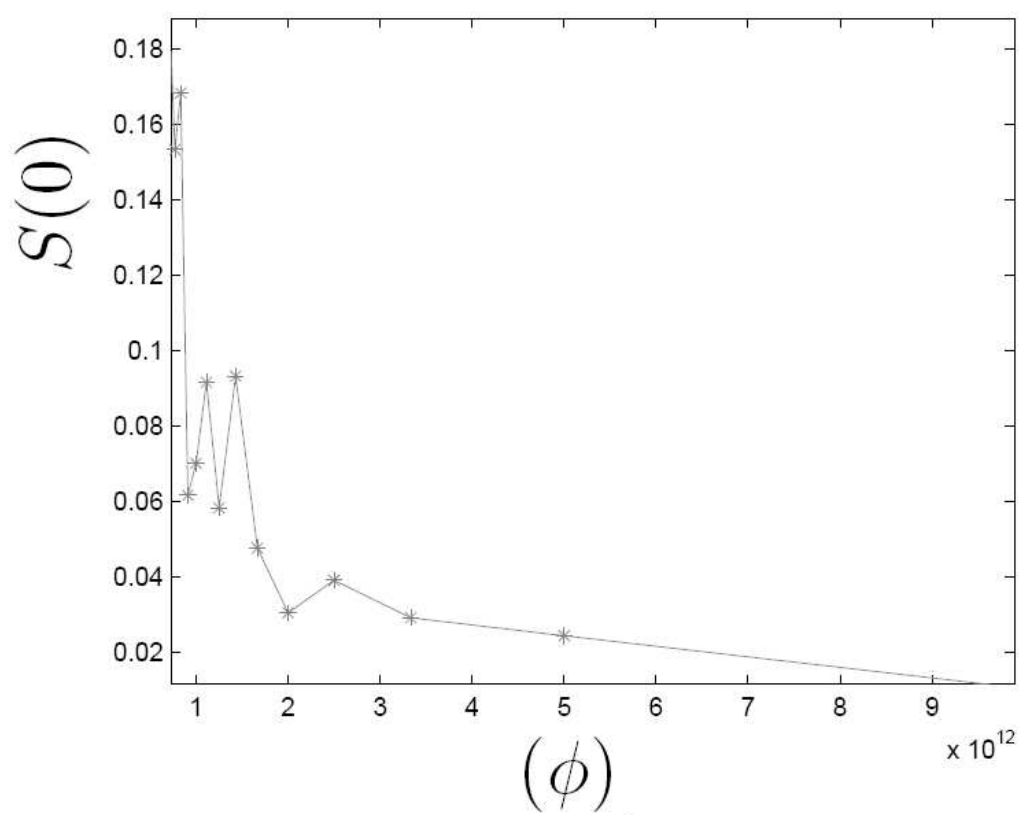


Figure 3.9: Synchronization error $S(0)$ decays with the increase in the fluctuation rate. Here the coupled Laser system is subjected to fluctuations that follow uniform distribution. $\widetilde{\Delta\omega} = 2.5409 \times 10^7$.

3.8 Conclusion

In this chapter we have shown that the effect of a fluctuating parameter involved in the dynamics of coupled systems is to destroy synchronization. The effect of such fluctuations on the quality of synchronization depends on the time scale associated with the fluctuations. In some cases a well defined relation can be found between the timescales and the similarity function $S(0)$. But in systems which are very sensitive to parameter mismatch, no such relation can be derived.

Bibliography

- [1] T. Yamada and H. Fujisaka, *Prog. Theor. Phys.*, 70, 1240, 1983.
- [2] L. M. Pecora and T. L. Carroll, *Phys. Rev. Lett* 4, 821, 1990.
- [3] T. L. Carroll and L. M. Pecora, *IEEE Trans. Circuits Syst.*, II, 38, 453, 1991.
- [4] T. L. Carroll and L. M. Pecora, *IEEE Trans. Circuits Syst.*, 40, 646, 1995.
- [5] T. L. Carroll and L. M. Pecora, *Eur. J. Biochem.* 235, 1996, 238.
- [6] L. Glass, *Nature*, 410, 277, 2001.
- [7] A. S. Pikovsky and M. Rosenblum and J. Kurths, *Synchronization: A universal concept in nonlinear sciences*, Cambridge University Press, Cambridge, 2001.
- [8] M. G. Rosenblum and A. S. Pikovsky and J. Kurths, *Phys. Rev. Lett.* 76, 1804, 1995.
- [9] M. G. Rosenblum A. S. Pikovsky and J. Kurths, *Phys. Rev. Lett.* 78, 4193, 1997.
- [10] G. D. Van Wiggeren and R. Roy, *Science* 279, 1198, 1994.
- [11] P. Colet and R. Roy, *Opt. Lett.* 19, 2056, 1994.
- [12] G. D. Van Wiggeren and R. Roy, *Phys. Rev. Lett*, 81, 3547, 1998.
- [13] G. P. Agrawal, *Appl. Phys. Lett.* 49, 1013, 1986.

- [14] Manu P John, Jijo P U and V M Nandakumaran, Effect of a fluctuating parameter mismatch and the associated timescales on coupled Rossler oscillators, to appear in Pramana-journal of physics, 2009.
- [15] M. P. John, P. U . Jijo and V. M. Nandakumaran, Effect of a fluctuating parameter mismatch in the synchronization of a chaotic system, National Conference on Current Trends in Material Science (CTMS-07), organized by the Department of Physics Christian College, Chengannur, March 25-27 2007.
- [16] M. P. John, P. U. Jijo, and V. M. Nandakumaran, Fast Fluctuations do not Destroy Synchronization, National Conference on Nonlinear Systems and Dynamics, Ramanujam Institute for Advanced Study in Mathematics, University of Madras, Chennai, 6-8, February 2006, Proceedings, Allied Publishers Chennai.
- [17] V. Bindu and V. M. Nandakumaran, J. Opt. A: Pure Appl. Opt. 4, 115, 2002.
- [18] H. W. Yin and J. H. Dai and H. J. Zhang, Phys. Rev. E 58, 9683, 1998.
- [19] L. M. Pecora and T. L. Carroll and G. A. Johnson, and D. J. Mar, Chaos 7, 520, 1997.
- [20] P. Ashwin and J. Buescu and I. Stewart, Phys. Lett. A 193, 126, 1994.
- [21] D. J. Gauthier and J. C. Bienfang, Phys. Rev. Lett. 77, 1751, 1996.
- [22] T. L. Carroll, Chaos 15, 13901, 2005.
- [23] V. Bindu and V. M. Nandakumaran, J. Opt. A: Pure Appl. Opt. 4, 115, 2002.
- [24] V. Bindu and V. M. Nandakumaran, Phys. Lett. A. 227 , 345, 2000.
- [25]
- [26] B. B. Zhou, R. Roy, Phys. Rev. E. 75, 026205, 2007.

- [27] N. Gross, W. Kinzel, I. Kanter, M. Rosenbluh, L. Klaykovich, *Opt. Commn.* 267, 464, 2006 .
- [28] E. Klein, N. Gross, M. Rosenbluh, W. Kinzel, L. Khaykovich, I. Kanter, *Phys. Rev. E.* 73, 066214, 2006. S. Rajesh and V. M. Nandakumaran, “Synchronization of chaos in unidirectionally coupled modulated self pulsating semiconductor lasers: Effects of delay and detuning,” *Perspectives in Nonlinear Dynamics 2004, Chennai, a satellit meeting of the STATPHYS 22, India.*
- [29] M. P. John, P. U. Jijo, and V. M. Nandakumaran, Effect of parameter fluctuations in directly modulated semiconductor laser systems, *Proceedings, Photonics 2004, Cochin, December 8-11, 2004.*

Chapter 4

Chaos in an intermittently driven damped oscillator

4.1 Introduction

It is generally known that continuous linear systems cannot exhibit chaotic time evolution. However recently it has been shown that chaotic behavior can occur in systems without explicit non linearities. Hirata et.al. [1] have shown that continuous chaotic wave forms can be constructed by the superposition of certain pulse basis functions. In a linear second order filter driven by randomly polarized pulses, chaotic behavior is observed when the time series is viewed backwards in time [2]. Further they have shown that by reversing the time series, folded band chaos similar to Rössler attractor can also be synthesized [3]. Even if the time reversal is not physical, this reveals the importance of pure randomness which is associated with chaotic behavior. In this chapter we study a weakly damped driven linear oscillator where the oscillator and the drive are coupled only when the trajectory is in a thin strip in the phase space [4].

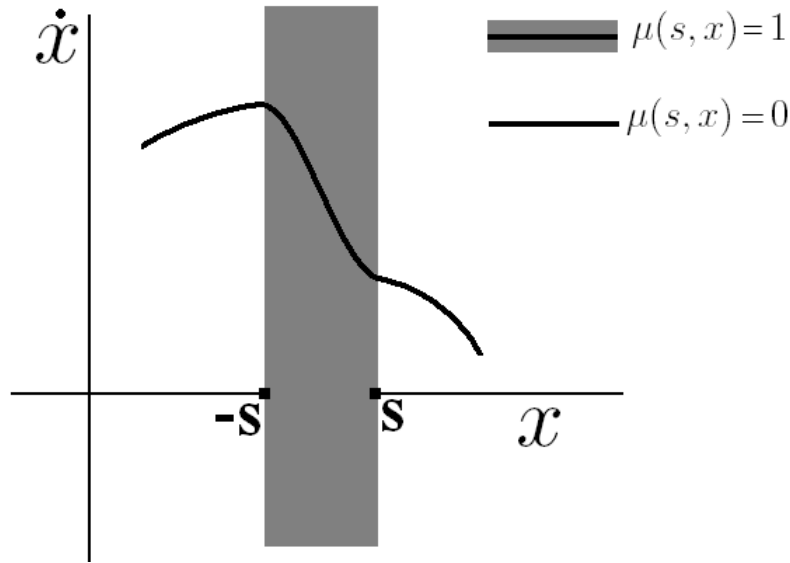


Figure 4.1: The schematic diagram of the driving. The drive and the oscillator are coupled when the trajectory is in side the strip located at the origin of the phase space.

4.2 Basic model

The basic model discussed in this chapter is a damped oscillator which is driven only in a thin strip of the phase space. that is, as the trajectory enters the strip the coupling between the drive and the oscillator becomes active. When not driven, the oscillator performs a damped motion and the drive runs freely. This is schematically shown in figure 4.1. We choose the origin as the location of the strip because orbits with lower energy may not encounter the strip, if it is located far from the origin. Such orbits will spiral towards zero as in the case of an ordinary damped oscillator.

First we consider a deterministic drive. The dynamics is characterized using standard techniques. We also study a model in which the oscillator is driven by a stochastic drive. That is, as the trajectory enter the strip, the oscillator is subjected to a random forcing. We show that the stochastic system mimics its deterministic analogue. Also it is shown that the effective forcing is associated with a timescale, this makes the forcing similar to the fluctuation that we have studied in the previous

chapter.

4.3 Deterministic driving

4.3.1 Dynamical equations

The dynamical equation for a harmonic oscillator, which is coupled to the drive only in a strip in the phase space can be written as,

$$\frac{d^2x}{dt^2} + \gamma \frac{dx}{dt} + \Omega^2 x = \mu(s, x) a \sin(\omega t) \quad (4.3.1)$$

where,

$$\mu(s, x) = \begin{cases} 1 & \text{if } |x| \leq s \\ 0 & \text{otherwise.} \end{cases} \quad (4.3.2)$$

Here, γ is the damping coefficient, Ω is the angular frequency of the oscillator and ω is the angular frequency of the drive. Thus with a deterministic drive, what the dynamical equations represent is a legitimate deterministic system in every sense.

4.3.2 Numerical results

Numerical simulations were done using the Runge-Kutta algorithm with a step size of 10^{-3} . We choose the following values for the parameters: $\Omega = 1.0$, $\gamma = 0.1$, $\omega = 0.3$, $s = 0.1$ and $a = 2.5$. The parameters were chosen by numerical trials to express the concepts clearly, and are fixed during the evolution of the system in time. Fig.4.2 shows the phase space plot of the system. Note that there is a discontinuity in a strip of width $2s$ near 0 in the the phase space, where the oscillator is coupled to the drive. A closer view of the strip is given in Fig. 4.3. It can be seen that the trajectories that approach the origin may either cross the strip with or without considerable modifications, or it may get reversed. Fig. 4.4 shows the time series $x(t)$ of the system. The amplitude of oscillations, and the number of oscillations between two consecutive crossings of the strip are irregular. This corresponds to the phase

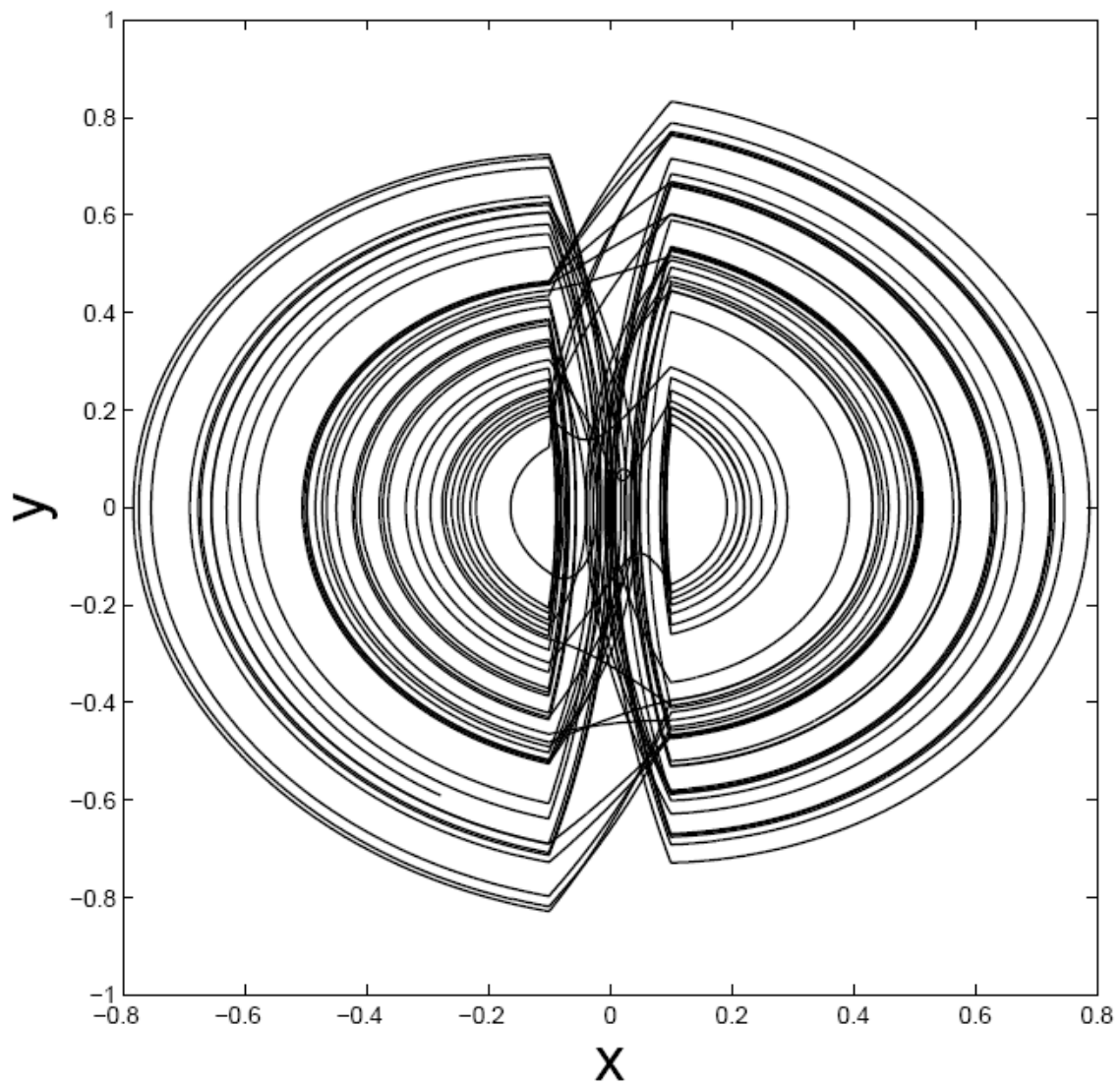


Figure 4.2: Phase space trajectory of the oscillator ($\Omega = 1.0$, $\gamma = 0.1$, $\omega = 0.3$, $s = 0.1$ and $a = 2.5$).

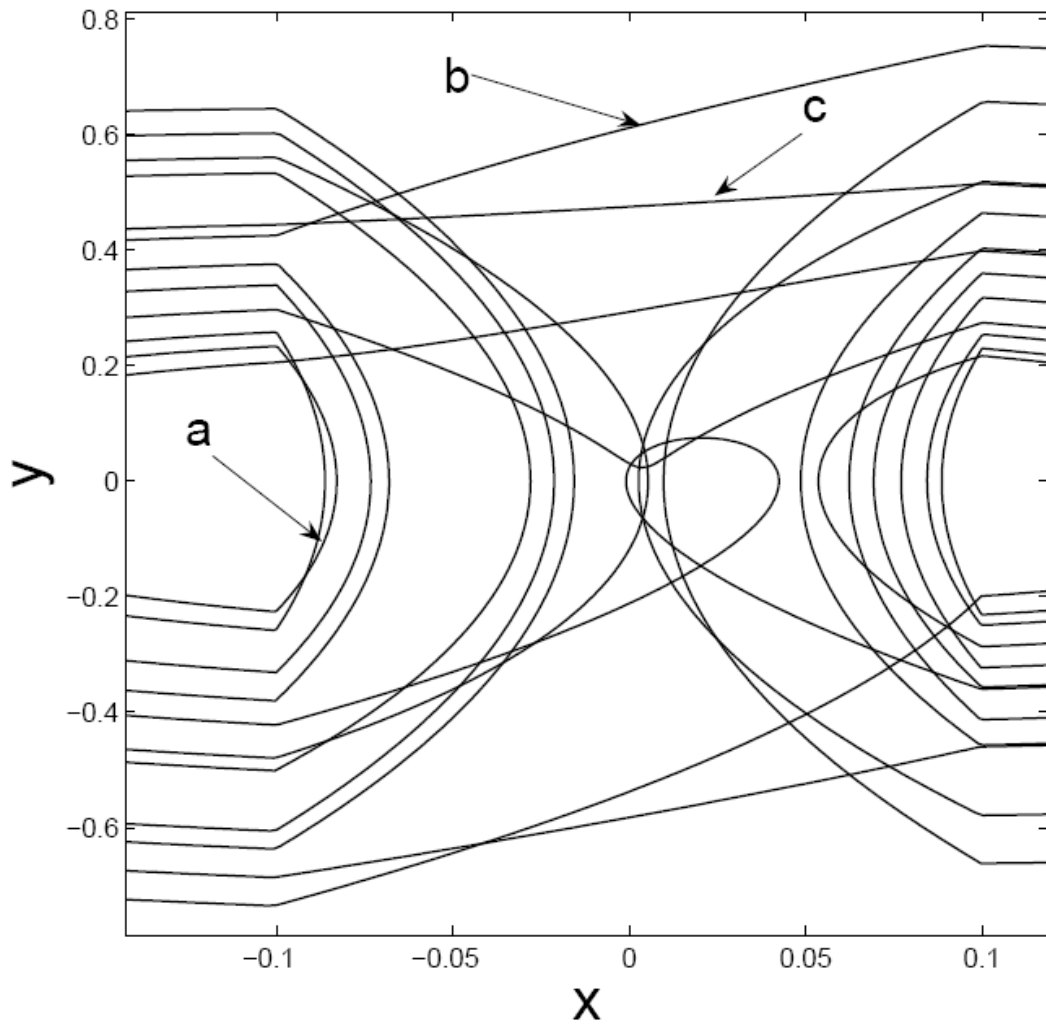


Figure 4.3: Close view of the strip. Note the trajectories: a) reverse direction b) cross the strip but suffers deformation, c) cross the strip without considerable modification.

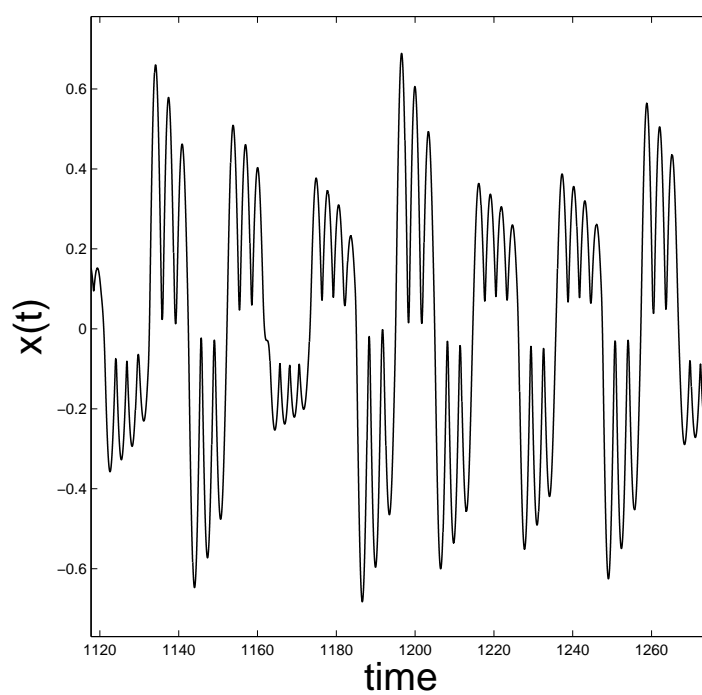


Figure 4.4: Time series of the system ($\Omega = 1.0$, $\gamma = 0.1$, $\omega = 0.3$, $s = 0.1$ and $a = 2.5$).

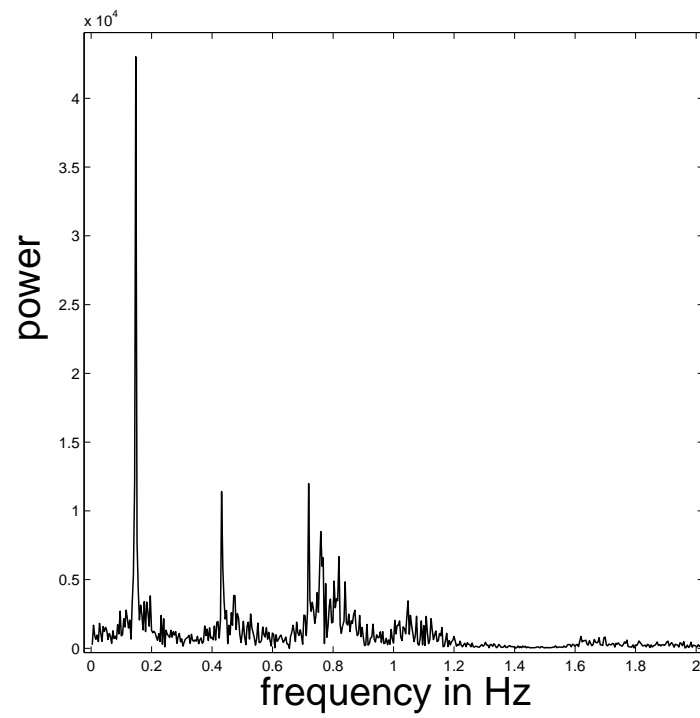


Figure 4.5: Power spectrum of the time series $x(t)$ ($\Omega = 1.0$, $\gamma = 0.1$, $\omega = 0.3$, $s = 0.1$ and $a = 2.5$).

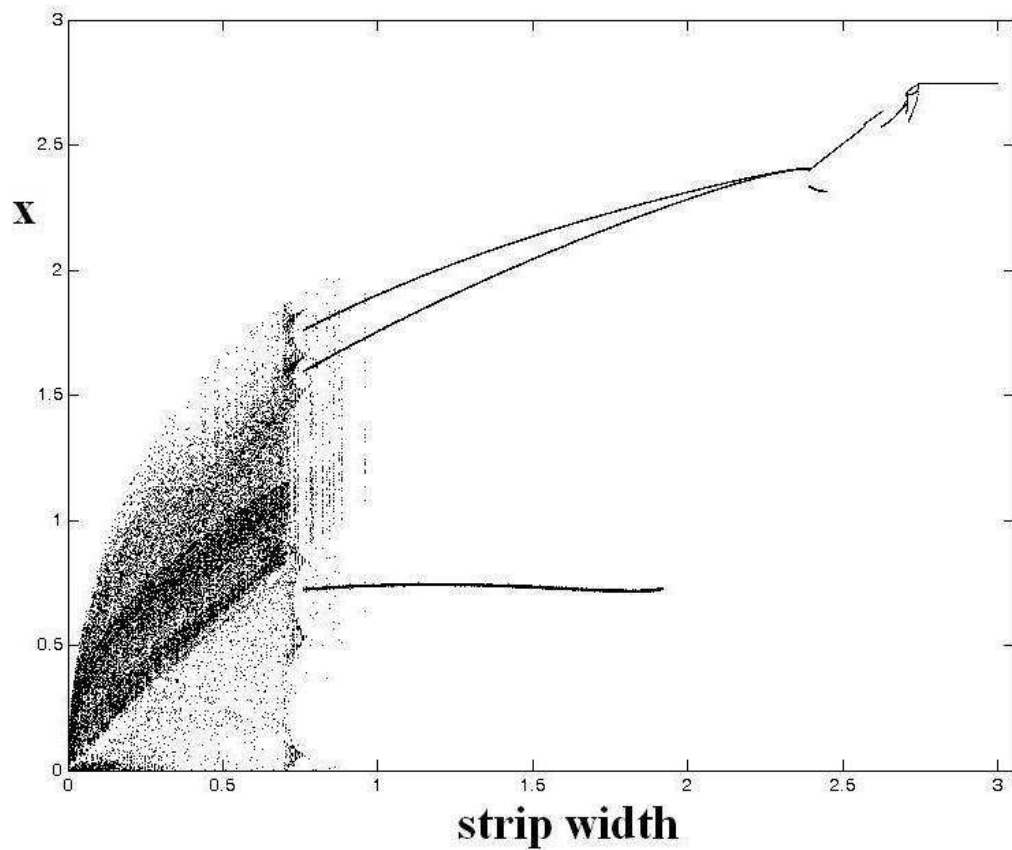


Figure 4.6: Bifurcation diagram obtained by varying the strip width s . Chaotic behavior disappears as the width of the strip is ($\Omega = 1.0$, $\gamma = 0.1$, $\omega = 0.3$ and $a = 2.5$).

space dynamics which consists of reflections in the strip and transitions which modify the trajectories. The power spectrum as shown in Fig. 4.5 is broad which confirms the aperiodic behavior in time.

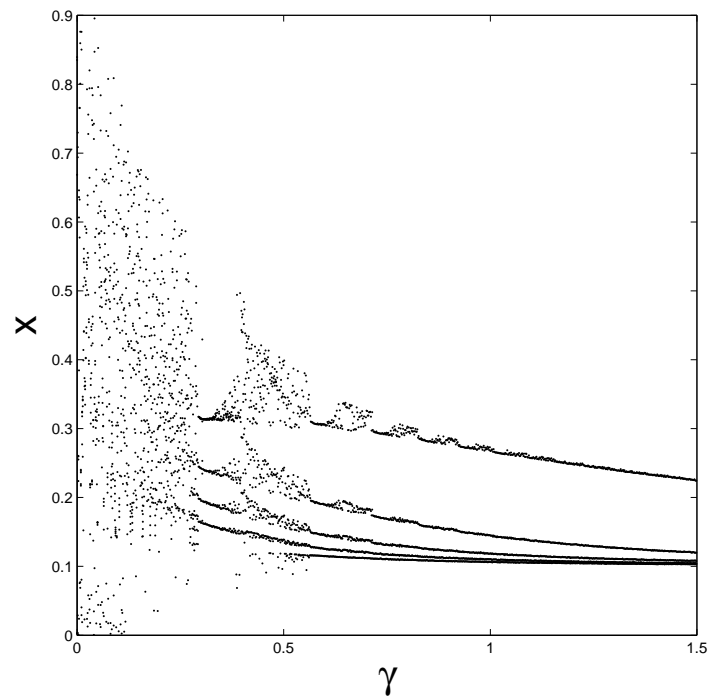


Figure 4.7: Bifurcation diagram obtained by varying the damping coefficient γ . Chaotic behavior is suppressed as the damping is increased ($\Omega = 1.0$, $\omega = 0.3$, $s = 0.1$ and $a = 2.5$).

Varying the parameters s and γ , the system exhibits both chaotic and periodic oscillations. From the bifurcation diagrams shown in Fig. 4.6 and Fig. 4.7, it can be seen that the chaotic behavior disappears for higher values of γ and s . Also note that for $s \simeq 1$ there is a transition to the case of an ordinary driven damped linear oscillator, where no chaotic behavior is expected.

We used *DATAPLORE*[®] [5] for the analysis of the time series. The time delay required for reconstructing a timeseries is a widely discussed topic [4]. With a delay of 1.56, it is found that the autocorrelation function falls to 0.5. With this delay, embedding dimension was calculated using False nearest neighbors method [7]. It is found that the percentage of nearest neighbors approaches zero with embedding dimension 3. Lyapunov exponents were calculated with embedding dimension 3, number of nearest neighbors 37 and the degree of the extrapolating polynomial 3. The result obtained is multiplied by the sampling frequency of the input signal to calculate the Lyapunov exponents. The Largest Lyapunov exponent is found to be 3.19. We obtained 2.148 as the Kaplan-Yorke dimension. The reconstructed phase space of the attractor is shown in fig. 4.8. It is similar in appearance to other chaotic systems in several respects. The trajectories are not closed and it fill the phase space, but not uniformly. The oscillations are bounded though the trajectories diverge locally.

4.4 Random driving

4.4.1 Dynamical equations

In this section we consider the effect of random driving on the oscillator dynamics. Random forcing is achieved by the drive assuming a random value ξ each time the phase space trajectory enters the strip. The amplitude of forcing ξ is Gaussian random

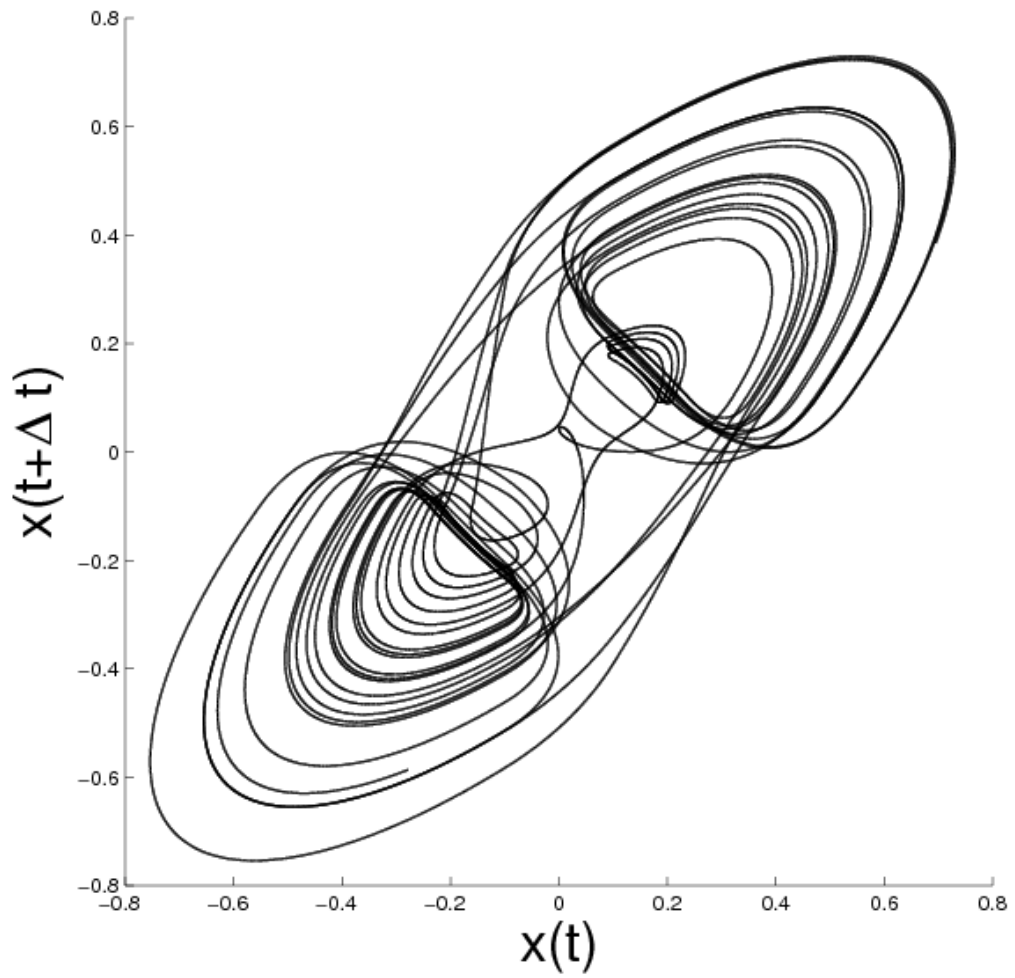


Figure 4.8: The delay reconstructed attractor ($\Omega = 1.0, \gamma = 0.1, \omega = 0.3, s = 0.1, a = 2.5$ and $\Delta t = 1.56$).

variable with variance $\sigma^2 = \frac{1}{\sqrt{2}}$ and zero mean. We define $\chi(s, x)$ as follows,

$$\chi(s, x) = \begin{cases} \xi & \text{if } |x| \leq s \\ 0 & \text{otherwise.} \end{cases} \quad (4.4.1)$$

Retaining $\mu(s, x)$ defined as in eq. 4.3.1 for comparison, the dynamical equation is,

$$\frac{d^2x}{dt^2} + \gamma \frac{dx}{dt} + \Omega^2 x = a\mu(s, x)\chi(s, x) \quad (4.4.2)$$

4.4.2 Numerical results

Replacing the deterministic drive with a random drive, the resulting system mimics its deterministic analogue in many respects. The position momentum space of the oscillator is shown in figure 4.9. Figure 4.10 shows the attractor reconstructed from the timeseries of the system by delayed coordinates. We used a delay of 1.1 seconds, a delay with which the autocorrelation function falls to half its original value [4], for reconstructing the attractor from its timeseries. reflection-transmission dynamics inside the strip is also similar to the deterministic case as shown in figure 4.11. We calculated the invariant parameters, it was found that the Lyapunov exponent is 2.92 and the Kaplan-Yorke dimension is 2.31. A positive Lyapunov exponent and Kaplan-Yorke dimension between 2 and 3 is a sure indication of chaos. The invariant parameters with both driving schemes is given in table 4.1 for comparison.

Invariant parameters	Deterministic driving	Random driving
Lyapunov exponents	3.19	2.92
Kaplan-Yorke dimension	2.148	2.31

Table 4.1: Invariant parameters of deterministic and random driving schemes

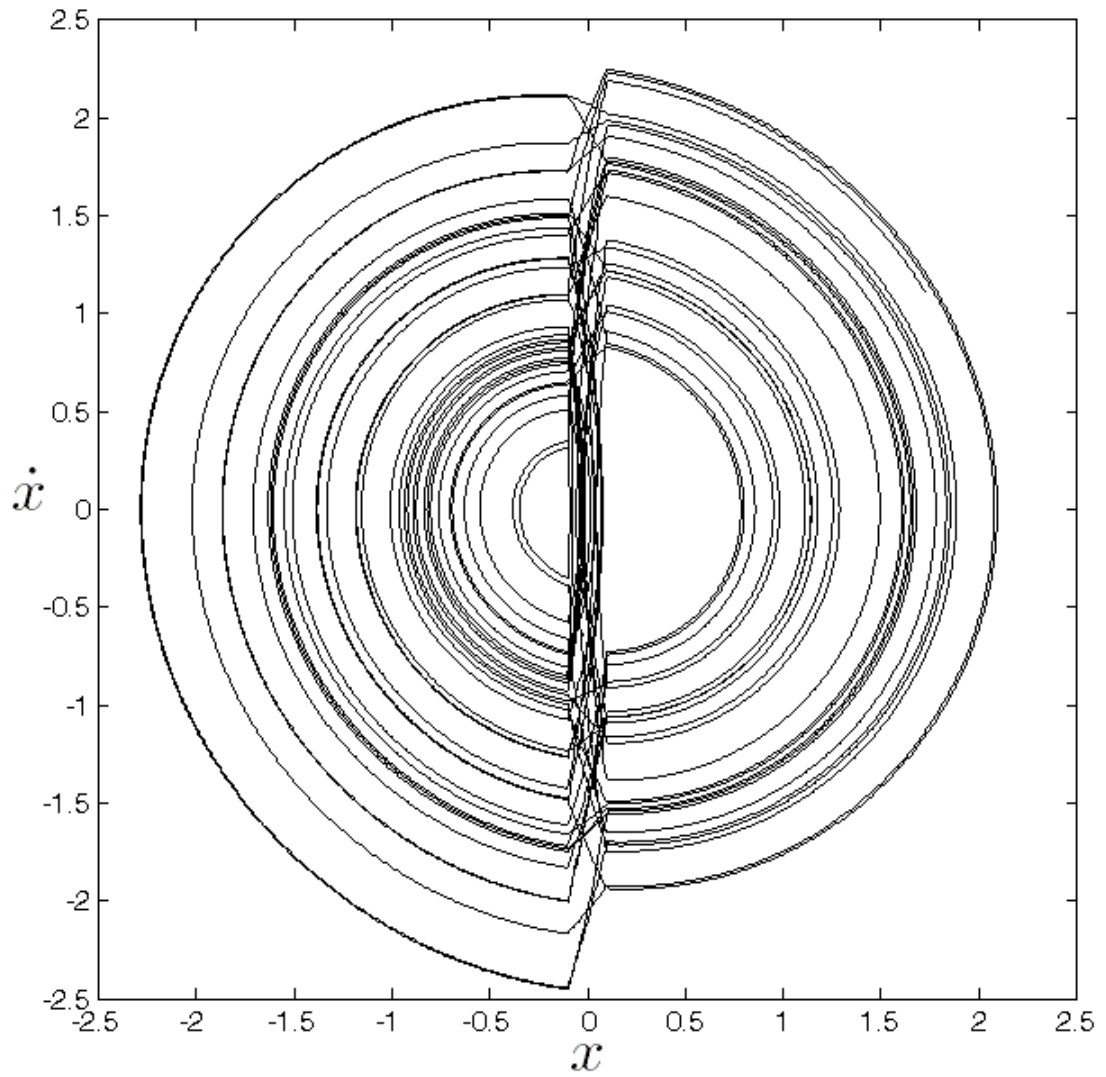


Figure 4.9: The position-momentum space of the oscillator under random driving. ($\Omega = 1.0$, $\gamma = 0.1$, $s = 0.1$, $a = 2.5$ and $\Delta t = 1.1$).

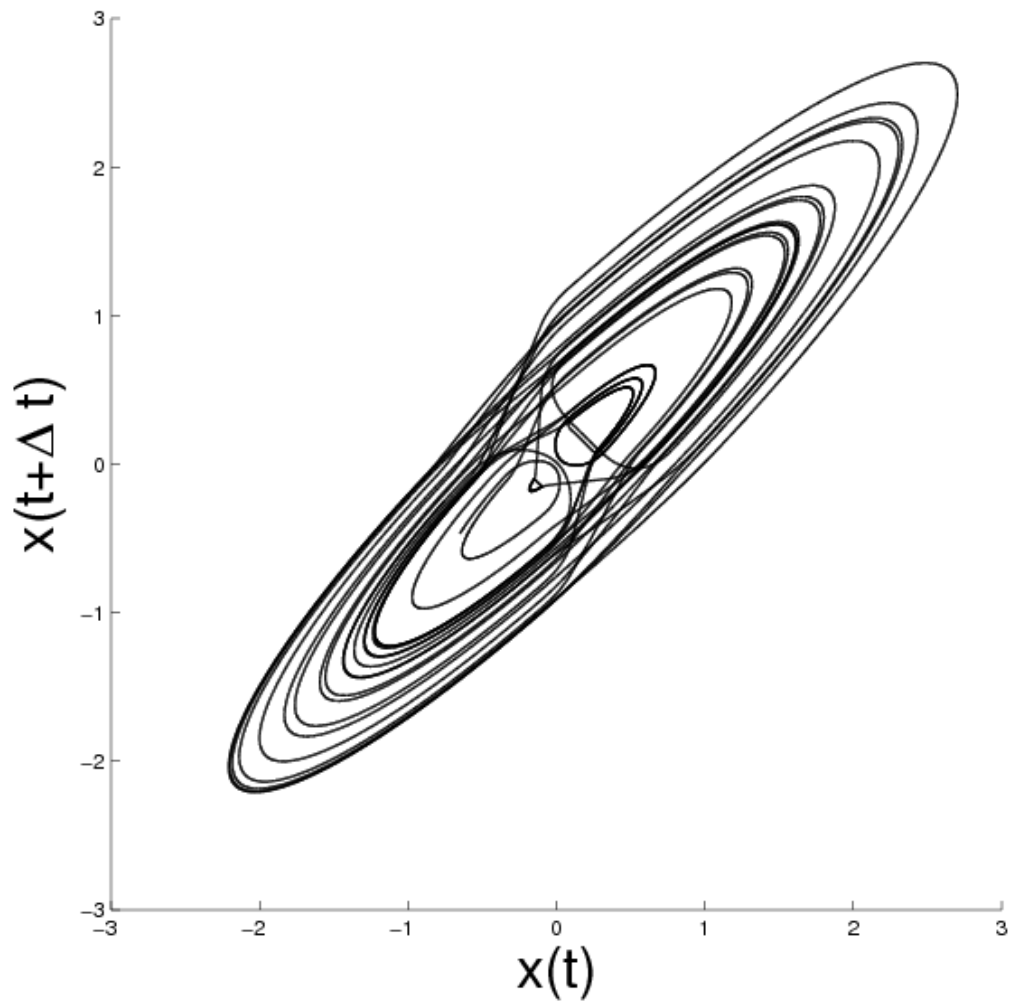


Figure 4.10: The reconstructed attractor resulting from random driving ($\Omega = 1.0$, $\gamma = 0.1$, $s = 0.1$, $a = 2.5$ and $\Delta t = 1.1$).

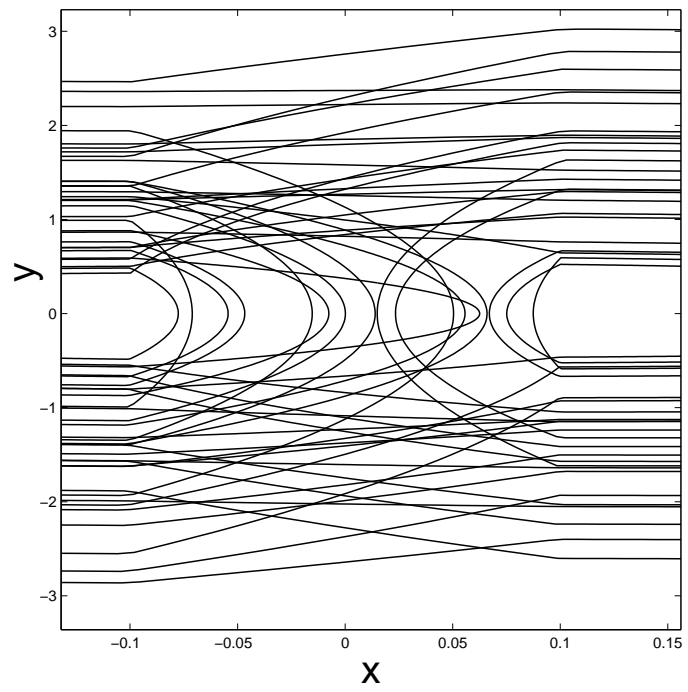


Figure 4.11: Close view of the phase space strip of a randomly driven oscillator.

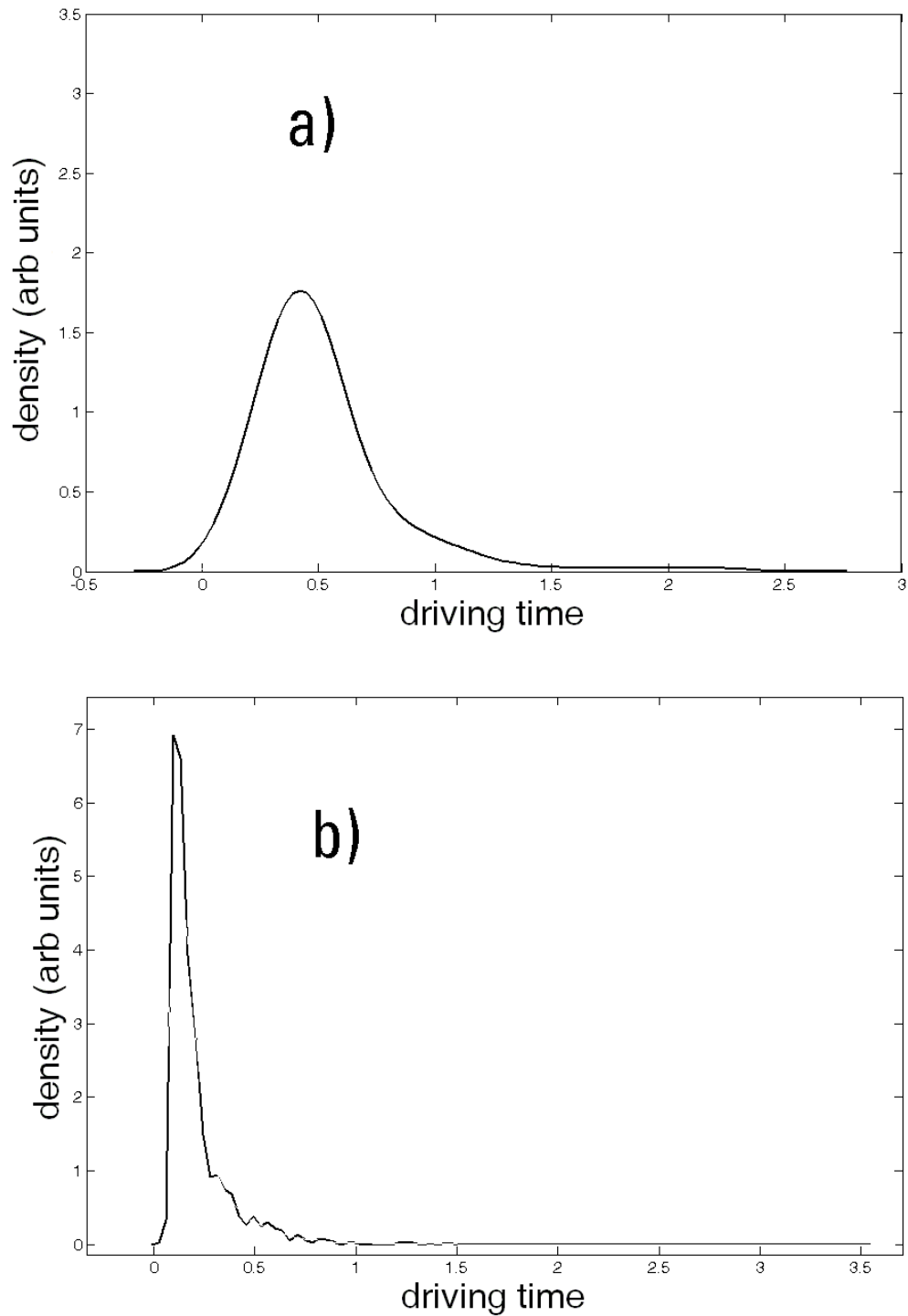


Figure 4.12: The density distributions of the driving times: a) deterministic driving
b) stochastic driving

4.5 Nature of the forcing

The effect of a forcing on the dynamics can depend on many factors. The most important are the amplitude and the time for which such a forcing persists. With Eq. 4.3.1 the dynamics of the system in terms of phase space variables is well defined. The only degree of freedom available for an irregular behavior is through the time interval in which the system is driven. It is shown in fig 4.12 that the distribution of the driving times is peaked in deterministic as well as in random drivings schemes. It is interesting to note that the nature of the distribution is the same but the distribution is more sharply peaked for the random forcing.

4.6 Conclusion

We have shown that weakly damped linear driven oscillator can exhibit chaotic behavior if the coupling between the drive and the oscillator are applied only at a narrow region of the phase space. Similar chaotic behavior can be observed with a purely random drive. Though physically similar mechanisms exist for such a behavior, mathematically, they are different. Under stochastic driving, the forcing term is constant inside the strip and the duration for which the forcing persists, is distributed with a distribution function which is sharply peaked. This implies that the net forcing experienced by the oscillator is similar to the kind of fluctuation that we have studied in Chapter III.

Bibliography

- [1] Y. Hirata and K. Judd, *Chaos* **15**, 33102, 2005.
- [2] N. J. Corron, S. T. Hayes, S. D. Pethel and J. N. Blakely, *Phys. Rev. Lett.* **97**, 24101, 2006.
- [3] N. J. Corron, S. T. Hayes, S. D. Pethel and J. N. Blakely, *Phys. Rev. E* **75**, 45201, 2006.
- [4] Manu P. John and V. M. Nandakumaran, Interplay of determinism and randomness in a piecewise linear chaotic system, communicated.
- [5] The official Weblink to Dataplore is

`http://www.ixellence.com/en/analyse/dataplore_index.html` and the
online manual can be found under
`http://www.ixellence.com/onlinedocu/index_dp.html`
- [6] P. S. Addison, *Fractals and Chaos*, Overseas Press, New Delhi, 2005.
- [7] H. Kantz and T. Schreiber, *Nonlinear time series analysis*, (Cambridge University Press, Cambridge, 1997.

Chapter 5

Harmonic oscillator with exponential damping

5.1 Introduction

In this chapter we study a system which is a modification of the system that we have studied in the previous chapter. We study an oscillator in which the drive is spatially modulated with an exponentially decaying function of the position variable. The significance of this study, in view of the present work is that achieving chaos in this system proves that the chaotic dynamics that we have studied in the previous chapter is structurally stable. That is, the nature of the attractor is not considerably modified with small changes in the dynamical equations of the system.

The dynamical equation of a damped driven harmonic oscillator [1, 2, 3] is given by,

$$\frac{d^2x}{dt^2} + \gamma \frac{dx}{dt} + \Omega^2 x = a \sin(\omega t). \quad (5.1.1)$$

Where the term γ represents the damping coefficient. In a mechanical system this is the damping force proportional to the velocity(\dot{x}). The term Ω represents the angular frequency of the oscillator which is given by $\Omega = \frac{k}{m}$ where k is the restoring force per

unit displacement from the equilibrium and m is the mass. ω represents the frequency of the drive and a represents the amplitude of the forcing applied by the drive.

The dynamical equation of a modified damped driven harmonic oscillator in which the driving term have a spatial dependence can be written as,

$$\frac{d^2x}{dt^2} + \gamma \frac{dx}{dt} + \Omega^2 x = a \exp(-\alpha x^2) \sin(\omega t). \quad (5.1.2)$$

. The driving term $\sin(\omega t)$ of the original harmonic oscillator is modified to $\exp(-\alpha x^2) \sin(\omega t)$.

This can also be written as a system of coupled equations,

$$\begin{aligned} \dot{x} &= y & (5.1.3) \\ \dot{y} &= -\Omega^2 x - \gamma y + a \exp(-\alpha x^2) \sin(z) \\ \dot{z}_1 &= \omega. \end{aligned}$$

The function $\exp(-\alpha x^2)$ with high values of α is a rapidly decreasing function of the space variable. Thus the driving becomes inhomogeneous and there will be regions in the phase space where the effect of the driving is practically absent. This is schematically given in the figure 5.1. The region shaded in grey represents the coupling strength between the drive and the oscillator in various spatial regions. Though the harmonic oscillator is a perfectly linear system, the spatial dependence of an exponential form introduces strong nonlinearities because the term $\exp(-\alpha x^2)$ can be written as,

$$\exp(-\alpha x^2) = 1 + \sum_{n=1}^{\infty} \frac{(-\alpha x^2)^n}{n!}.$$

To study the chaotic dynamics of the system, parameter values which are best suited for the illustration of the concepts are chosen. These values are, $\Omega = 1.0$, $\gamma = 0.1$, $a = 6.25$, $\alpha = 80.0$ and $\omega = 0.3$. In figure 5.2 The phase space of the system is given. The reconstructed attractor is shown in figure 5.4. It can be seen that the topology of the reconstructed figure possess many similarities to that of other chaotic systems. We used a time delay of 0.5s as the time lag required for reconstructing the dynamics [4].

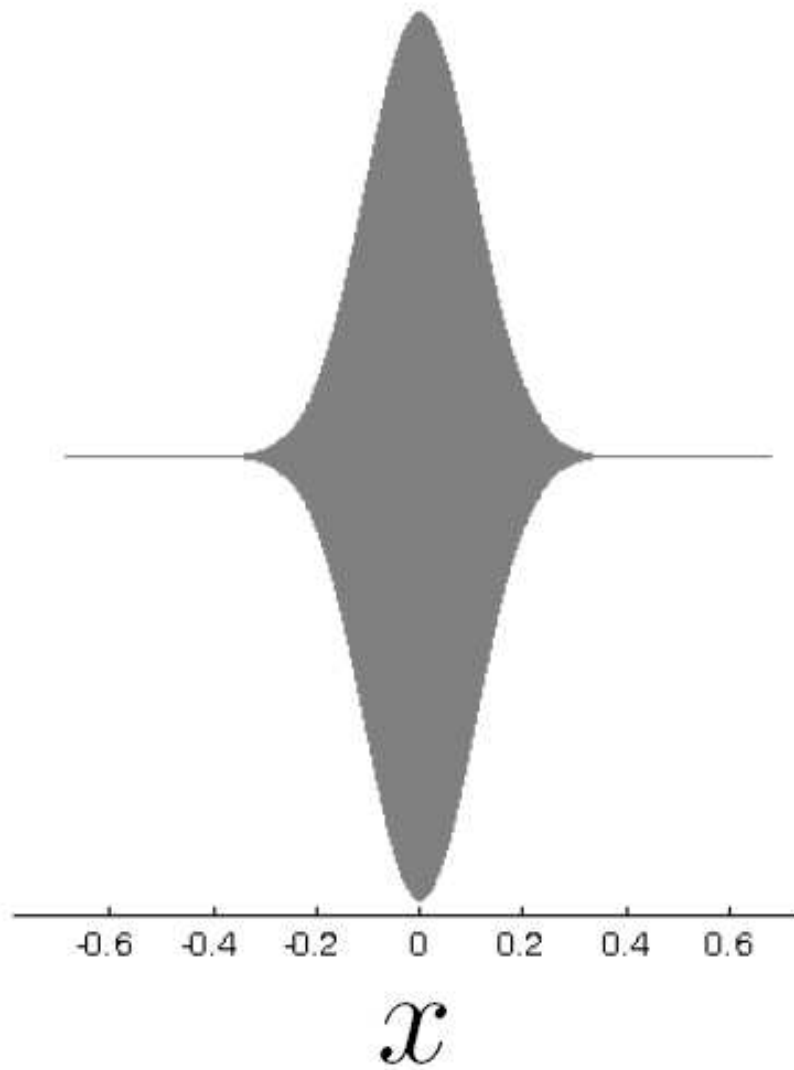


Figure 5.1: Spatial modulation of the drive. The shaded region denotes the spatial modulation experienced by the drive. Thus with an exponential dependence on the space variables the effect of the drive is restricted to a smaller region in phase space. Also there are regions where the effect of the sinusoidal forcing is absent.

The power spectrum of the time series in the chaotic regime is shown in figure 5.3. It can be seen that the power spectrum is broad which indicates aperiodic behavior of the system. The Lyapunov exponents of the attractor is computed using a Matlab version of the Fortran program provided by Wolf. et. al [5]. It can be seen from figure 5.5 that the Lyapunov exponents of the system converges to positive, zero and negative values: which is a clear indication of chaotic behavior. The longer time needed for the convergence of the Lyapunov exponents is a common characteristic of driven systems [3].

5.2 Parameter variations

Many of the nonlinear systems exhibit chaos depending on the parameter values of the system. As we have seen in chapter I, varying the parameters of a system leads to orbits of different periodicities and also chaotic behavior. The key element in the dynamics of this system is the parameter α . We study the effects of varying this parameter keeping all other parameters constant as defined earlier.

The parameter α enters the dynamics through the term $\exp(-\alpha x^2)$. Thus when $\alpha = 0$ or for the smaller values of α , one can expect a regular dynamics similar to that of the damped driven harmonic oscillator. On increasing α the nonlinearities starts to influence the dynamics. Here we can expect periodic oscillations. With higher values of α the nonlinearities affect the dynamics strongly such that the dynamics becomes different from that of the original harmonic oscillator and can result in chaos.

The bifurcation diagram of the system is given in figure 5.6. It can be seen that as α increases the system become chaotic through successive period doublings. There are also periodic windows and successive period doublings in the bifurcation diagram, that are characteristics of chaotic dynamics.

Varying the parameter ω the system exhibits some interesting oscillatory behaviors. The system is chaotic when the drive frequency is considerably less than that of the drive. However when the drive frequency and the natural frequency of the

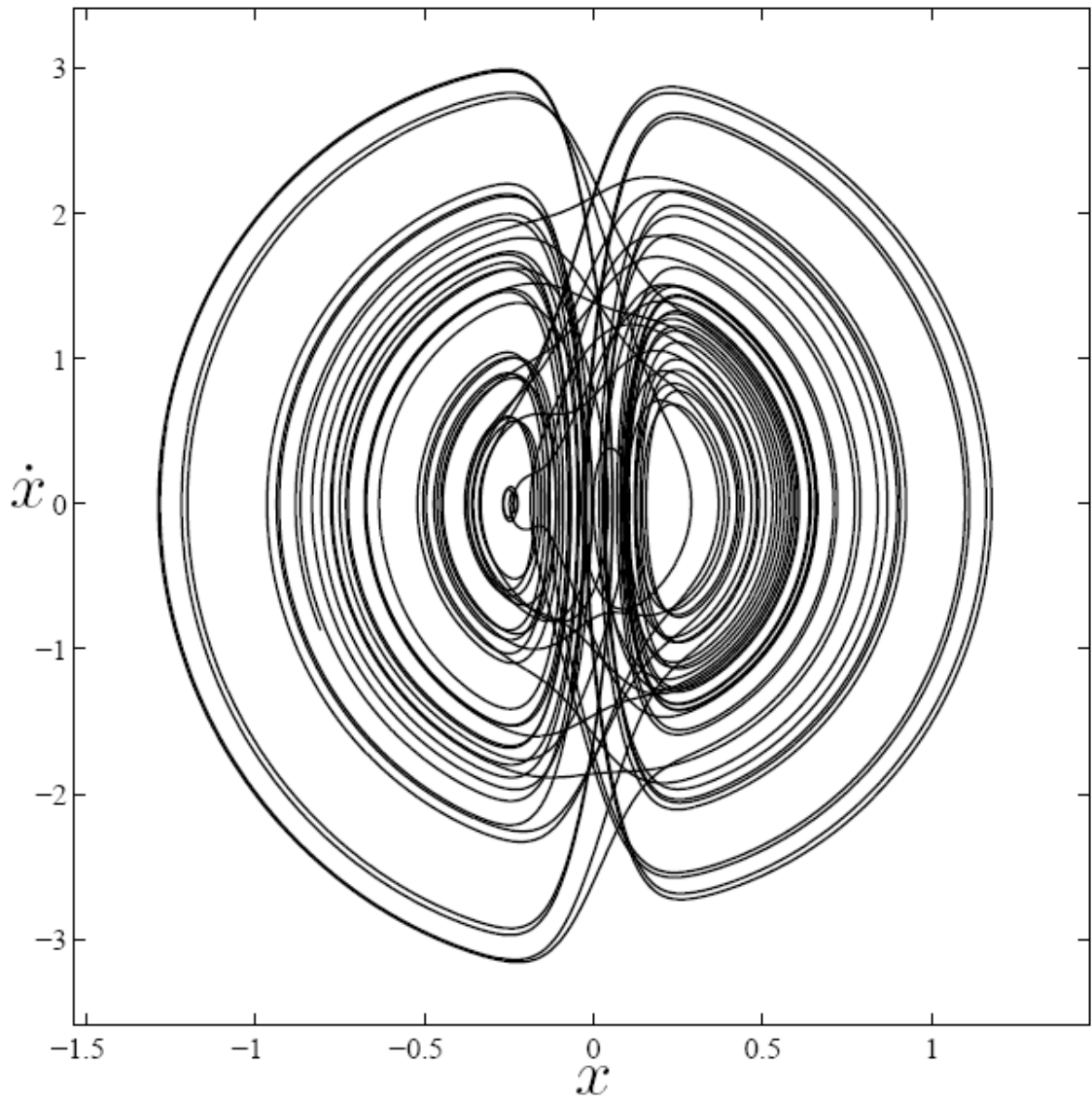


Figure 5.2: The displacement-velocity space of the oscillator in the chaotic regime.

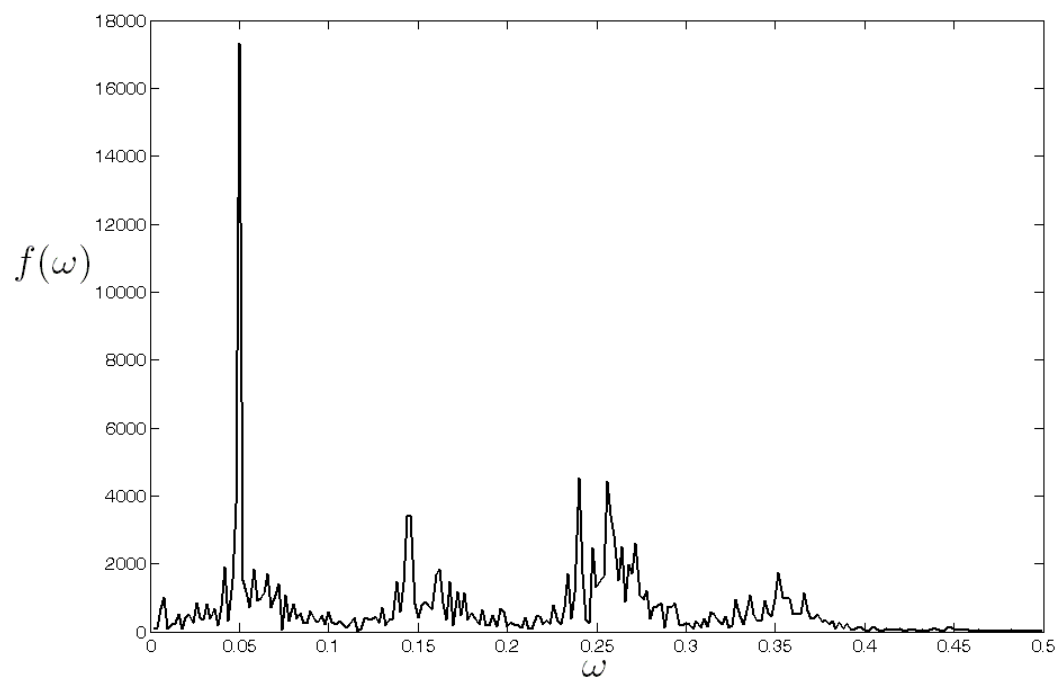


Figure 5.3: The power spectrum of the time series for the parameter values $\Omega = 1.0$, $\gamma = 0.1$, $a = 6.25$, $\alpha = 80.0$ and $\omega = 0.3$.

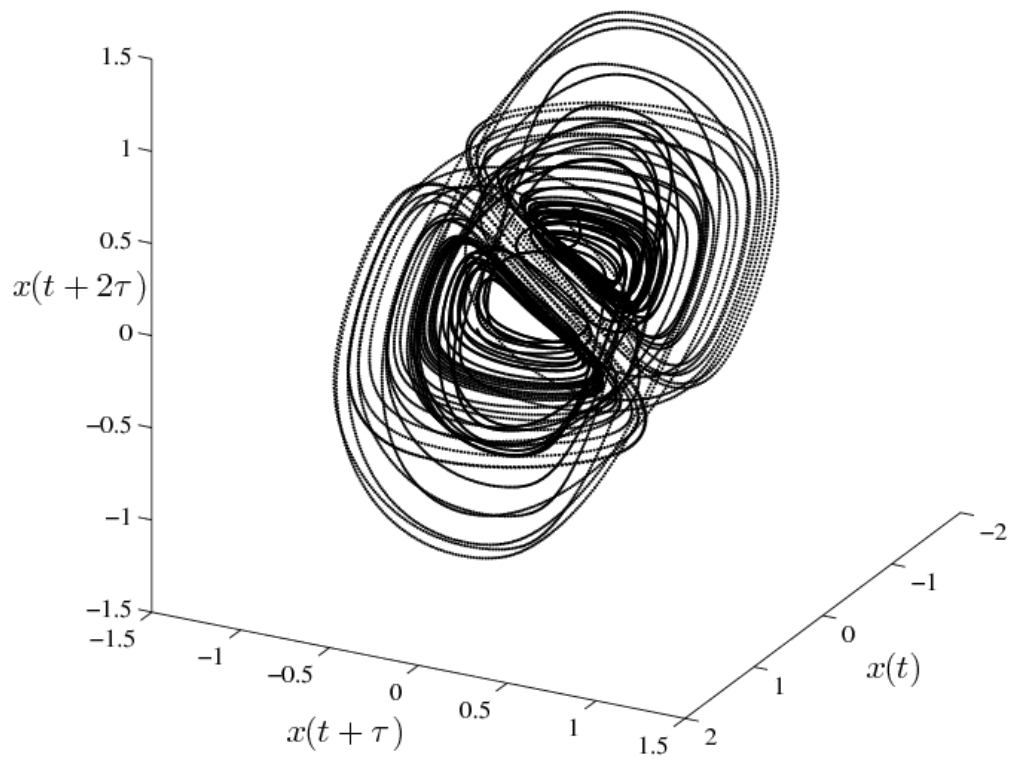


Figure 5.4: The delay reconstructed phase space of the oscillator.

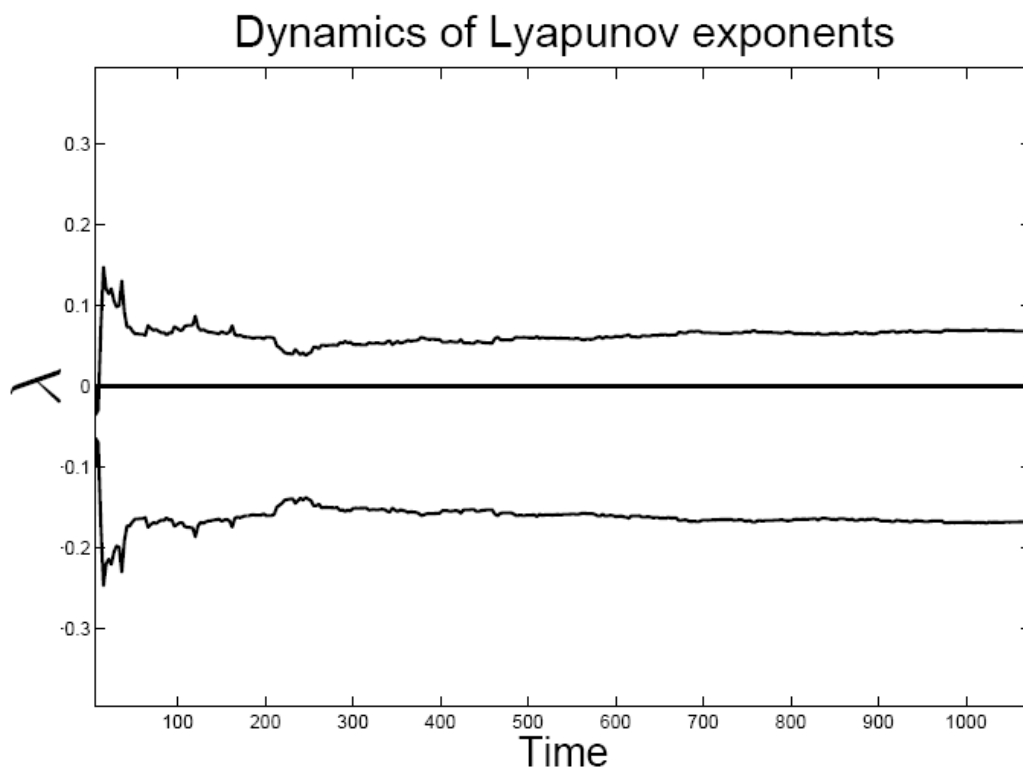


Figure 5.5: Convergence of the Lyapunov exponents as $t \rightarrow \infty$.

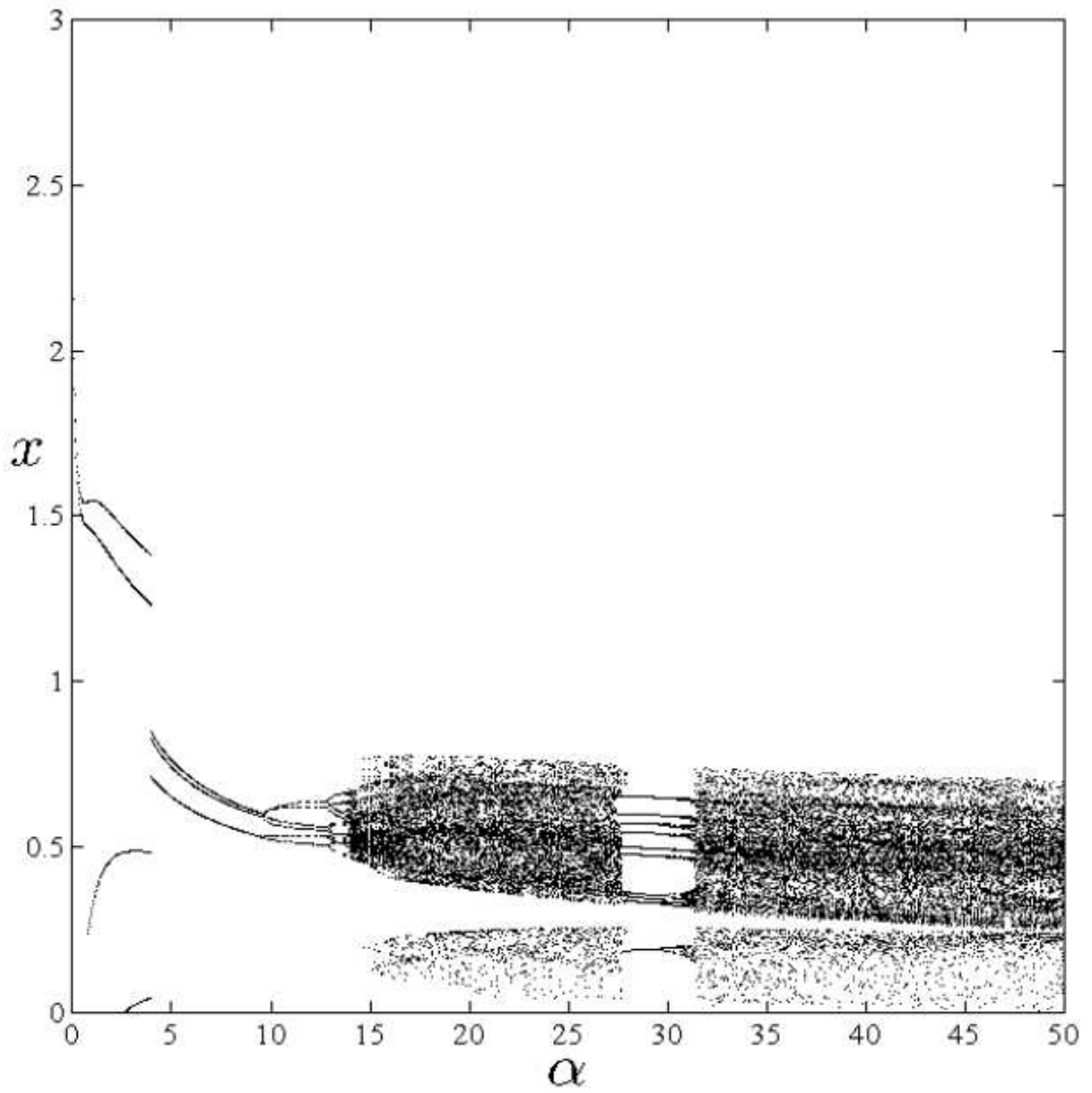


Figure 5.6: The bifurcation diagram of system under the variation of α .

oscillators match it can be seen that the system becomes periodic. The maximum amplitude of oscillations in the periodic regime occurs when the frequency of the drive and the natural frequency of the oscillator match. However, periodic orbits are possible when the frequency of the drive is higher than that of the oscillator. The bifurcation diagram corresponding to the variation of ω is given in figure 5.7. From figure 5.8 it can be seen that chaotic behavior does not occur if the damping coefficient is high. At high values of damping, orbits of different periodicities can be observed.

5.3 Synchronization

In this section, we study the synchronization properties of the oscillator in the chaotic regime. Synchronization is achieved by diffusive coupling. The coupled equations can be represented as,

$$\begin{aligned}
 \dot{x}_1 &= y_1 + c(x_2 - x_1) & (5.3.1) \\
 \dot{y}_1 &= -\Omega^2 x_1 - \gamma y_1 + a \exp(-\alpha x_1^2) \sin(z_1) \\
 \dot{z}_1 &= \omega \\
 \dot{x}_2 &= y_2 + c(x_1 - x_2) \\
 \dot{y}_2 &= -\Omega^2 x_2 - \gamma y_2 + a \exp(-\alpha x_2^2) \sin(z_2) \\
 \dot{z}_2 &= \omega,
 \end{aligned}$$

where c denotes the coupling strength. The schematic diagram of the coupling scheme is given in figure 5.9. The Conditional Lyapunov exponents (**CLE**) [6] of the coupled systems are calculated. The variation of maximal conditional Lyapunov exponent with respect to coupling strength is plotted in figure 5.10. It can be seen that with both unidirectional and bidirectional coupling, chaotic synchronization is achieved between the oscillators. The synchronization plot of the systems coupled bidirectionally with a coupling strength of 0.2 is given in figure 5.11.

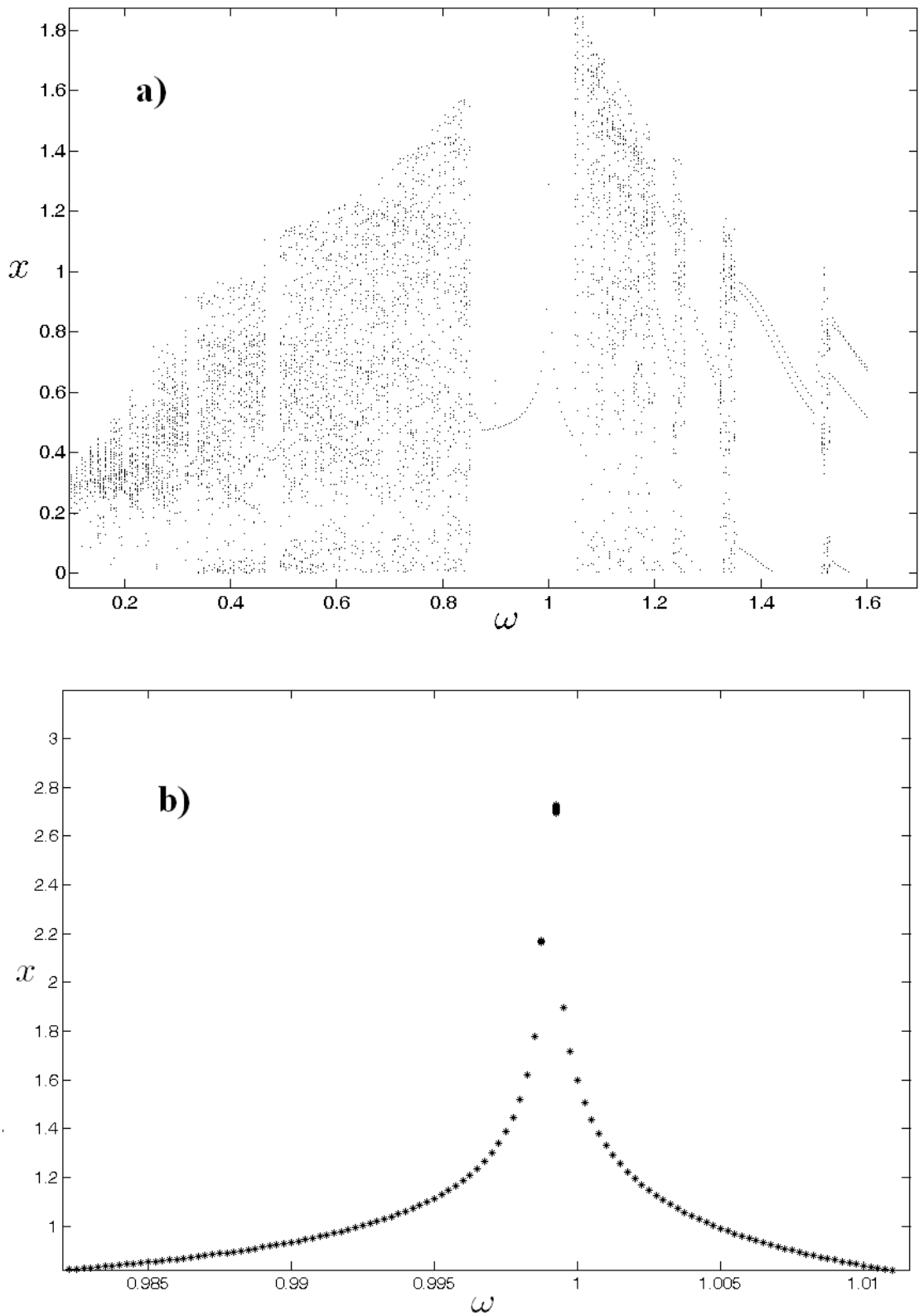


Figure 5.7: a) The bifurcation diagram of system under the variation of ω , b) zoomed view of the resonance part

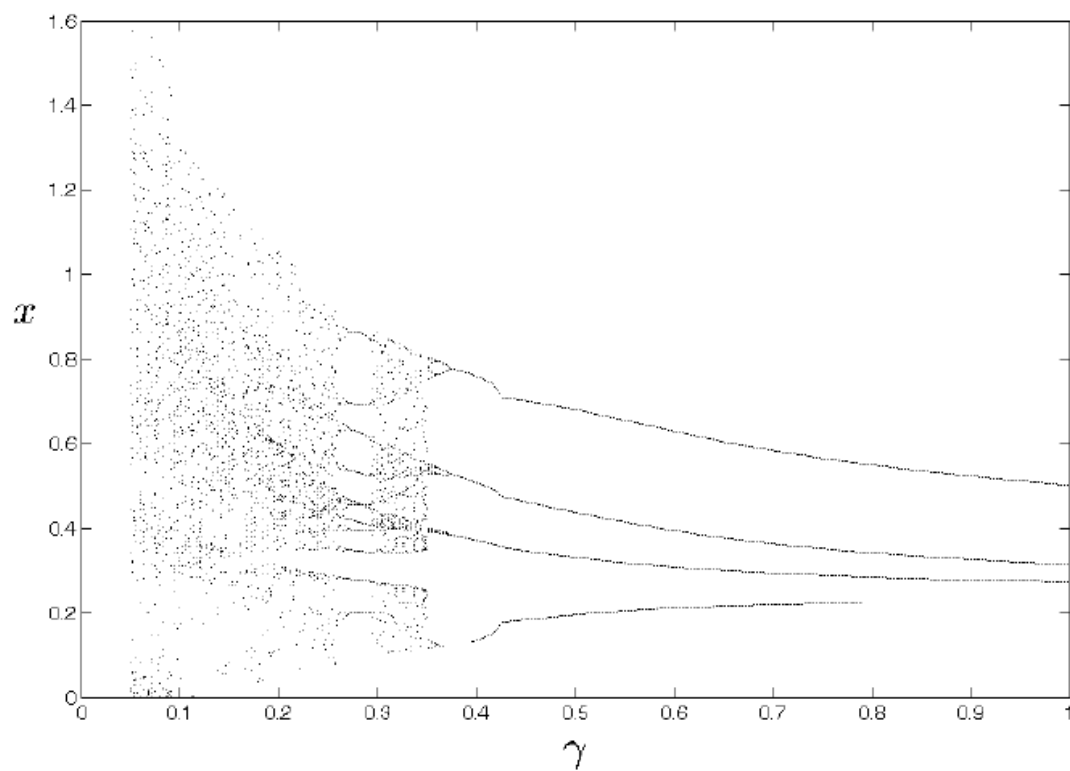


Figure 5.8: The bifurcation diagram of system under the variation of γ .

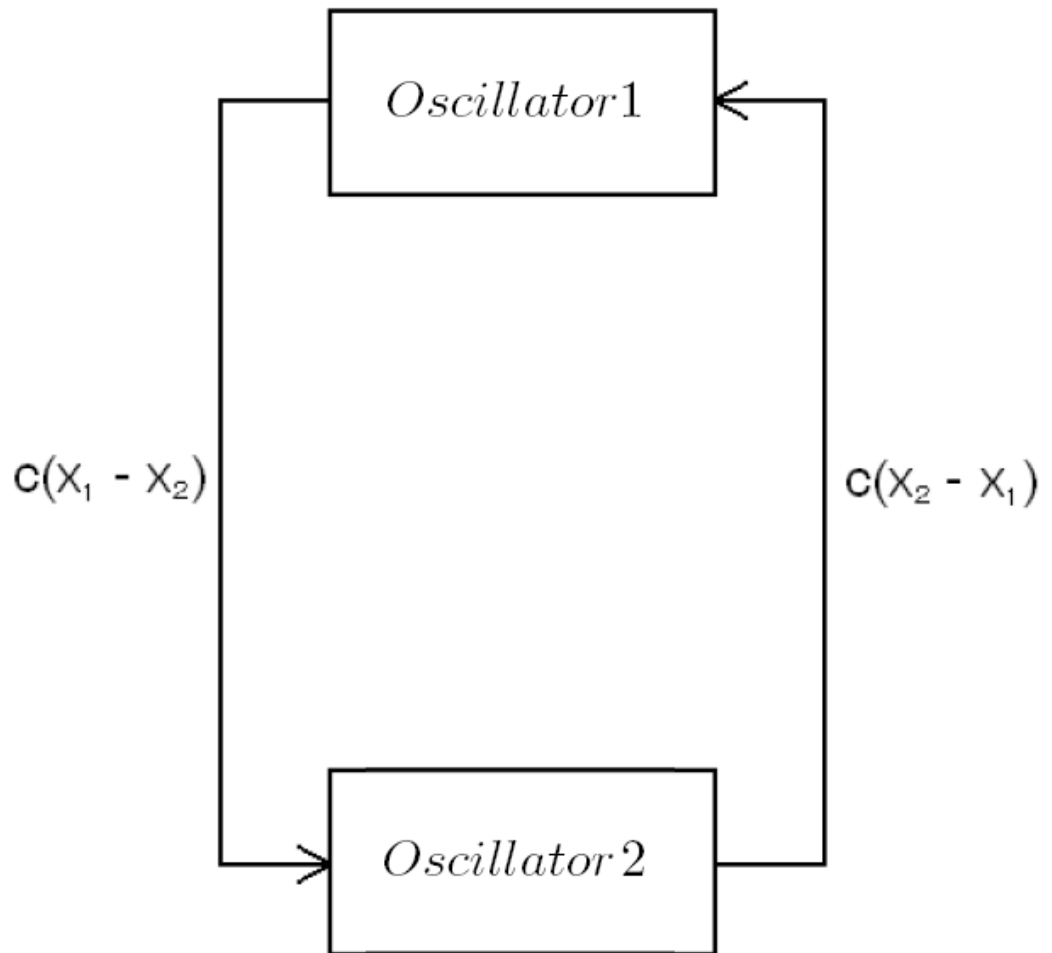


Figure 5.9: Diffusively coupled spatially modulated harmonic oscillators: a schematic representation.

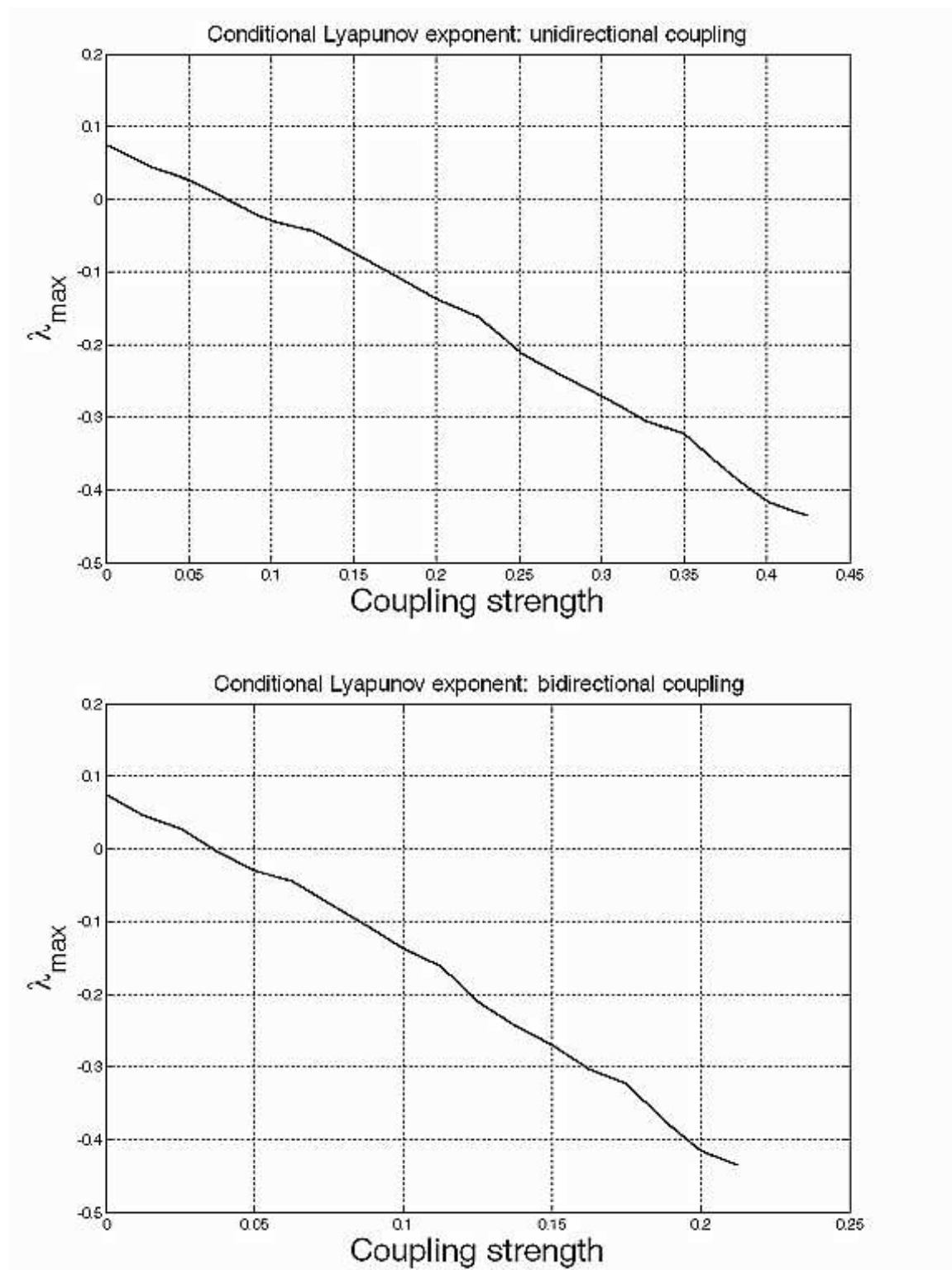


Figure 5.10: Variation of the maximal Conditional Lyapunov exponent with increase in coupling strength.

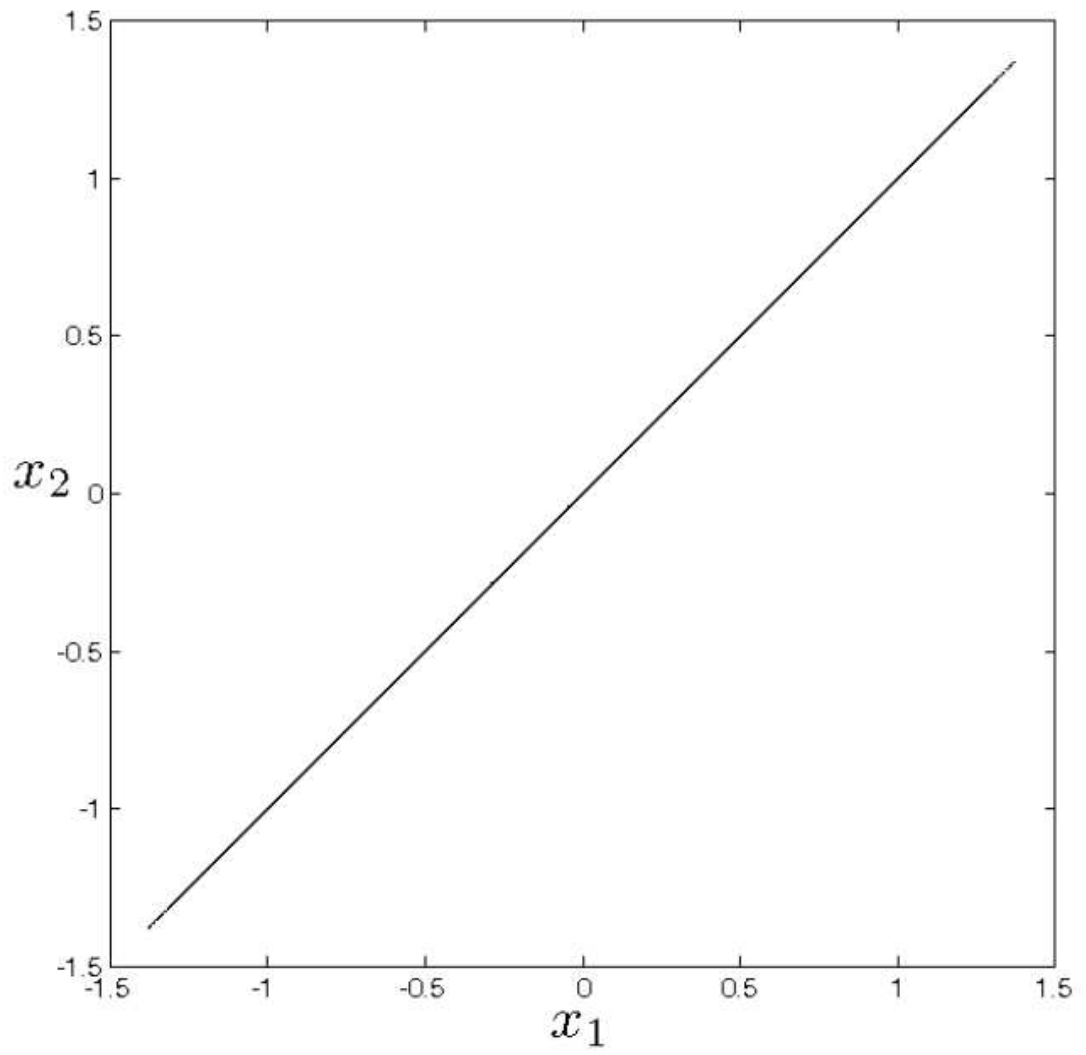


Figure 5.11: The synchronization plot of the coupled modulated harmonic oscillators.

5.4 Conclusions

The driven damped harmonic oscillator can be transformed to a chaotic oscillator by modifying the driving term with a spatial dependence of an exponential nature. The system follows the familiar period doubling route to chaos. Synchronization of such systems is possible for a wide range of coupling strengths.

Bibliography

- [1] "Simple Harmonic Motion" from The Wolfram Demonstrations Project
<http://demonstrations.wolfram.com/SimpleHarmonicMotion/> Contributed
by:Paul Rosemond.
- [2] "Driven Damped Oscillator" from The Wolfram Demonstrations Project
<http://demonstrations.wolfram.com/DrivenDampedOscillator/> Contributed by:
Mark Robertson-Tessi.
- [3] J. C. Sprott, *Chaos and Time-series analysis*, Oxford University Press, Oxford,
2003.
- [4] P. S. Addison, *Fractals and Chaos*, Overseas Press, New Delhi 2005.
- [5] A. Wolf, J. B. Swift, H. L. Swinney and J. A. Vatsano, *Physica D* 16, 285, 1985.
- [6] Louis M. Pecora, Thomas L. Carroll, Gregg A. Johnson, and Douglas J. Mar,
Chaos 7, 520, 1997.

Chapter 6

Summary, conclusions and future prospects

6.1 Summary and conclusion

We have shown that a randomly fluctuating parameter on synchronization of chaotic systems destroys the synchronization. In some systems, it is possible to establish the relation between the characteristic timescales associated with the fluctuation and the quality of synchronization. But there are also situations in which this is not possible.

We studied a modified harmonic oscillator in which the drive and the oscillator are coupled only when the phase space trajectory is inside a small strip in the phase space. The resulting oscillator exhibits chaotic behavior. A stochastic analogue of this system can also be constructed by replacing the deterministic drive with a random one. It was found that such a system mimics its deterministic analogue.

In stochastically driven chaotic oscillator the effective driving is the *random forcing with associated timescales*, where the timescales are distributed with a density function which is peaked. The peaked nature of the distribution suggests that a timescale which is characteristic to such forcing exists.

Replacing the strip in the earlier chapter, we studied a damped harmonic oscillator in which a spatial modulation which is an exponential function of the position variable, is applied to the drive. The system exhibits chaotic dynamics which is much similar to the familiar chaotic systems. This shows that the dynamics of the stochastically driven oscillator and its deterministic analogue is not much different from the behavior of regular chaotic systems.

To conclude, a fluctuating quantity which is associated with characteristic timescales destroys synchronization. On the other hand, such fluctuations can also induce chaos. Thus we have shown that phenomenon which is equivalent to chaos and that cannot be synchronized exists. Also we have established one of the close relations between determinism and randomness in nature.

6.2 Future prospects

In future we would like to extend our studies to modified versions of the intermittently driven system. This include driving with random forcing which follows other distributions, and hence to find out what the actual distribution with which the dynamics is most similar to chaos. Though the previous results that describe chaotic behavior under random driving involves time reversal, it also has a similarity to our system: the system is driven by random pulses. Establishment of a connection between our model and the model given by Corron et. al. is also proposed. In future, we also plan the physical realization of the mathematical models that we have studied.